January 2013

A Distributed Local-Leg Feedback Algorithm for Robust Walking on Uneven Terrain

Mayur Ramakant Palankar
University of South Florida, palankarmayur@gmail.com

A Distributed Local-Leg Feedback Algorithm for Robust Walking on Uneven Terrain

by

Mayur Palankar

A dissertation submitted in partial fulfillment
of the requirements for the degree of
Doctor of Philosophy
Department of Computer Science and Engineering
College of Engineering
University of South Florida

Major Professor: Luther Palmer III, Ph.D.
Yu Sun, Ph.D.
Kyle Reed, Ph.D.
Kathryn De Laurentis, Ph.D.
Scott Campbell, Ph.D.
Yael Arbel, Ph.D.

Date of Approval:
May 1, 2013

Keywords: biologically-inspired, force-threshold, foot-forces, force-feedback, position-control

DEDICATION

Commitment and effort were the important cornerstones for the completion of my doctoral dissertation but support of my family was even more important. I dedicate this important professional achievement to my parents, Ramakant and Mangala Palankar. I would not have achieved my goal without their support.

ACKNOWLEDGMENTS

I would like to thank to my adviser, Dr. Luther R. Palmer III, for his leadership and support during these years. I am very grateful for his scientific advice and knowledge. His astute insights, and valued comments and suggestions, have been of such great benefit for improving my work, and in writing the manuscript. He is my primary resource for getting my questions answered and is instrumental in helping me finish this dissertation.

I would like to thank the Department of Computer Science and Engineering for providing me with assistantships though these years. I would like to thank the members of my committee, Dr. Yu Sun, Dr. Kyle Reed, Dr. Scott Campbell, Dr. Kathryn De Laurentis and Dr. Yael Arbel.

I want to thank the current and former members of the Biomorphic Robotics Lab including Nellie Bonilla, Caitrin Eaton, Carlos Ezequiel, Jeffrey Price, John Rippetoe, Bradley Savon, Robert Skinner, Daniel Standish, Miguel Veliz, and Jeffrey Vickers for their contribution, however great or small, to my research. I would particularly like to thank Jeffrey Price for his work with the RobotBuilder simulation environment. Also, I would like to thank Miguel Veliz, Bradley Savon, John Rippetoe and Nellie Bonilla for their work on the hexapod hardware at various stages of development. Lastly, I want to thank all my friends and colleagues for their support.

I want to thank my girlfriend, Jill Weber, for always believing in me and for motivating me to finish my dissertation. Finally, I thank my parents, Ramakant and Mangala Palankar, to whom I dedicate this dissertation. I also want to thank my brother, Vishal Palankar. I know this dissertation makes them proud.

TABLE OF CONTENTS

iii

LIST OF TABLES

LIST OF FIGURES

vi

ABSTRACT

Legged animals can traverse significantly more of the Earth's land mass than man-made wheeled and tracked vehicles [1]. Their impressive mobility is largely due to multiple dexterous legs and the robust algorithms that coordinate and control them. A legged animal such as a squirrel can exhibit multiple locomotion modes such as walking, running and jumping and also multiple gaits or leg phase timings within each mode. A robot that could mimic this level of robust locomotion would be highly useful for planetary exploration, military reconnaissance, and time-critical search and rescue in cluttered or collapsed buildings.

A number of biological studies on animal walking have provided information concerning the underlying control system. Studies in insect walking have revealed a distributed local-leg control that generates quasi-rhythmic movement by sensing the environment using local feedback loops. Ground reaction forces produced by an insect during walking and running, along with joint angles, have been recorded by various studies. The primary goal of this research is to develop a distributed local-leg control algorithm to generate walking behaviors on uneven terrain using local force feedback. The intended purpose of this research is to pursue a biologically-inspired control algorithm that can be used as a scientific tool to study walking and provide a better understanding of local-leg control.

Control of a multi-jointed robot system has traditionally been done using position control. But as the number of degrees of freedom in systems started increasing, position control of each actuator using a centralized controller became cumbersome. The control of a walking robot is a

more complex problem as stability also becomes an issue. Much research has been concentrated towards creating rhythmic or quasi-rhythmic movements which can be used for walking in predictable environments. However, walking on uneven terrain requires one to incorporate different issues, such as but not limited to, the mechanical properties of the leg, coordination between legs, as well as higher level decisions based on external information and internal body states. Much of the current research in legged robots is directed towards sensing the terrain so that the walking sequence of the robot can be pre-determined. This requires a large array of sensors, off-line as well as in real-time, to accurately sense the terrain increasing the cost and complexity of the robot. Even if the body path and footholds are planned, a real-time module is required to handle small perturbations and slips adding to the complexity. Like animal walking, using force feedback can greatly improve walking behavior in a robot. However, due to the unreliable nature of force sensors, no other control algorithm for walking has been able to use continuous force feedback for walking on uneven terrain.

The distributed local-leg controller developed in this research, called Force Threshold-based Position (FTP) controller, is able to generate walking behaviors robust to terrain elevations without using visual sensors, a priori terrain information, inertial sensing, or inter-leg communication. The controller uses local force feedback to control each leg and is, therefore, very responsive to terrain changes when compared to a centralized controller arbitrating all of the joint positions in a high degree of freedom system. The controller is implemented with gait phasing dictated by a static timer. By integrating force feedback with position control, the FTP controller combines the advantages of position control with robustness to uneven terrain. This work provides the minimum interaction needed between joints or legs for the robot to navigate a rugged terrain. This work provides insight into the role of active elements in the local leg feedback controller that allow for responsiveness over uneven terrain, and can be used to reveal the underlying structure insects use to generate the forces needed for different behaviors and gaits on flat and uneven terrain.

The FTP controller has been realized and studied on a full 3D simulation model and on an experimental hexapod system. Multiple gaits along with turning and side stepping have been implemented and tested on the system. The FTP controller is built as an low-level reflexive system which would be guided by a high level controller overseeing its operation, intermittently passing directional commands and control information. The objective is to make the walking behavior a background process such that the robot can focus on its mission objectives. The FTP controller also has potential for expansion to bipeds, quadrupeds and other biologically-inspired forms.

CHAPTER 1: INTRODUCTION

1.1   Motivation

Legged animals have a remarkable ability to adapt their walking behavior based on the terrain and threat level. Animal legs appear in many arrangements and morphologies, and are capable of multiple locomotion modes. Despite the versatility in arrangement seen in nature, every leg operates under the same intermittent paradigm of flight and stance phases (Fig. 1.1). All terrestrial animals appear to exhibit spring-mass dynamics, whether moving on two, four, six or eight legs [2]. Foot forces are applied to the ground to propel and stabilize the body during the stance phase, and the leg is returned from its posterior position to a forward position during the flight phase.

A single leg morphology can utilize multiple mobility modes to circumvent obstacles or gaps in the terrain, which further outpaces the capabilities inherent to wheels that can nominally move over near-horizontal terrain. Even within a single mobility mode, such as quadruped running, legs can be coordinated to transition between the canter, trot, or gallop in order to increase stability or conserve energy in response to the terrain or threat level. This level of versatility can be achieved because of the high number of degrees of freedom (DoFs) apparent in many legs.

Biological evidence supports the notion of a hierarchical control system that distributes the leg coordination and control effort to multiple systems in the body [4]. Research on decerebrated cats shows that the brain is not required for gait selection and coordination over a range of walking and running speeds [5]. This research illuminated some of the local leg feedback algorithms that

1
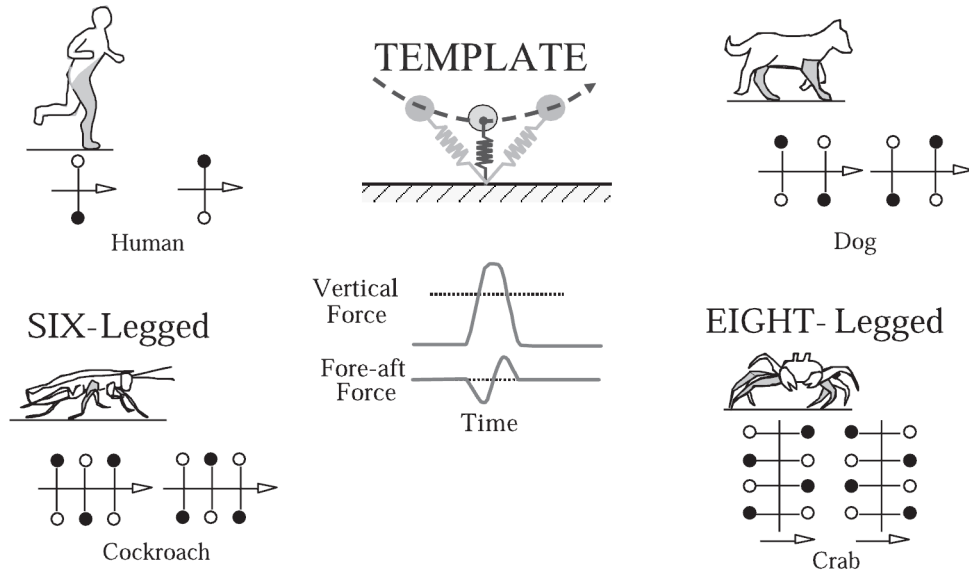
Figure 1.1: Center-of-mass (COM) dynamics for running animals with two to eight legs. All terrestrial animals appear to exhibit spring-mass dynamics, whether moving on two, four, six or eight legs. Multiple legs act in concert to produce the effective leg-spring dynamics. (Taken from [3] - see Appendix B.1)

may be responsible for joint-level coordination during leg movement. These control loops sense and command control elements only within a single leg, and the limited number of control elements combined with the short transmission lines allow these control loops to be much more responsive than a higher-level controller potentially responsible for sensing and controlling multiple legs.

The main motivation behind distributing the leg coordination and control is that the control of a high degree of freedom multi-legged robot can potentially be done using small, fast and energy efficient control systems which are highly responsive to terrain changes while indirectly providing motion control and tilt stability.

1.1.1 Need for Legged Systems

Legged systems have the potential for use in planetary exploration, time-critical search and rescue, military reconnaissance, and a wealth of other tasks in which the terrain is complex or rife

www.manaraa.com

with uncertainty. Mobility comparable to biological systems such as squirrels, cockroaches and even humans will be necessary to effectively perform in these arenas.

Wheels are excellent on constructed surfaces but perform poorly on natural uneven surfaces. The main advantage of legged systems is that on uneven surfaces, selection of each leg foothold can be optimized to provide support and result in forward movement irrespective of the terrain. Unlike a wheeled system, which needs a continuous path to travel, a legged system can step over isolated paths to travel over uneven surfaces without much loss of stability. Since multiple mobility modes can be implemented on a legged system, they are a prime candidate for terrains rife with uncertainty. The legged mobility mode can be chosen based on the terrain and/or the situation.

The benefit of legged systems over wheeled vehicles is not only more mobility over highly irregular terrain, but it also holds potential for jumping, climbing, and swimming.

1.1.2 Difficulties with Walking

A high number of degrees of freedom (DoFs) can result in versatility and robustness, but can be very difficult to coordinate and control. To make this control problem more manageable, gaits have been isolated and studied individually [6–10]. Although legged systems with articulating joints have been developed to perform singular mobility tasks [11–13], many of the underlying control algorithms for these systems are gait or task specific, and no link to multi-modal or multi-gait mobility is laid out.

The control of legs requires the interplay between supervisory commands, central pattern generators (CPGs), and neural feedback. Control algorithms have been developed which alter the timing of leg CPGs based on sensory feedback such as foot contact and body tilt angles [14, 15]. In some CPG implementations, the joint torques during the stance phase are direct outputs of the CPG, and in other implementations, the CPG controls the leg phasing between stance and flight,

3

and joint torques are computed using other feedback-based equations. In both controller types, inertial measurements of pitch and roll are used as feedback. Inertial signals, however, can be plagued by significant noise, delay and drift, and algorithms dependent on accurate inertial sensing become very vulnerable at high running speeds.

Joint torques can also be computed by solving the inverse dynamics problem for all legs in contact with the ground [16]. In biped control, the system is over determined during periods of single-leg ground contact and only moderate tilt and velocity correction can be achieved. Periods of overlapping foot contact result in an underdetermined system and allow for additional constraints on the joint outputs to achieve significant correction. During high-speed running, the coupling of legs during the double support phase presents a challenging logistics problem for the rapid communication of all joint positions for all legs in contact with the ground. This problem is amplified for quadruped and hexapod systems, and becomes impractical for higher order arthropods.

1.2 Legged Robot Control

Some researchers have achieved remarkable mobility in a single mode, and utilizing a single gait, by implementing extracted principles of legged locomotion on systems with significantly reduced DoFs [17–20]. Some of the significant contributions in the field of legged robots are discussed in this section.

1.2.1 Legged Robots on Uneven Terrain

To navigate through natural or uneven terrain, legged systems have been developed which are capable of sensing the terrain in order to plan their steps accordingly [21, 22]. The sensed terrain can be mapped and used to plan a sequence of steps to reach the goal position and also to find the optimal foot placement. Even gait selection could be done using the mapped terrain.

4

This requires the terrain information to be accurate and many systems pre-compute the terrain information to pre-plan each step before execution [23]. Some systems then use reactive behaviors to re-compute and re-plan their steps in real time in case of a false step or failure [24]. Such systems require fast and accurate body state information and use off-board cameras and motion capture systems for proper functioning [21].

RHex [25] is able to achieve remarkable mobility over uneven terrain by utilizing extracted biological principles of legged locomotion with reduced degrees of freedom (DoF) legs. By using legs with passive compliance, RHex is able to navigate through uneven terrain without the need for visual terrain sensing. Many dynamic behaviors have been implemented on the RHex such as running [26], stair climbing [27] and swimming [28]. Like RHex, Whegs [29] series of robots also use reduced DoF legs and combine the advantage of wheels and legs to generate a method of locomotion able to climb obstacles higher than an equivalent wheeled vehicle could climb. The use of systems with reduced DoF have also been adapted by other researchers with good results [17–20]. However, by using reduced degrees of freedom, systems sacrifice maneuverability needed for applications like planetary exploration.

A biologically inspired control mechanism, developed by Goldschmidt et al. [30], tries to generate basic walking behavior in a hexapod robot by using a neural control mechanism. The hexapod robot uses ultrasonic, contact, and infrared sensors which act as input to the reactive neural controller whose outputs drives each joint in the robot.

Lewinger et al. [31] developed a computationally simple intra-leg joint coordination algorithm called SCASM (Sensory Coupled Action Switching Modules) which uses a joint state machine to determine whether each joint should be flexing or extending. Transitions between states were based on local leg feedback loops created using synthesized biological data [32]. SCASM was able to produce basic walking motions on different uneven terrains on a multiple legged platform [33].

5

Other biologically inspired robotic systems make use of compliance in the legs to achieve dynamic and versatile locomotion. StarlETH [34] is a compliant quadruped robot that uses linear compression springs to decouple the motor and gearbox from the joint and is robust against falling impacts. StarlETH requires accurate body state information for locomotion and uses a Microsoft Kinect sensor along with a motion capture system for operation. Since the use of compliance reduces the need to model the terrain, systems like StarlETH are able to perform highly dynamic maneuvers. Even though many significant biologically-inspired robotic systems have been built, missing from the current horizon of legged research on uneven terrain is of implementation of biologically-inspired local leg feedback algorithms.

1.2.2 Robots Using Force Feedback

The Spring-Loaded Inverted Pendulum (SLIP) model derived from studies on animal loco-motion has been used as a basis for a large number of walking robots [2]. Figure 1.2 shows the use and implementation of the SLIP model in robots. The ground reaction forces found in cockroach locomotion are recreated using oscillators and springs to generate a running behavior [35]. The lower panel shows the typical vertical and fore-aft forces experienced during rapid running by each system.

BigDog [37] from Boston Dynamics adapts to uneven terrain by adjusting the footfall placement to control the body posture. By coordinating the kinematics of the legs with their ground reaction forces, BigDog is able to navigate slopes without higher level terrain sensing. The BigDog robot uses approximately 50 sensors [37] including inertial sensors as well as sensors at the joint level for sensing the position, motion and force. Beyond very general principles, not much information about the leg level controller is given. BigDog has been observed using a walking canter and running trot but it is unclear if these two gaits are using similar control algorithms or vastly different approaches. The Legged Squad Support System (LS3) [38] is one of

6
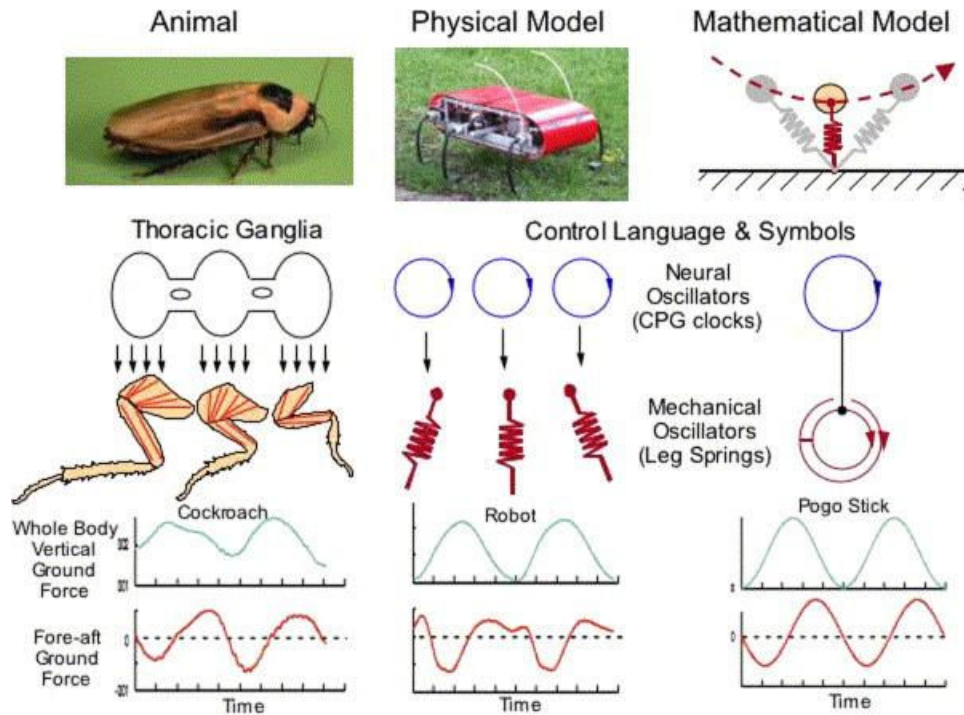
Figure 1.2: The Spring-Loaded Inverted Pendulum (SLIP) as a model for the center-of-mass (COM) dynamics of animals and legged machines. (Taken from [36] - see Appendix B.2)

the newer robots from Boston Dynamics that can walk outside over complex terrain, but not much information about its control algorithm has been published either.

A quadruped walking algorithm developed by Kalakrishnan et al. [39] uses learning algorithms to pre-process an uneven terrain to generate an approximate body path and joint trajectories at each step that are modified in real time to increase robustness. The system is implemented on Boston Dynamics LittleDog quadruped robot [40]. The joint trajectories are adjusted in real time using the measured foot forces and position-based torques previously calculated. Due to its reactive component, the controller is robust towards non-perceived obstacles. However, the system requires an external motion capture system and inertial data as well as force and position sensors.

Emergent gaits based on neurobiological mechanisms have been introduced by Lewinger and Quinn [41]. The de-centralized joint control network proposed by them decouples the joints whose direction of motion is influenced using the sensory information. The sensory information

7

such as joint angle and joint load are used to generate stepping motion and achieve elevator and search reflexes in rough terrain. The joint load gives information about the interaction of the leg with the environment influencing the stepping pattern of the leg as well as other legs in the system. For example, a foot touchdown causes the joint loads for the leg to be changed causing it to retract but also influence other legs that can start to protract and enter the swing phase. The joint load is used only to influence the stepping pattern of the legs. Disadvantage of using such this mechanism is explained in Section 3.4.3.

1.3 Objectives

Extensive research in the area of local leg control needs to be done to find the scope in multi-legged robots. Such research will not only provide an insight to the possibilities a local leg controller can achieve but also the ease at which local leg control can be implemented.

Mimicking the performance of the biological local leg controller is the primary pursuit of this work. An effective local leg controller will enable legged systems to rapidly coordinate high degree of freedom legs by distributing the control effort, as opposed to a single controller coordinating all legs. The afferent communication from all joints, computation of the appropriate response, and efferent communication back to the joints can be burdensome for a single controller, which has led much of the research in legged locomotion toward legs with a reduced number of controllable joints at the expense of dexterity. Achieving more complex maneuvers like jumping, climbing, and swimming require legs with high dimensionality for control and biology provides the means to rapidly coordinate these joints: the local leg controller.

A fully functioning local-leg controller should result in or allow for the following:

1. Distributed local-leg controller: Distributed controller for each leg with no explicit information exchanged between them during walking.

8

2. High leg dimensionality: Each leg should have at least three degrees of freedom.

3. Localized control: Walking pattern only dependent on the local sensed information.

4. Ground reaction forces: Local ground reaction forces are used for effective control.

5. No feedback of body state: No inertial information about the body should be required for leg control.

6. Blind system: No information about ground is pre-programmed or sensed before walking.

7. Limited sensing: No additional sensors should be required for walking while using force feedback.

1.4 Contributions

The main contribution of this research work is the development of a local leg feedback controller and its implementation in experimental hardware. This biologically inspired control strategy enables the application of biological hypothesis to hardware models for testing and enhancement. Advanced maneuvers such as turning and side stepping have also been implemented and tested. Another contribution of this research work is the implementation of multiple gaits to walk on uneven terrain. The implementation of multiple gaits along with maneuvering capabilities on a distributed local-leg controller, to the best knowledge of the author, is the first among its type.

1.5 Organization

Chapter 2 provides a brief background of the biological studies that have been done over the years in terms of animal locomotion. This chapter also presents the main inferences drawn from these studies which inspire this research work.

Chapter 3 describes the current use of position control along with its advantages as well as disadvantages. The possible use of position control in creating a distributed local-leg algorithm is investigated in this chapter along with their possible advantages and disadvantages. This chapter represents the evolution of the local feedback algorithm providing an insight during various stages of development.

Chapter 4 describes the distributed local-leg feedback algorithm, called the Force Threshold-based Position (FTP) controller, developed for walking over uneven terrain. A detailed description of the algorithm along with walking states and their intended operation is provided in this chapter.

Chapter 5 describes the structure of the hexapod, developed in simulation and in hardware, to implement and test the FTP algorithm. This chapter describes the necessary hardware required for the FTP algorithm to work smoothly over uneven terrains.

Chapter 6 provides a detailed list of test results, both in simulation and hardware, showing the working of the FTP algorithm along with its limitations. Analysis of the system in terms of code and hardware is provided along with discussion on the distributed nature of the system.

Chapter 7 describes the modifications done to the FTP algorithm to include turning and side stepping apart from straight walking. The limitations of the current hardware system are presented and a solution working under the limitations is provided along with results in both simulation and hardware.

Chapter 8 summarizes the contributions of this work and future research topics are presented.

10

CHAPTER 2: BACKGROUND RESEARCH[1]

2.1   Introduction

Biological studies of animal and human behavior have often contributed to the field of legged robotics. Models drawn from animal or human behavior and movement have been well studied and used as a basis for creating control algorithms for mechanical devices.

2.2   Biological Studies

Biologists comparing legged animals with differing morphology have observed general force patterns during stance while animals walk, run, jump and climb [45–48]. Biologists have also observed that legged animals employ whole-body dynamics during locomotion in which each leg produces a similar ground force pattern that sums up to produce the whole-body pattern [35, 49]. Some of the studies influencing this research work are listed in this chapter.

2.2.1   Ground Reaction Forces

Full et al. [50] measured the three dimensional ground reaction forces produced by individual legs of the cockroach while running. Full et al. found that vertical ground reaction forces were similar for each leg but found differences in lateral and fore-aft forces between fore, middle and

---

[1]Portions of these results have been adapted from previously published publications {[42], [43], [44]}.

11

hind legs. Similar force patterns were also found by Goldman et al. [35] while recording forces of vertically climbing cockroaches and geckos (Fig. 2.1), and by Cruse [51] for a walking stick insect. Even though the magnitude of force recorded in these experiments was different and dependent on the morphology and locomotion of the animal, the force patterns were similar. The magnitude of the force was dependent on the weight of the animal. Figure 2.2 shows the general template for vertical ground reaction force. At each step, a vertical ground reaction force greater than the body weight of the animal is produced by the active legs during walking.
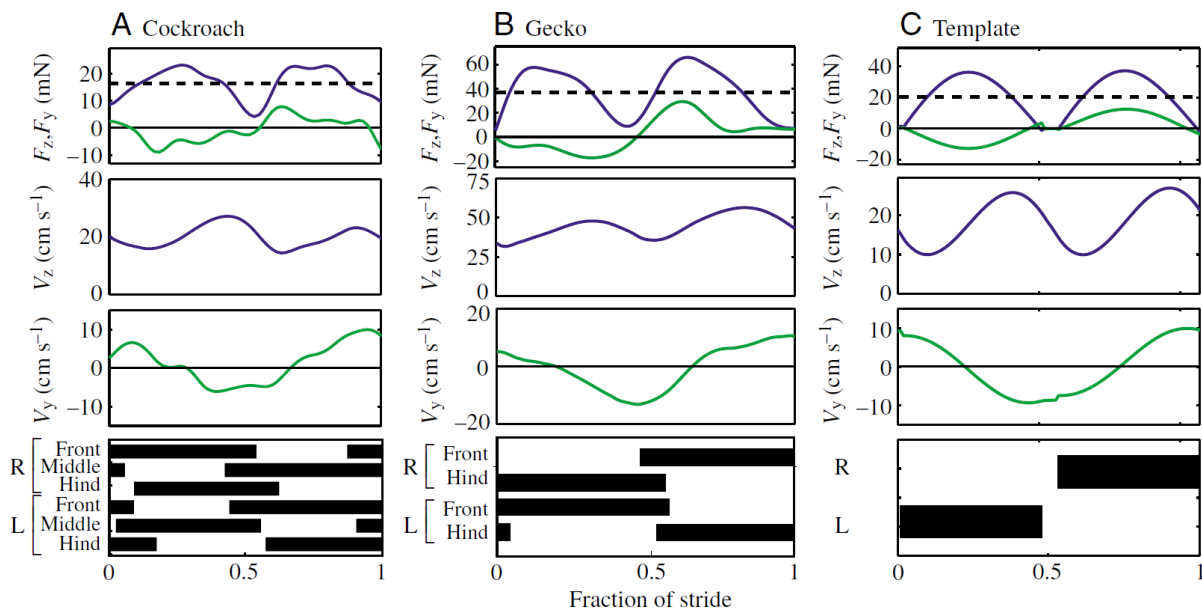
Figure 2.1: Fore-aft (blue) and lateral (green) ground reaction forces during walking for (a) a cockroach, (b) a gecko and (c) the spring-mass model template. Broken lines indicate body weight. Black bars represent stance period and white spaces the swing period. (Taken from [35] - see Appendix B.1)

For a distributed local-leg controller to work, each leg will have to produce the required force to support the body. Ground reaction force templates (similar to one in Fig. 2.2) will be used in this research to make sure appropriate foot forces are produced by each leg to support the body weight.
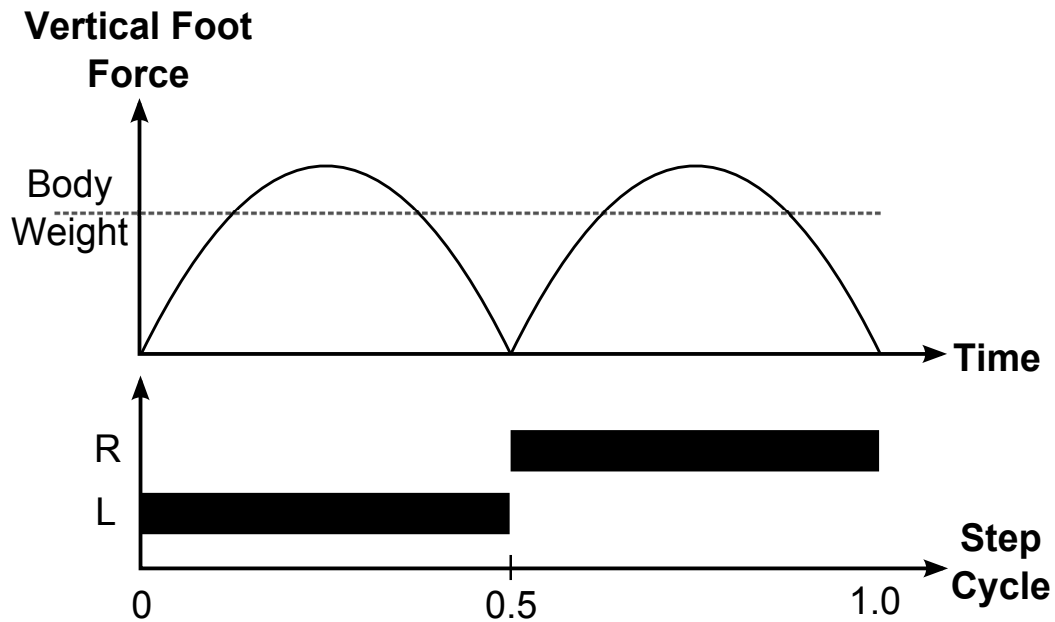
Figure 2.2: A spring-mass model template for vertical ground reaction force during a typical running step. The vertical foot forces during walking have a much less predictable shape because of the overlapping ground contacts and numerous stepping patterns achievable. Dashed line indicates body weight of the animal. The black bar represents the stance period and white space the swing period. (Adapted from [42])

2.2.2 Local Sensing

Insect and mammalian legs use load measuring sense organs. Cockroach legs have sense organs called *Campaniform Sensilla* that act as a strain gauge that detect the load on the leg through strains in the exoskeleton [52]. Research has found the presence of force feedback loops in the local control circuits of insect and mammalian legs which react rapidly to changes in load. Positive force feedback has been found to be an important component contributing to load compensation during sudden changes in the load due to instability or oscillations in the body [53].

Sensors measuring the foot forces, equivalent to the load measuring sense organs, will be used in this research as force feedback to make sure appropriate force is being produced by each leg.

13

2.2.3 Leg Coordination

Work by Bender et al. [54] showed differences in leg coordination between the cockroach alternating tripod gait when moving at relatively slow speed versus higher speed running. It was hypothesized that the triggers for elevation and depression of the leg at low speed are largely dictated by the sensory reflexes in the local leg networks. As these controllers have no direct interaction with each other, it is not surprising that the resultant leg phasing is not strictly synchronized. The tightly coupled leg phasing observed at high speeds is potentially the result of a higher level pattern-generated circuit.

This research is targeted towards fast walking and therefore, tightly coupled leg phasing is used. Tightly coupled leg phasing between different legs can be generated without communication by either using a global clock or by using a start signal. Once a start signal is provided to all legs, each leg can keep track of their walking phases.

2.2.4 Leg Coupling

Studies done by Cruse et al. [55, 56] on stick insects suggested that each individual leg acts as an independent height controller for the body on uneven surfaces. The study also showed that no neural couplings between the legs of the stick insect needs to be assumed to exist and only mechanical coupling between legs is sufficient to explain the results found in the study. Other studies [55, 56] support the idea of creating a distributed local controller for walking.

2.2.5 Control of Body Height

Based on the experimental results on a stick insect walking over obstacles, one study [57] concluded that each leg of the stick insect acts as an elastic system which controls the distance

14

between body and surface independent of the other legs. This statement was based on indirect evidence as the data produced by the study could only be explained if each leg was assumed as an independent height controller. This elastic system could either be represented by muscle elasticity or a resistance reflex system.
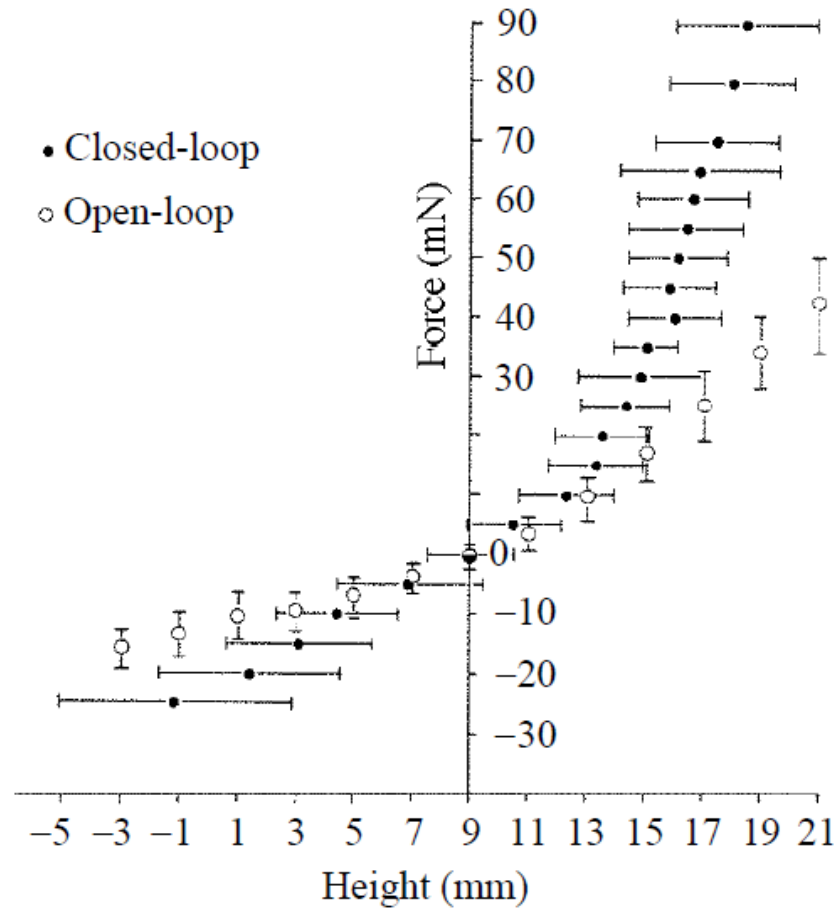
Figure 2.3: The force-body height characteristic for a stick insect during open-loop system (○) experiment and closed-loop system (●) experiment. In open-loop results, the independent variable is height and for closed-loop results, the independent variable is load. (Taken from [58] - see Appendix B.1)

Another study by Cruse et al. [58] confirmed the results found in the previous study [57]. Cruse et al. found that as the distance between the body of the stick insect and the ground is

changed, each leg tried to pull or push on the ground to achieve a certain leg length. During the study, the stick insect was attached to a fixed plate with its legs on a wheel platform. In one experiment, the distance between the stick insect and the wheel platform was fixed and force on the wheel platform by the leg was recorded (open-loop experiment) and in another, the wheel platform was not fixed and the stick insect was allowed to select the distance between its body and the platform (closed-loop experiment). Figure 2.3 shows the results from the study. Cruse et al. found a specific distance where the force was zero called the 'zero-force distance'. The study found as the distance between the stick insect body and platform became higher (than the zero-force distance), the leg produced a force that tried to pull the platform towards its body (to achieve zero-force distance) with a force proportional to the distance and, conversely, as the distance became smaller, the legs produced a force that pushed the wheel away from the body.

The idea of an individual leg acting as an independent height controller for the body can be used by a local-leg controller to control the body height of the robot. By controlling the length of each leg, the 'zero-force distance' or the body height can be achieved. Even though the biological reasons for selecting a specific 'zero-force distance' by the stick insect is not known, a body height for a robot can be chosen dependent on other criteria such as the ability to walk over various kinds of terrains.

2.2.6 Body Posture

Cruse [57] provided a study which tried to find the body position of a stick insect when walking on uneven surfaces. The body of the stick insect is divided in to three thoracical segments (prothoracic coxae, mesothoracic coxae, and metathoracic coxae) which are at different heights from the ground. Figure 2.4 shows the schematic of a stick insect along with the three height of the three thoracic segments. The height of these three thoracic segments was measured in this study as the stick insect walked over various terrains.

16
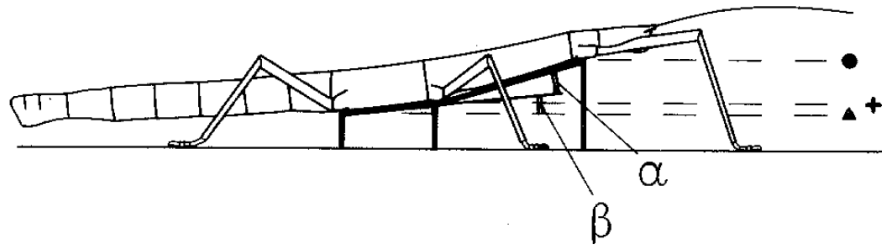
Figure 2.4: Schematic presentation of the stick insect showing heights of the coxae of the three thoracical segments (prothoracic coxae [●], mesothoracic coxae [+], and metathoracic coxae [▲]) and body angles (α and β) with respect to the horizontal baseline. (Taken from [57] - see Appendix B.3)

Figure 2.5 shows the heights of the coxae of the three thoracical segments as the stick insect walks over three separate terrains (a step up, a step down and an obstacle). Cruse found that each pair of legs of one segment tried to maintain a definite height for its segment. Cruse found that as when the terrain changes were smaller (shown in Fig. 2.5), the body angles (α and β) had positive angles and there was little change in the body posture. As can be seen in Fig. 2.5, the three thoracical segments heights return back to their original height after the insect walks over the change in terrain. However, when terrain change is larger, the body angles and thoracical segments heights change to walk over the terrain.

Similar results were found on cockroaches by Watson et al. [59]. The cockroach was able to scale smaller obstacles with little change in running movements and body posture while higher obstacles required altered gaits, leg positions and body posture. Body adjustments necessary for climbing over higher obstacles were done before approaching the obstacle. The cockroach can assess the height of the obstacle and change its body posture to approximately match the change in height to climb over it.

Since insects are able to scale moderate terrain changes without the need for posture control, adding a body joint is not considered in this research.

17
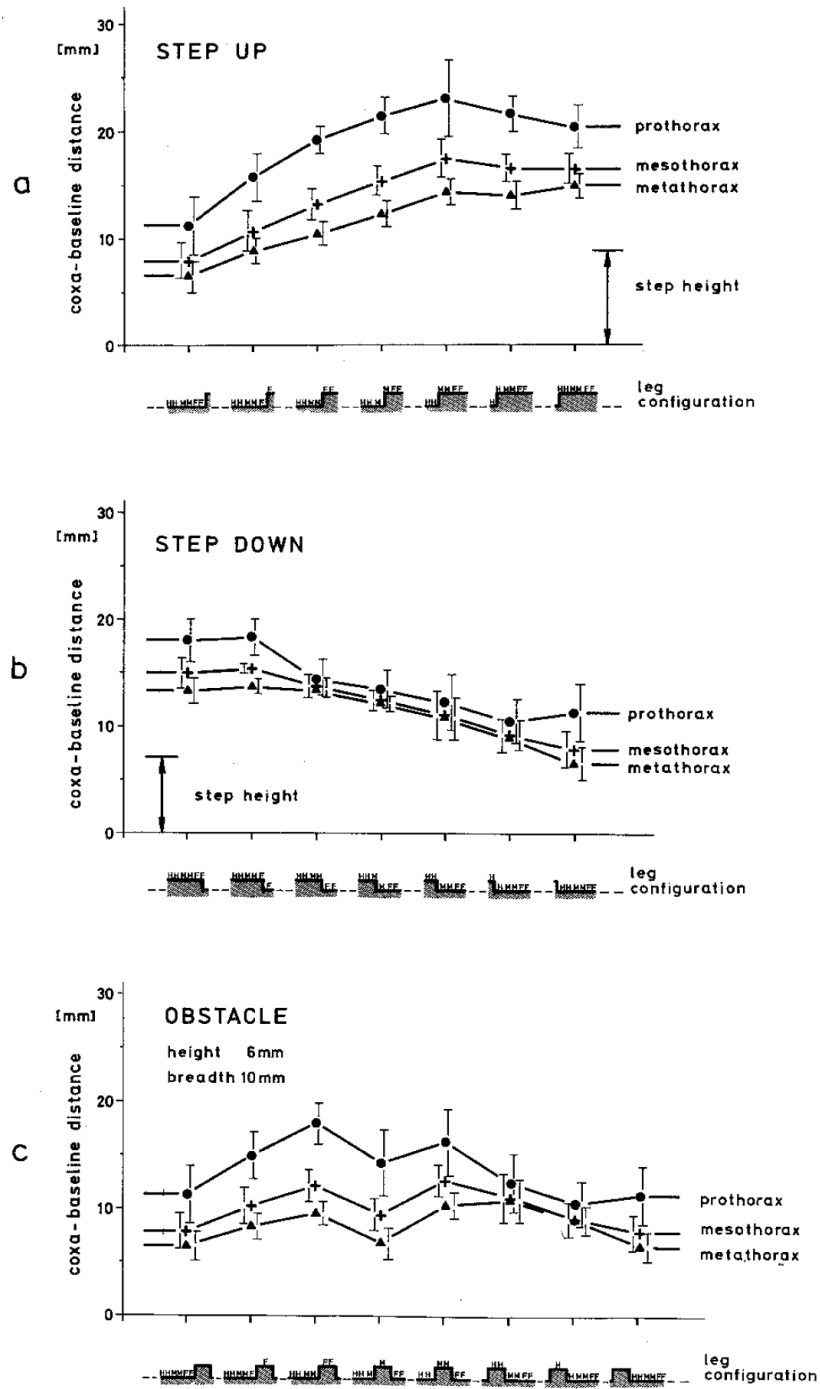
Figure 2.5: The heights of the coxae of the three thoracical segments when the insect walks over (a) a step up, (b) a step down, and (c) an obstacle. (Taken from [57] - see Appendix B.3)

18

2.2.7 Terrain Sensing

Judging by the relatively poor performance of the legs when rapidly walking over uneven terrain [60], it seems clear that the legs do not have an accurate model of the ground and the interaction from the supervisory controller is likely nothing more than a binary cue to initiate and conclude the stance phase. The local leg controller is then responsible for seeking and interacting appropriately with the ground in a way that propels the body without destabilizing the body tilt axes. And because of the rapid stride period when running, it is also unclear what role, if any, inertial sensing can have in a single step [61].

Since this research is targeted towards fast walking, no sensing of the terrain or a priori terrain information will be used for walking. The research will focus towards creating a blind walking behavior using only local sensing.

2.3 Summary

This chapter gave a very brief introduction to the biological studies trying to find the underlying control used by animals for walking on uneven terrain. Even though not every scenario and environmental stimulus has been studied, information is present which can provide a limited understanding of animal locomotion. Using some basic information, this research work tries to create a local-leg control system which can provide a better understanding of the local-leg control and shed more light in understanding animal locomotion.

3.1   Introduction

For many years, position control has been used to control walking systems [64–67]. Once joint angles are chosen for the leg touchdown position and the desired body motion during stance is known, the desired joint angles throughout the stance phase can be computed kinematically. This chapter explains the use of position control along with its potential use in distributed local-leg control algorithm.
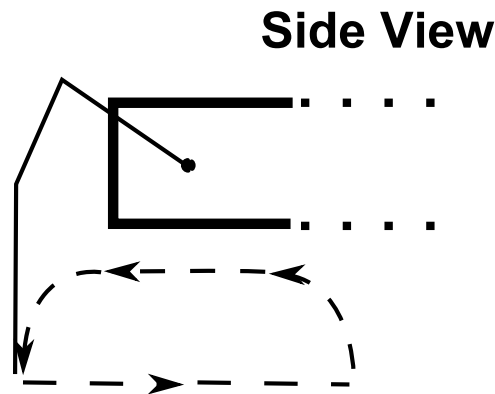
Figure 3.1: Controlling a single leg using a position controller.

Figure 3.1 shows a typical example of a leg trajectory under position control. The dotted line with arrows shows the desired trajectory and the direction of foot with respect to the body. The leg tries to achieve this trajectory by comparing the current position of the leg with the desired position. A proportional controller generates the foot force to track the desired trajectory by

[1]Portions of these results have been adapted from previously published publications {[42], [62], [63]}.

$$f_{position} = k_P \cdot (p_{desired} - p_{measured}).$$ (3.1)

The proportional gain, k_p, is tuned to generate smooth error correction. In the hexapod alternating tripod gait, three legs cycle in phase together to form a tripod of support when in stance phase. Position control of each leg is executed independently, without knowledge of the other leg states, or even if those legs have achieved ground contact. During periods when all six legs are on the ground, each leg continues to execute its desired position trajectory and has no need for interleg sensing or communication. The vertical position is shown here, but $f_{position}$ is a 3-dimensional vector representing the desired force in three directions.

3.2 Advantages of Position Control

A strength of position control is the inherent motion control and tilt stability that arise from well-designed trajectories. Because these trajectories are often kinematically-computed from stable and smooth body motions on well-modeled terrain, legs moving through their desired position can result in smooth body motions without the use of vestibular sensing of the body or information about the terrain. On complex terrain when only feed-forward trajectories dictate the desired foot position, the interaction of the foot with the ground becomes unpredictable causing sluggish forward movement and, in some cases, no forward motion is possible.

3.3 Position Control on Uneven Terrain

Figure 3.2 shows the advantages and disadvantages of using position control. While position control works well on a flat terrain (as seen in Fig. 3.2a), the controller becomes unstable on uneven or natural terrain. Figure 3.2b shows the situation when a pure position controller steps on

21

Top View

Right
Side

Left
Side

━━━━━ **Left Tripod (Stance Phase)**

- - - - **Right Tripod (Swing Phase)**

Side View

← Direction of
Movement

(a): Flat terrain

**Missed Ground
Contact**

(b): Terrain - Step up
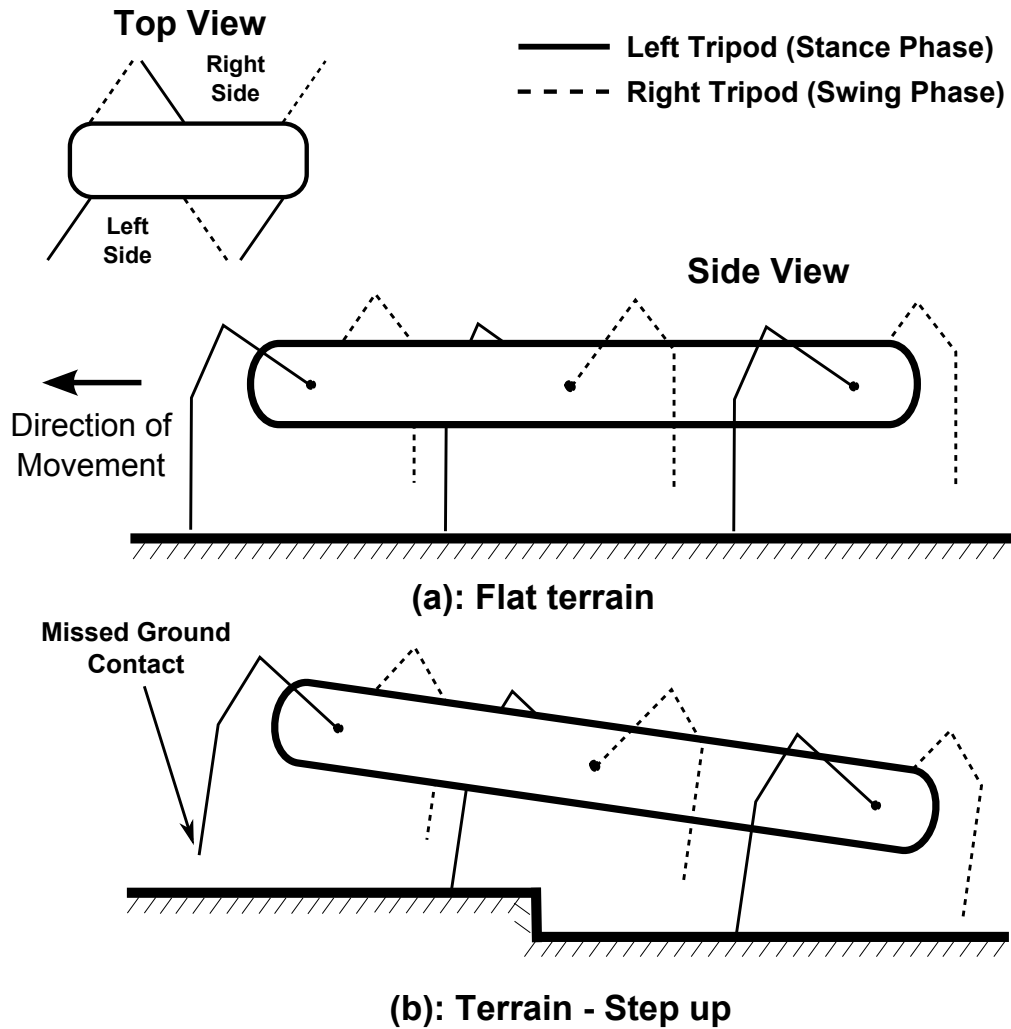
Figure 3.2: Advantages and disadvantages of using a position controller.

a terrain height which is higher than the desired level. This causes body height to increase and may cause tilt.

One way to alleviate this problem is to sense the whole terrain before walking and create a trajectory based on the sensed terrain. This approach needs the terrain to be pre-processed using a number of sensors so that a reliable trajectory can be generated before the robot can walk. However, even a reliable trajectory generation may not lead to successful walking due to some perturbations or slips during walking. Therefore, a reactive component is required, along with a separate set of

22

sensors, to update the trajectory when an anomaly happens. Such an approach is usually costly and complex and is used to generate walking behaviors on highly uneven terrain.

Another way is to change the walking pattern at each step based on the terrain height sensed by each leg using local sensors. This approach needs only local sensor information like ground forces to effectively generate a walking pattern in real time. This approach does not need any pre-processing or information about the terrain leading to a faster system more responsive to the terrain. This approach is usually used on relatively moderate terrain.

3.4   Using Force with Position Control

Ground reaction force profile patterns described by biological research can be used in conjunction with position control to alleviate the problems of position control while walking on uneven terrain. Following section describes some of the ways in which these force profiles can be used.

3.4.1   Hybrid Force Position (HFP) Control

One way to create the required force profile for each leg is to compute the torque which would create the necessary force profile needed for each leg. The vertical ground reaction force template like the one shown in Fig. 2.2 can be used as the desired vertical force needed at each step for walking. The Hybrid Force Position (HFP) controller tries to achieve the force profile at each step. Figure 3.3 shows the behavior as the HFP controller walks on flat and uneven terrain. The top subplot of Fig. 3.3 shows the expected vertical ground reaction forces for a single leg during two steps. When the ground is flat, the foot touchdown happens at the expected time and desired force profile can be created by the HFP controller. However, if the foot touchdown happens later due to lower terrain or step, the foot forces generated using the HFP controller will not be sufficient to lift

23

the body (Thick dotted line in Fig. 2.2). This is because the HFP controller tries to eliminate the force error at each step. Unless the step period for each step is made variable and dependent on when the touchdown happens, matching the force profile using the HFP control would be difficult.
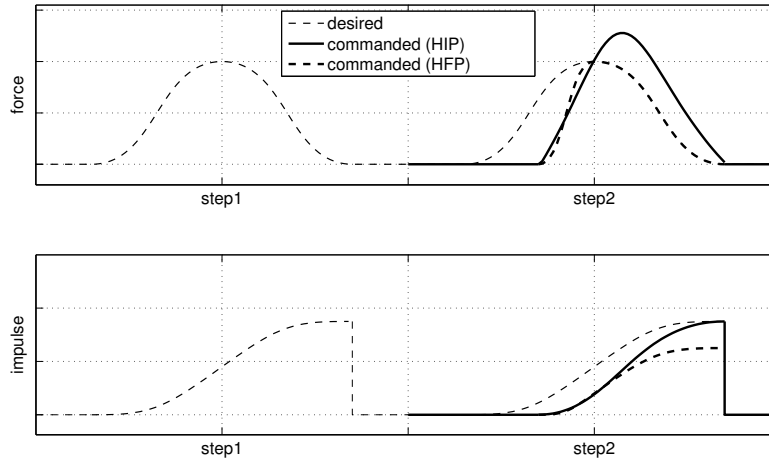
Figure 3.3: Expected ground reaction forces (and equivalent impulse) when walking on a flat terrain (step 1) and a lower terrain (step 2) using separate controllers. (Adapted from [63])

3.4.2 Hybrid Impulse Position (HIP) Control

The vertical force trajectory can also be represented as an impulse, drawn in the bottom subplot of Fig. 3.3. The impulse, or area under the force curve, is used as the reference trajectory for the HIP controller. This is different from the HPF controller that uses force error directly. Step 2 in Fig. 3.3 illustrates this difference. Ground contact is delayed likely due to an unexpected drop in the terrain. After contact, the commanded foot force from the impulse component to the HIP controller is computed by

$$f_{impulse} = k_I \cdot (I_{desired} - I_{measured})/\Delta t. \tag{3.2}$$

24

The measured impulse immediately after contact is zero since the leg has not applied any forces on the ground. The proportional gain, k_I, is chosen to generate smooth error correction. Ultimately, the commanded force increases above the desired force profile in order to eliminate the error on the impulse curve.

If the ground is not detected when expected, the impulse controller will generate forces at the foot that seek the ground. Without these forces, the foot may not contact the ground at all. The HIP controller, however, goes further by requiring legs that contact the ground late to still generate the desired impulse. Vertical impulse is responsible for lifting the body, and a less-than-desired impulse will result in inadequate body height for walking over rough terrain.

Once the position and impulse forces have been computed, $f_{position}$ and $f_{impulse}$ respectively, the following equations are used to determine the joint outputs τ_{out}:

$$f_{out} = \alpha_1 f_{impulse} + \alpha_2 f_{position}, \text{ and then} \tag{3.3}$$

$$\tau_{out} = J^T f_{out}. \tag{3.4}$$

where

$$
\begin{aligned}
\tau_{out} &= \text{the joint torques to be delivered,} \\
J^T &= \text{the transpose of the single leg Jacobian,} \\
\alpha_1, \alpha_2 &= \text{hybrid weights,} \\
f_{impulse} &= \text{foot force that satisfies the impulse controller, and} \\
f_{position} &= \text{foot force that satisfies the position controller.}
\end{aligned}
$$

$$\tag{3.5}$$

25

After computing the output leg force, the measured impulse can be updated for use in the impulse component of the HIP controller. This is done by

$$\text{if contact,} \qquad I_{measured}[h+1] = I_{measured}[h] + f_{out}\Delta t$$

$$\text{else} \qquad I_{measured}[h+1] = I_{measured}[h] \qquad\qquad (3.6)$$

where h is the index of the current control step. As shown in Fig. 3.3, the measured and desired impulses are reset at the end of each stance phase.

The HIP controller is able to achieve ground contact at each step and is able to navigate though some uneven terrain. However, the controller is very dependent on the force profile used. Since exact force profile patterns cannot be generated for every possible scenario, approximate force profile patterns have to be used. This may cause instability when a wrong force profile is used. Even if a large number of force profiles for different terrains and gaits are provided, the controller might still be ineffective to an unknown terrain.

3.4.3 Force Feedback Control

Instead of computing the force profile at each step, force feedback can be used by the position controller to control the trajectory of the leg. This means instead of creating a particular force, the position of the leg is changed based on the force being generated. In force feedback control, the leg is depressed until the ground contact is detected by reading the foot forces. Once ground contact occurs, the leg depression value is used as desired position throughout the stride period of that step. Therefore, at each step the desired leg depression changes based on the terrain. This makes the controller independent of the force profile pattern being used and is able to navigate

26

more terrains, including unknown ones, using force feedback. The behavior of the force feedback control can be shown in Fig. 3.4.
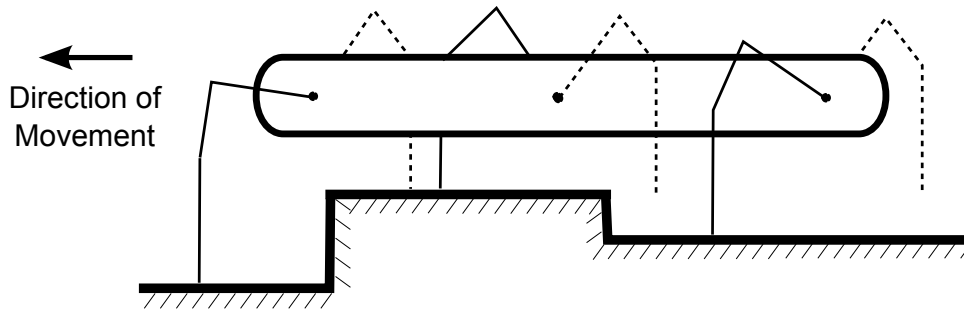
Figure 3.4: Sensing uneven terrain using force feedback.

(a): Walking down a step
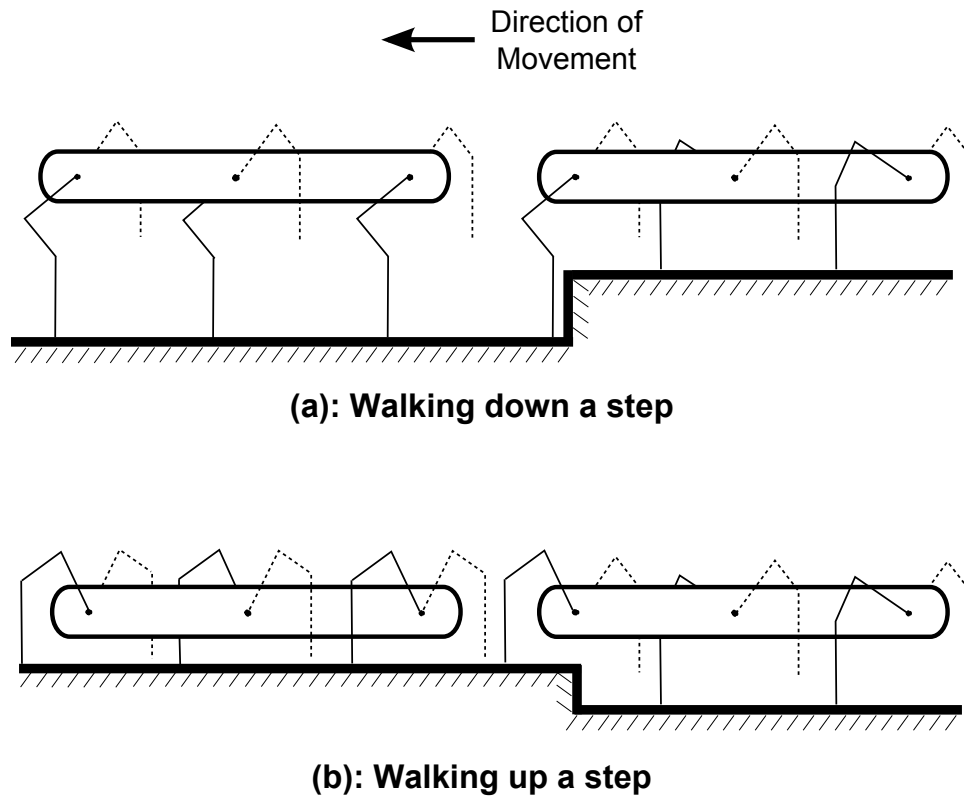
(b): Walking up a step

Figure 3.5: Force feedback control: Effect on body height walking up and down a step.

Figure 3.4 shows the hexapod body walking on uneven terrain using the force feedback controller. This, however, creates a problem when walking on a changing terrain like a slope or

27

(a): Walking down a slope
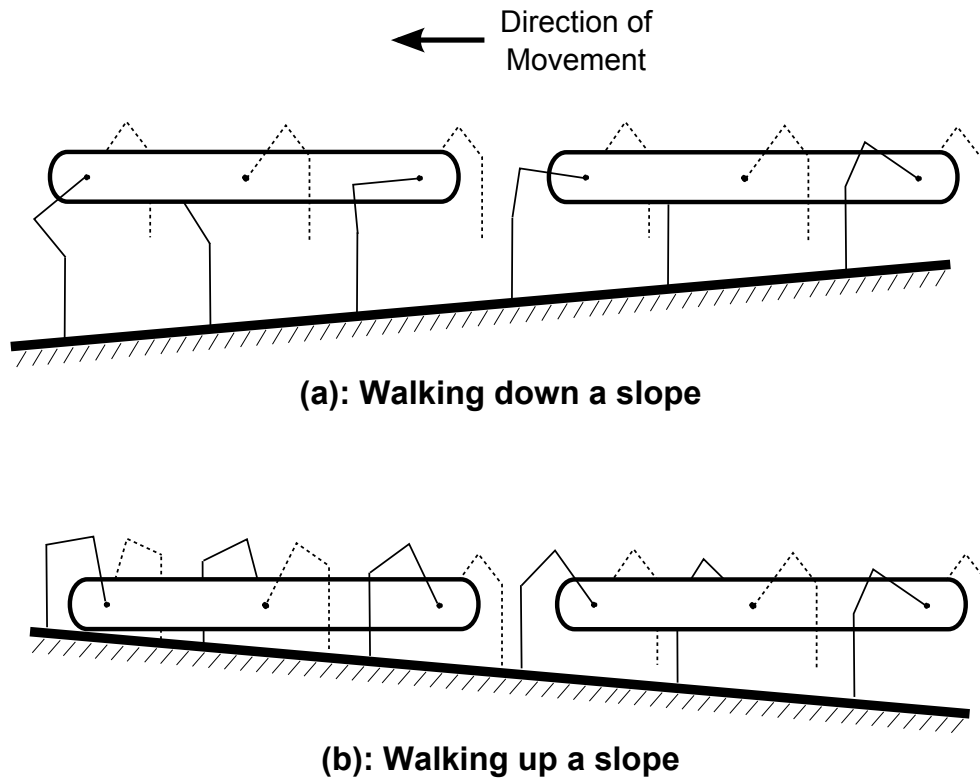
(b): Walking up a slope

Figure 3.6: Force feedback control: Effect on body height walking up and down a slope.

a series of steps. Since the legs constantly change their trajectory based on the ground contact and due to the nature of local leg control, the overall body height of the hexapod changes with respect to the terrain. However, the force feedback controller has no mechanism such that the original walking height of the hexapod can be restored or maintained. This can be clearly seen in Fig. 3.5. The figure shows the hexapod walking down and up a step. In subplot (a), the hexapod leg reaches down to make ground contact and hold the body. Before the first tripod can complete the step, the other tripod reaches down and makes ground contact. This means the body height keeps increasing during the step and once the step is cleared, the hexapod will continue walking with the same increased body height. In case of a series of steps, the body height of the hexapod will continue to rise until the legs reach their physical limits. The opposite is true for the hexapod going up a step. The body height will be decreased and it will stay decreased. While walking up

28

a series of steps, the body height will continue to decrease until the body is being dragged on the ground. The same thing happens when the hexapod goes down and up an incline (Fig. 3.6).

3.5 Summary

This chapter gave a brief description of some of the controllers that use foot forces in conjunction with the position controller. Since ground reaction forces are dependent on the terrain the robot is navigating, trying to produce a specific foot force on a leg can only be beneficial if the ground reaction force patterns are known before walking. Using such a controller on unknown terrains can make the system unstable. Force feedback control is a good idea for control since it can potentially work on unknown terrains and widely used by legged animals. However, independent terrain sensing by each leg can result in the height of the robot becoming dependent on the terrain. Independent height control, similar to one seen in stick insects (Section 6.2.2), has to be implemented. The Force Threshold-based Position (FTP) controller, described in Chapter 4, combines force feedback with independent body control through individual legs to create a robust walking controller able to navigate uneven terrains.

CHAPTER 4: FORCE THRESHOLD-BASED POSITION (FTP) CONTROL[1]

4.1   Introduction

The Force Threshold-based Position (FTP) controller attempts to create necessary ground reaction forces for each leg of the system such that the leg can propel and stabilize the body during every step. This is done best when the leg achieves ground contact during each step regardless of the terrain. However, as discussed in the previous chapter, trying to assign and achieve an exact vertical force pattern for all possible scenarios during walking is nearly impossible. Also, replicating one specific force pattern for all scenarios can lead the system to become unstable in challenging cases. Therefore, the FTP controller tries to achieve at least a minimum force magnitude at each step using specific force thresholds to control the position of each leg. This not only provides a stable walking pattern on flat terrain but also works very well on irregular terrains.

4.2   Force Thresholds

Even though every animal generates foot forces relative to its body weight, the foot force generated by each leg is different and dependent on the gait and number of legs on the ground. Figure 4.1 shows a force template for the vertical ground reaction force for two steps. By assigning force thresholds to the vertical ground reaction force template, we can distinguish the amount of support provided by the leg based on the ground reaction force. A leg is described to be in *full*

---

[1]Portions of these results have been adapted from previously published publications {[42], [43], [44]}.

support (FS) of the body when the leg is supporting a significant load. A leg is in *no support* (NS) when small or no load is being supported, which will typically be perceived as a leg not in contact with the ground. The leg is in the *weak support* (WS) phase when the leg is in contact with the ground but not supporting much force. The low (F_L) and high (F_H) thresholds are used by the FTP controller to distinguish these phases; and are hand tuned. Currently, no generalized procedure has been developed to find optimum thresholds for different morphologies based just on their body weight and walking gait.
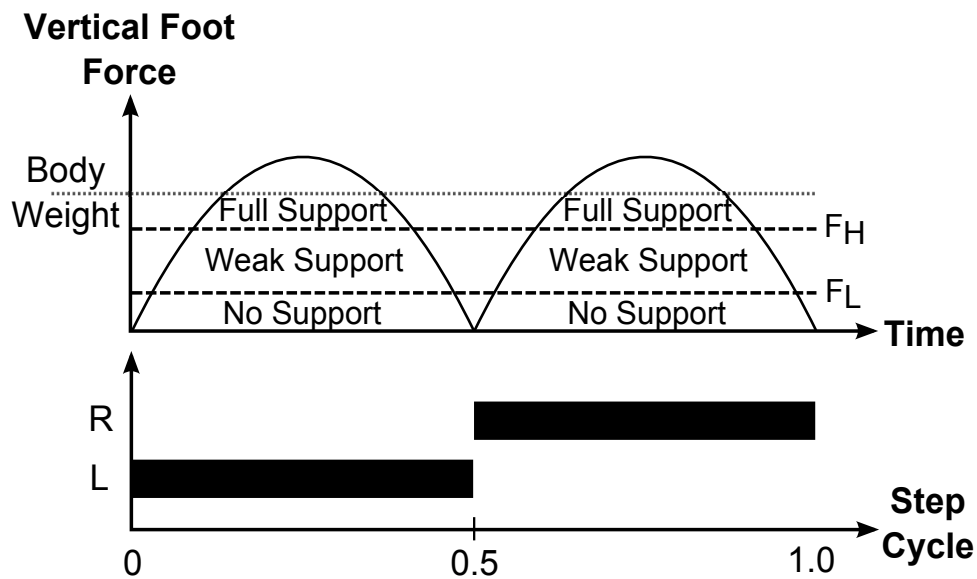
Figure 4.1: Vertical ground reaction force template along with force thresholds during a typical running step. The vertical foot forces during walking have a much less predictable shape because of the overlapping ground contacts and numerous stepping patterns achievable. Dashed line indicates body weight. The black bar represents the stance period and white space the flight period. (Adapted from [42])

For a walking behavior to work properly on uneven terrain, the trajectory of the leg should be adjusted based on the terrain height. If the ground is lower than expected, the controller must depress the foot to reach the ground and maintain the foot depression to support the body. If the ground is higher than expected, the controller must attenuate the foot depression so as not to lift the body higher than desired. The force thresholds can be used to decide if the foot should be

31

elevated or depressed and at what rate based on the ground reaction forces as well as the current foot position. Using this approach, the stance phase can be divided into a series of states that dictate foot depression and elevation. Even though force thresholds are used, the controller tries to achieve the level of support required by each leg and not the actual forces and, the FTP controller therefore, is able to produce ground reaction forces dependent on the terrain.

4.3   Maintaining Body Height

As with stick insects, individual legs can be used to maintain the body height independently. This means that each leg or a pair of legs should have a desired foot depression which, when attained by all legs, would result in achieving the desired body height. Since for effective walking, ground contact has to be made at each step; each leg has to first produce ground contact after which based on the ground reaction forces the foot position can be either elevated or depressed to effectively decrease or increase the body height respectively. The notion of the zero-force height explained in Section 6.2.2 can now be replaced by preferred foot depression for an individual leg resulting in similar behavior displayed by the stick insect. The preferred foot depression is currently a user selected number not based on an optimal solution.

4.4   FTP States

The inputs to the FTP algorithm are the current desired foot depression and measured foot force. The output is a desired depression or elevation rate, which may also be zero. The output can be further categorized into either a fast or a slow rate, narrowing the output states into one of the following five states; fast depress, fast elevate, slow depress, slow elevate and maintain position. In addition to depressing and elevating the foot in response to force feedback, the FTP controller attempts to stabilize the height of the body by moving the foot to a preferred foot depression that

32

can be set by the operator. Loss of body support should be avoided during stance because it may result in unwanted body tilt that is difficult to overcome. Foot depression and elevation is coupled with foot force and body support as described below:

1. While a foot is on the ground, further depressing this foot with respect to the body temporarily results in larger foot forces and greater support of the body. Depressing the foot too much may tilt the body away from this leg and eventually cause the foot forces to decrease.

2. Elevating a foot that is in contact with the ground temporarily reduces foot forces and body support, although continued elevation may cause the body to tilt toward this leg and result in increased forces.

By example, if the foot depresses past the preferred level as it seeks the terrain, elevating the foot back toward the preferred level immediately after contact may cause the leg to lose contact with the ground and the body to stumble. Care must be taken to elevate the foot appropriately to avoid this outcome.

The input space for the FTP algorithm is divided into four states, shown in Fig. 4.2. The F_L and F_H thresholds correspond to the level of support currently provided by the leg (Fig. 4.1), and the preferred foot depression, D_{PRE}, is the level at which the body walks at a user-selected height. If all stance legs achieve D_{PRE}, the body will be level on the pitch and roll axes, as is true with a simple position controller. The foot force generated by the leg at the previous step is compared with thresholds and based on the current foot depression, the foot is either depressed or elevated. The slow/fast foot elevation or depression is represented in terms of change from the current foot position. The rates are Δ_{FD} (fast depress), Δ_{SD} (slow depress), and Δ_{SE} (slow elevate). Δ_{FE} (fast elevate) is used during swing phase of walking and as the FTP controller is used in stance phase only, this rate is not seen during the working of the FTP algorithm. The states shown in Fig. 4.2 are explained below:

33
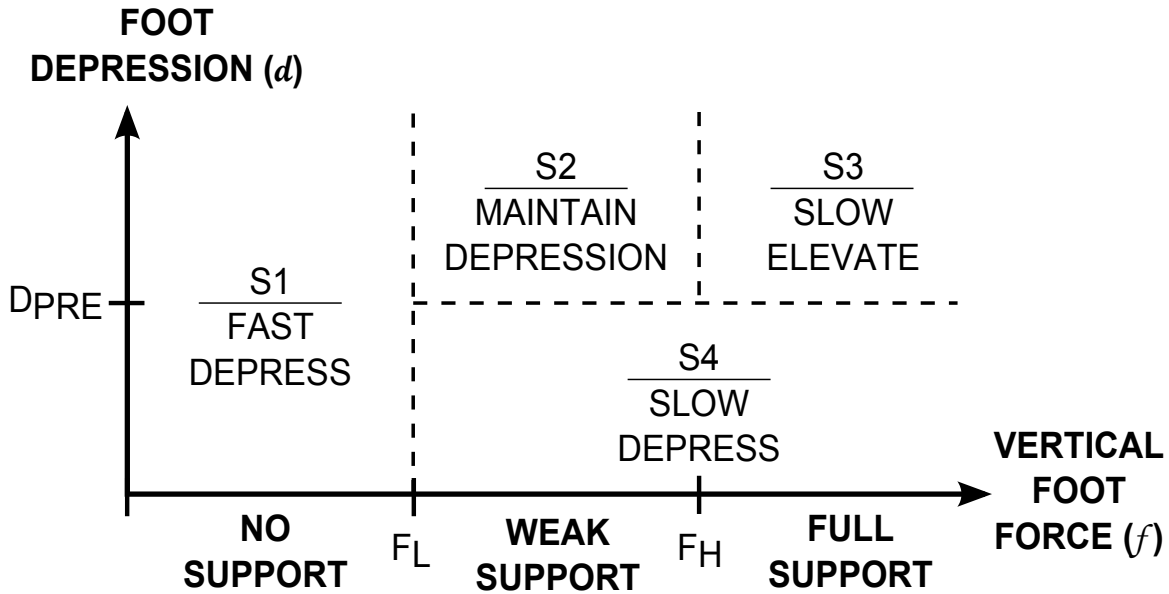
Figure 4.2: Force Threshold-based Position (FTP) controller states. During stance, the foot is either commanded to depress further or elevate upwards based on the foot force feedback and current foot depression. (Adapted from [42])

S1 The leg enters $S1$ at the start of the stance phase, and the foot is directed to fast depress toward the terrain at a constant rate Δ_{FD} until ground contact is made. If ground contact is lost at any point during the stance phase, which is perceived by the foot force decreasing below F_L, the leg re-enters state $S1$ and is depressed rapidly in order to re-engage the terrain.

S2 In this state, the foot depression level is directed to remain unchanged because the foot has made ground contact and is depressed further than preferred, but the leg is weakly supporting the body. Elevating the foot toward the preferred level while only weakly supporting the body may cause the leg to lift off the ground and the body to tilt inappropriately.

S3 When the leg is in full support of the body, the foot can be elevated slowly toward D_{PRE} if needed. The rate of elevation (Δ_{SE}) must be limited such that the algorithm can rapidly stop this elevation when the foot force drops below F_H and the leg is in danger of losing support of the body.

34

S4 In this state, the foot is depressed slowly toward D_{PRE} at a constant rate Δ_{SD}. If the leg is in weak support, the depression should increase the foot force and result in greater support of the body as desired.

The FTP states shown in Fig. 4.2 can also be briefly summarized below.

Table 4.1: Explanation of the FTP states.

State	Condition	Explanation
$S1$	$f < F_L$	No ground contact Depress foot at a high constant rate (Δ_{FD})
$S2$	$(f > F_L) \wedge$ $(f < F_H) \wedge$ $(d > D_{PRE})$	Foot too far depressed but not supporting body Maintain foot depression
$S3$	$(f > F_H) \wedge$ $(d > D_{PRE})$	Foot too far depressed and fully supporting body Elevate foot at a slow constant rate (Δ_{SE})
$S4$	$(f > F_L) \wedge$ $(d < D_{PRE})$	Foot too far elevated and supporting body Depress foot at a slow constant rate (Δ_{SD})

It should be noted that the FTP algorithm works best when transition from one state to another occurs immediately after the foot force crosses the threshold. For example, if the leg in fast depress is not able to react to the change in the force, the body will rise too high and cause unwanted tilt. This requires the foot forces to be read very quickly. The local leg controller allows for rapid responsiveness as the number of sensors it has to read and the number of motors to communicate the desired position is smaller compared to a central controller. A central controller has to read all sensors of all legs before it can communicate the desired to the motors.

The FTP states and the relationship between them can be further elaborated using a finite state machine diagram shown in Fig. 4.3. At every stance phase, the leg enters the fast depress state and based on the interaction of the leg with the terrain, the leg changes state. Please note that even though the vertical foot force during state $S1$ can suddenly drop from being greater than F_H to being less than F_L in a single time step, it is assumed that the force will decrease slowly causing the state to go from $S3$ to $S2$ and then $S1$. Therefore, there is no transition shown between $S3$ and $S1$.

35

Also, in state $S2$ the foot depression is maintained and not changed. Due to this, the state $S2$ can transition either to $S1$ or $S3$ but not $S4$ since the leg can enter that state only if the foot depression goes below the preferred foot depression D_{PRE}.
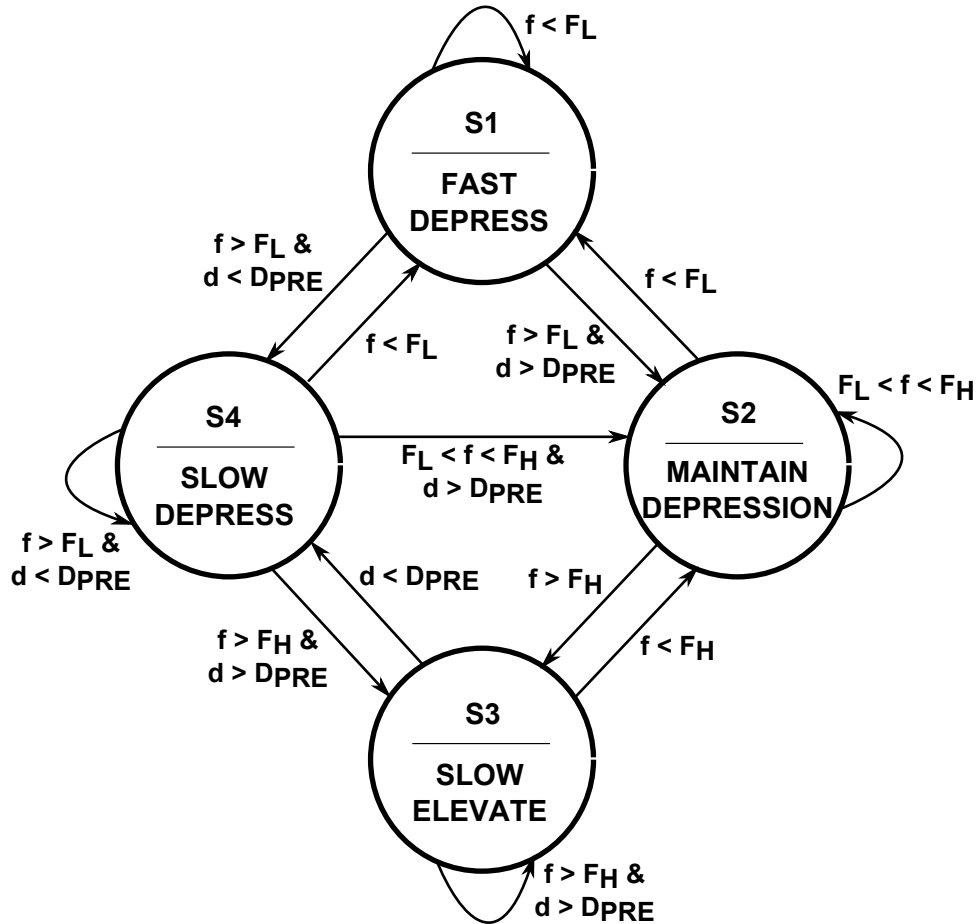
Figure 4.3: Finite state machine (FSM) diagram for the FTP controller states.

4.5 FTP Walking Behavior

Figure 4.4 shows the cyclic behavior used by the FTP algorithm for walking on flat terrain. Part (a) of the figure shows the position of the foot with respect to the leg attachment to the body in the X and Z plane. The Y plane is kept constant and chosen such that the workspace of the foot

36
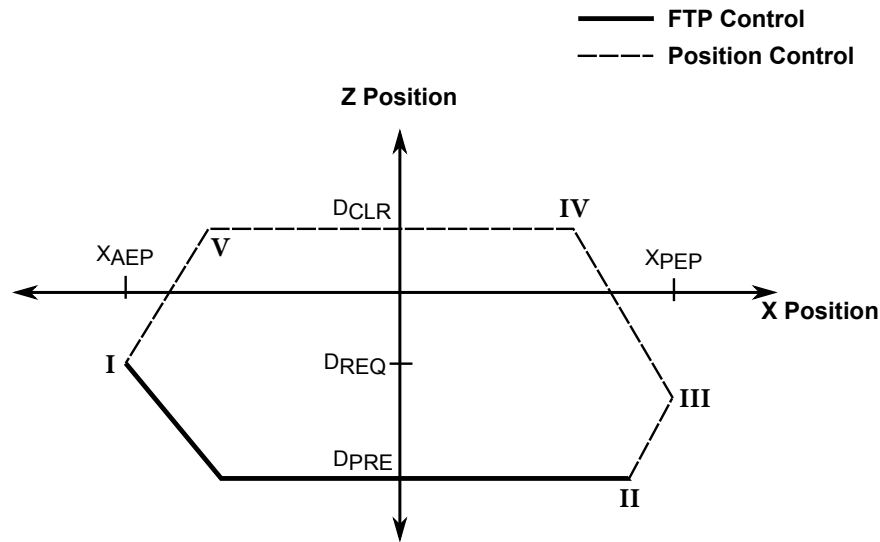
(a): Position of foot in X and Z plane
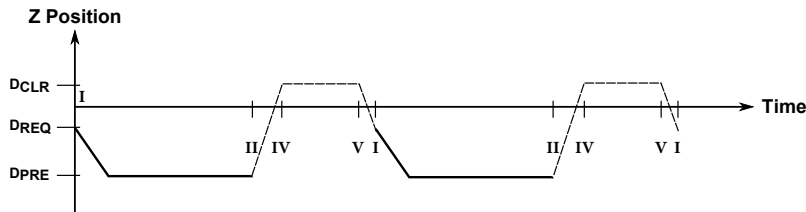
(b): Timing cycle in Z plane
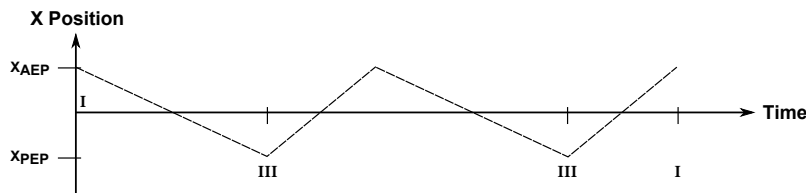
(c): Timing cycle in X Plane

Figure 4.4: Cyclic walking behavior using the FTP algorithm on flat terrain. (a) Position of foot in the X and Z plane (foot position in Y plane is kept constant) during a step: The behavior is governed by six position variables which determine the extreme positions of the foot in the X and Z plane (Only five shown in figure). (b) Timing cycle in the Z plane: The FTP controller controls the leg during the stance phase while the position controller swings the leg back to its original position. (c) Timing cycle in the X plane: The movement in the X plane is completely controlled by position control. D_{CLR} is the preferred clearance while D_{REQ} and D_{PRE} are the required and preferred depression in the Z axis. X_{AEP} and X_{PEP} are the anterior posterior extreme position in the X axis. (Adapted from [42])

37

is largest in the Z plane. Six extreme positions in the X and Z plane govern the position of the foot during the walking step. The anterior extreme position (X_{AEP}) and posterior extreme position (X_{PEP}) control the most anterior and posterior position in the X plane that can be reached by the leg during walking. Since the position in the X plane is controlled by position control, the movement between X_{AEP} and X_{PEP} is deterministic regardless of the terrain.

The foot position in the Z plane is commanded by the FTP controller during the stance phase while position controller commands the foot position during the swing phase. The foot position in the Z plane during swing phase changes from the position at the end of previous stance phase dependent on the terrain height to a deterministic initial position before the start of the next stance phase. The foot position during the stance phase is based on the terrain height and the interaction of the foot during that phase. The four positions which govern the position in Z plane are the preferred clearance D_{CLR}, required depression D_{REQ}, preferred depression D_{PRE}, and maximum depression D_{MAX} (not shown in Fig. 4.4). The preferred depression D_{PRE} has been discussed in the previous sections while the preferred clearance D_{CLR} is the position the foot has to reach during the swing phase such that the leg can walk over obstacles. D_{CLR} can be the maximum upward position reachable by the leg configuration. If the terrain is flat, the position in the Z plane would oscillate between D_{PRE} and D_{CLR}. The required depression D_{REQ} is the foot position such that the body is lifted slightly from the ground. This is done so that regardless of the terrain height, the body is lifted slightly above the ground by all legs so that lower side of the body does not hit or rub against the ground. During the swing phase, the position controller commands the foot position to go to D_{CLR} and then down to D_{REQ} such that the stance phase begins with the foot at the required depression D_{REQ}. The maximum depression D_{MAX} is the maximum depression reachable by the leg configuration and forms an upper limit for the foot depression during the stance phase. If the terrain is lower than the maximum D_{MAX}, the leg stops depressing the foot further and maintains that depression.

38
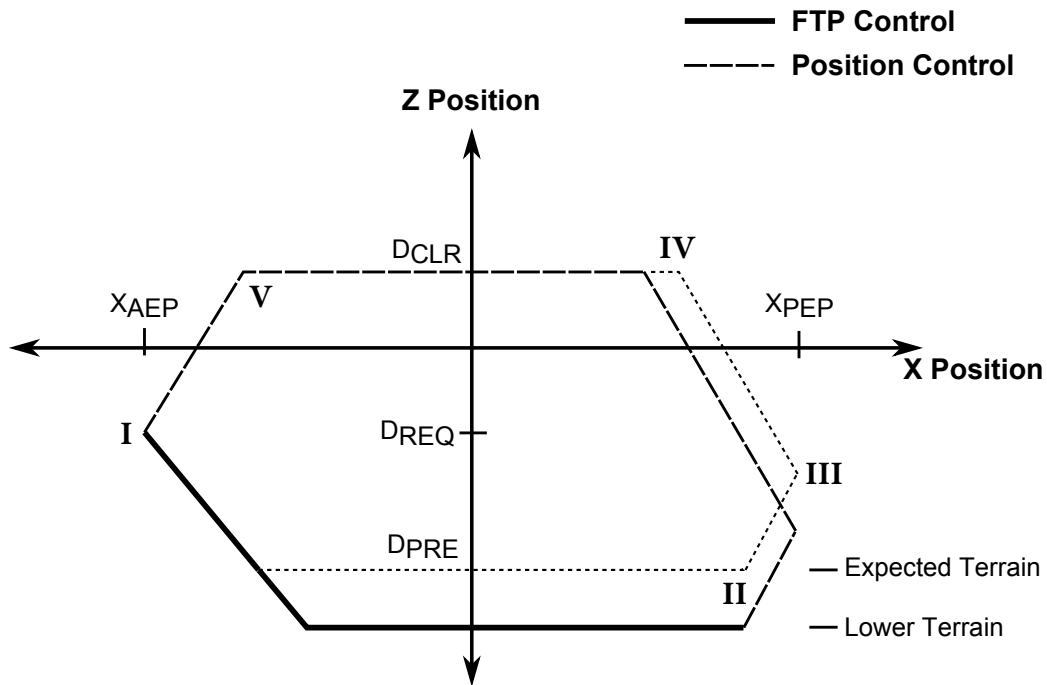
(a): Position of foot on a terrain lower than expected

(b): Timing cycle in the Z plane on a terrain lower than expected

Figure 4.5: Cyclic walking behavior using the FTP algorithm on a terrain lower than expected. (a) Position of foot in the Z plane (foot position in Y plane is kept constant) changes during a step (b) Timing cycle in the Z plane. D_{CLR} is the preferred clearance while D_{REQ} and D_{PRE} are the required and preferred depression in the Z axis. X_{AEP} and X_{PEP} are the anterior posterior extreme position in the X axis.

Part (b) in Fig. 4.4 shows the desired Z foot positions with respect to time while part (c) shows the desired X foot positions with respect to time. Stance duty factor ($0 < D_S < 1$) controls the ratio of time between the stance and swing phase during a single step. Stance phase starts at time step *I* and ends at *II* (swing phase goes from time step *II* to *V* and ends at *I*). Retraction duty

39

factor ($0 < D_R < 1$) controls the ratio of time between retract and protract phase during a single step. Retract phase starts at time step I and ends at III (protract phase goes from time step III to V and ends at I). D_R is chosen to be greater than D_S in order to delay protraction until the foot has been elevated from the terrain. For the hexapod to walk in tripod gait, D_R and D_S have been selected to be 0.8 and 0.7 respectively. The time duration for a single step is kept constant for all legs. Thus, even though all the legs are independently controlled, starting the execution of the FTP controller on the legs at the same time makes them synchronous with each other.

On flat terrains, the position plot is similar from one step to another and behaves almost as a position controller. However, on uneven terrains, based on the force feedback, foot depression changes from step to step in order to match the terrain. Figure 4.5 shows the cyclic behavior used by the FTP algorithm for walking on a terrain lower than expected. As can be seen in Part (a) of Fig. 4.5, the leg continues to do fast depress until the force feedback increases above the minimum threshold and, in effect, makes ground contact. This changes the behavior for the remaining step. Since the timing for the whole step is time controlled, the time steps (I to V), except IV, occur at the same time every step. The foot position in the Z plane depends on the terrain height and, therefore, the time step (IV) the foot reaches D_{CLR} changes at each step. Figure 4.6 shows the cyclic behavior used by the FTP algorithm for walking on a terrain higher than expected. The behavior observed is similar to the one in Fig. 4.5. Please note that in Fig. 4.5 and Fig. 4.6, after touchdown, based on the measured foot forces, the leg would be slow elevated or depressed to reach the preferred depression D_{PRE}. This behavior is not shown in Fig. 4.5 and Fig. 4.6 and can be considered a simplified version of the walking behavior on uneven terrain.

4.6 Multiple Gaits

Even though the alternating tripod gait is the fastest hexapod gait [68], other gaits like the wave and ripple gait offer more stability. For example, when the terrain is slippery, the wave and

40
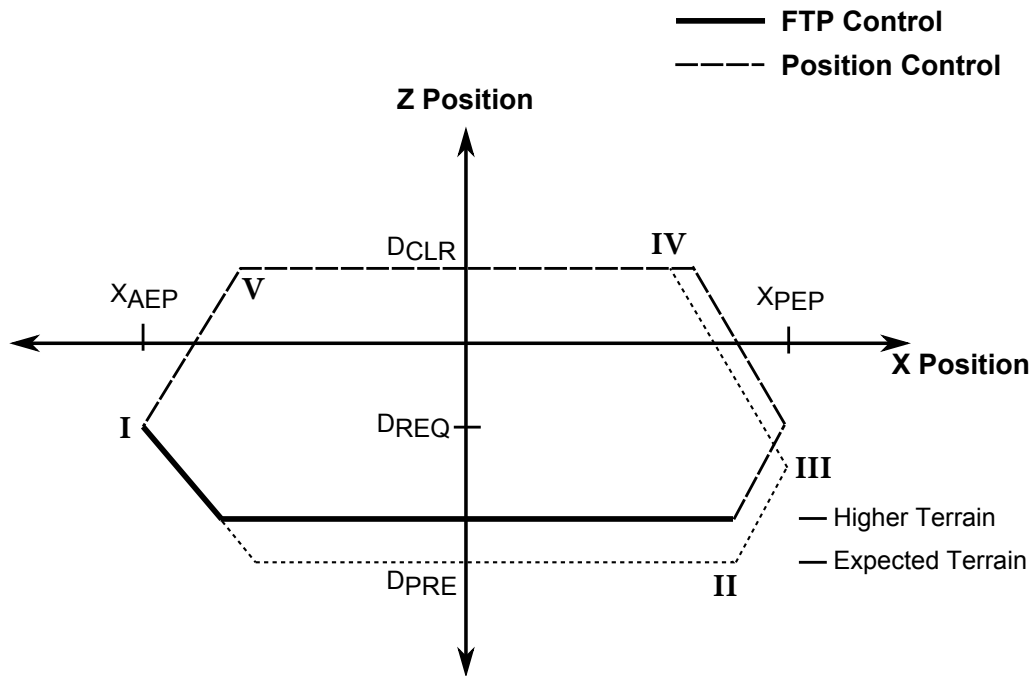
(a): Position of foot on a terrain higher than expected
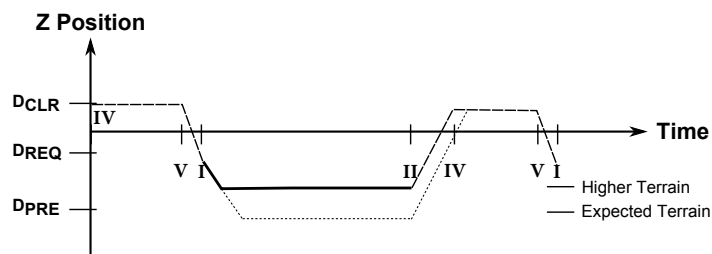
(b): Timing cycle in the Z plane on a terrain higher than expected
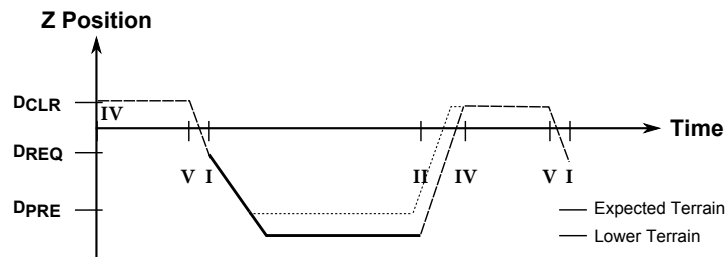
Figure 4.6: Cyclic walking behavior using the FTP algorithm on a terrain higher than expected. (a) Position of foot in the Z plane (foot position in Y plane is kept constant) changes during a step (b) Timing cycle in the Z plane. D_{CLR} is the preferred clearance while D_{REQ} and D_{PRE} are the required and preferred depression in the Z axis. X_{AEP} and X_{PEP} are the anterior posterior extreme position in the X axis.

ripple gaits are more stable as the number of legs on the ground at any given time is higher, which serves to increase the size of the support polygon formed by the feet. Figure 4.7 shows the timing patterns of all the three gaits. Each gait still operates by alternating between the swing phase and the stance phase. The difference between the different gaits is the relative phasing between the

41

legs and the amount of time spent in the stance phase. In the alternating tripod gait, each tripod starts their phases at the same time with a phase difference between them. In wave and ripple gait, individual legs start their phases independent of each other which cause the time period for each step to be increased. The time period for each time step (addition of the swing and stance time period) for wave gait is 3 times more than the time step for a tripod gait while the time period for the ripple gait is 1.5 times more than the tripod gait time period.
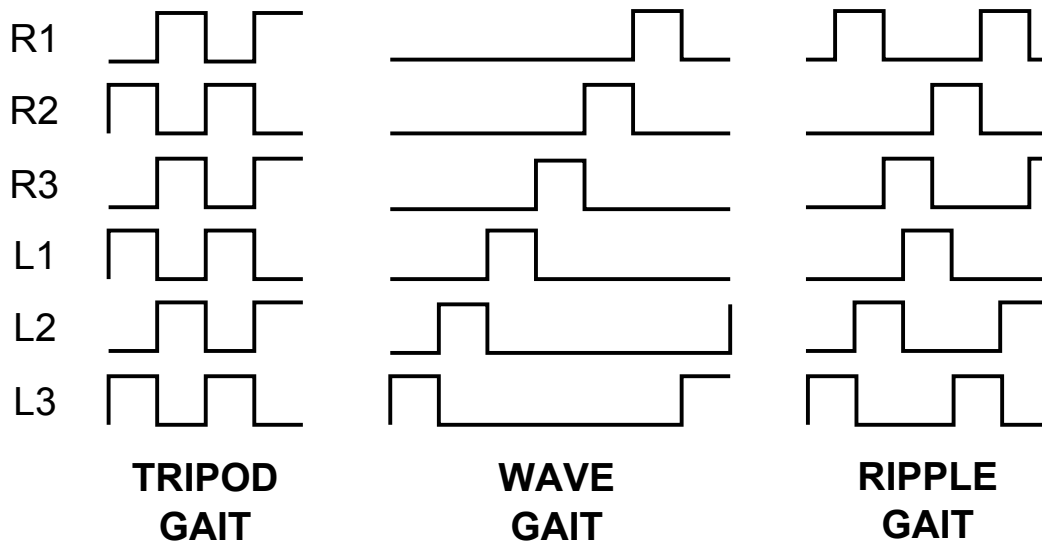
Figure 4.7: Timing plot for tripod, wave and ripple gaits. (Adapted from [69]).

4.6.1   Multiple Gaits Using FTP Control

As the modifications required for different gaits are in terms of phasing and time period, wave and ripple gaits can be implemented using the FTP algorithm without any major modifications. Since the FTP algorithm is not dependent on the force profile pattern, the only change needed is the high force threshold F_H value. In the alternating tripod gait, the middle leg needs to produce more force to lift the body up, but this is not the case for the other gaits. Since more legs are on the ground at any given time compared to the tripod gait, the F_H for the middle legs

42

in wave and ripple gaits could be reduced by half. However, the high force threshold F_H value for the alternating tripod gait can also be used for the wave and ripple gaits without any change in the walking behavior. So by changing the time period and individual leg phasing, multiple gaits can be implemented using the FTP controller. Results are provided in Chapter 6.

4.6.2   Gait Change in FTP Control

Animals change their gait depending on the terrain, the walking speed as well as environmental parameters. However, the stimulus for gait change during insect walking is not completely understood. Some stimulus that produce behavioral transitions from one walking gait to another have been found but the list is not yet complete. Transition steps taken in between two separate walking behaviors have been found [70]. Such transition steps orchestrate the legs to move from one walking behavior to the next without the loss of stability. However, the studies required to understand every transition and stimulus that causes walking transitions are yet to be done. Also, the dependency of the transition on the context of the environment makes this an open ended question.

Currently, the transition between gaits using the FTP controller is not automatic but preselected. The FTP controller also does not use a transition step which changes the walking behavior from one to the other but simply starts a new step using defined state variables. The walking behavior simply reads the necessary variables required for walking and completes the step with the behavior implied by the variables. For example, after a completion of a step, if the variable for time period is multiplied by 3 and the time period variables are set appropriately, the walking behavior changes from tripod gait to wave gait. Since the FTP algorithm uses deltas to change the position at each step, there is no loss of stability when changing the walking behavior. Also, no specific transition step is implemented.

43

4.7 Summary

The Force Threshold-based Position (FTP) controller is presented in this chapter. By dividing the vertical ground reaction force profile based on the amount of support it provides, the FTP controller is not dependent on any force profile patterns. Also, by trying to achieve the level of support required by each leg, the FTP controller is able to produce ground reaction forces dependent on the terrain. This is a great advantage because the FTP algorithm can walk on uneven terrain producing the necessary ground reaction forces without having to know what kind of ground forces are needed for that terrain or to store them.

The FTP controller is also able to maintain the body height by independently controlling the leg length based on the force feedback. Due to this independent height control, the robot is able to walk easily oven terrain changes without any loss of stability. Currently, the preferred foot depression D_{PRE} is user selected and is selected in such a way that the leg can step over or step down over a wide range of terrain changes.

The next chapter describes the hexapod structure built in simulation and hardware and parts needed to implement the FTP controller.

44

5.1   Introduction

The following sections describe the structure of the hexapod developed for testing the Force Threshold-based Position (FTP) controller in simulation and hardware. The goals of the leg design are three degrees of freedom per leg with the ability to sense ground force, or foot force, continuously throughout the step for use by the FTP controller. Traditionally, foot force has been difficult to measure rapidly and accurately. One strategy has been to measure the motor current and use the torque constant to determine how much force is being generated. In addition to the current measurements typically being very noisy signals, this torque constant is an idealized term that does not truly model the motor torque, particularly when the motor is turning at high speed. Other options are the use of sensors at the tip of the foot, but there are challenges associated with this as well. This chapter describes the leg structure, force feedback assembly, and the hexapod design. Information about the force feedback assembly and working is provided. Mechanical as well as electrical assembly of the hexapod developed is provided.

5.2   Leg Structure

The hexapod leg is modeled similar to a stick insect and has three degrees of freedom on each leg (Fig. 5.1). The three joints are modeled similar to the joints of the stick insect; ThC

[1]Portions of these results have been adapted from previously published publications {[42], [43], [44]}.
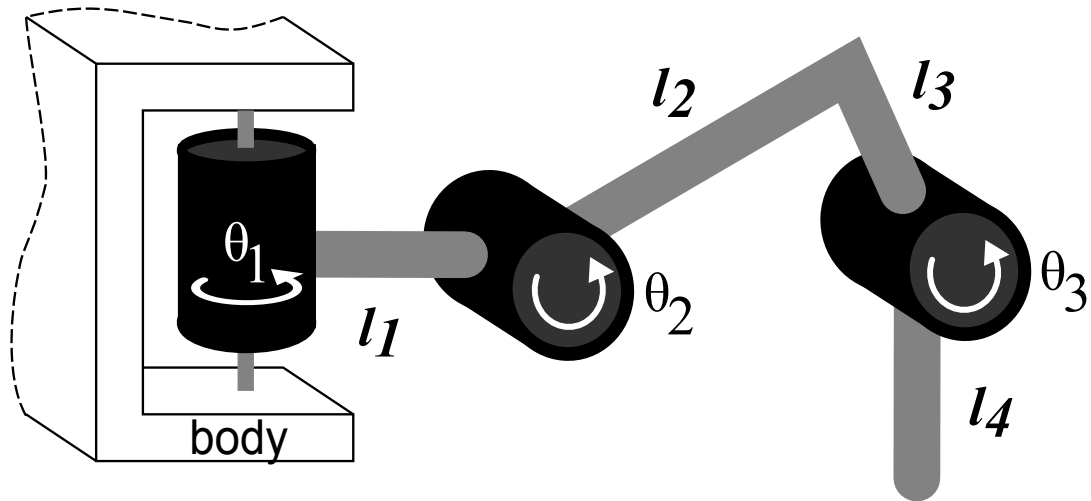
Figure 5.1: Hexapod leg structure: Each leg has three actuators and is described by four link lengths. (Adapted from [42])

(Thorax Coxa) joint, CTr (Coxa Trochanter) joint, and FTi (Femur Tibia) joint. Three joints (θ_1, θ_2 and θ_3) are used to control the position of the foot. The first or ThC joint θ_1 controls the fore-aft motion of the leg while the remaining two, CTr and FTi joints (θ_2 and θ_3), control the foot elevation and depression. Leg links l_2 and l_3 form a rigid $90°$ angle between them. The dimensions of the hexapod leg are given in further sections.

5.3 Force Sensing

One of the main criteria for the hexapod leg design is the need to accurately measure the foot forces at a high rate. This is needed so that the FTP algorithm can respond quickly to the change in terrain while achieving the maximum possible forward movement in a single stride. The accuracy of the foot force data is crucial to the success of the algorithm. Inaccurate force reading can lead to unpredictable leg behavior of the robot while slow reading of the force can lead to changes in the overall body pitch and roll due to excessive foot depression by one or more legs of the robot.

5.3.1   Using Force Sensitive Resistor (FSR)

One of the ways force could be successfully read is by using a force sensing or force sensitive resistor. A force sensitive resistor (FSR) is a material whose resistance changes when a pressure or force is applied at its surface. This resistor could be applied to a DC voltage and the value could be read using a data channel. Although the force value from the resistor could be read at a high frequency, the accuracy of the force data depends on the position of the FSR on the leg. If the FSR is positioned on the end effector of the leg, the value of the FSR depends on the angle of foot touchdown. Also, friction has an effect on the FSR causing discrepancies in readings. Placing one or more sensors in between joints or links makes the force data more reliable but causes a lot of wear and tear on the sensor. Based on the configuration of the leg, multiple force sensors are required to accurately measure the foot force for that leg. Noise in the readings also makes it harder to use with the FTP algorithm. Using a software filter increases data reliability but reduces the responsiveness to terrain changes. This kind of sensor setup is difficult to read and also difficult to maintain.

5.3.2   Using a Separate Actuator as a Force Sensor

Some actuators in the market use a position controller with selectable gain to determine the output torque of the actuator. The compliance of the actuator can be used to measure the corresponding load by reading its position and determining the error. This can be achieved by setting the proportional gain low, making the actuator compliant enough to deviate from the zero position when a load is applied. These small position changes can be monitored to find the corresponding load on the actuator. Since the output torque grows as the position deviates from the zero position, we can make an approximate estimation of the force on the actuator. The actuators from Dynamixel [71] use the combination of compliance margin and compliance slope values

47

to determine the output torque and in effect, the compliance of the actuator. If the actuator can be positioned on the hexapod leg such that the corresponding load is due to the foot forces, the position error can be used to measure the foot forces.
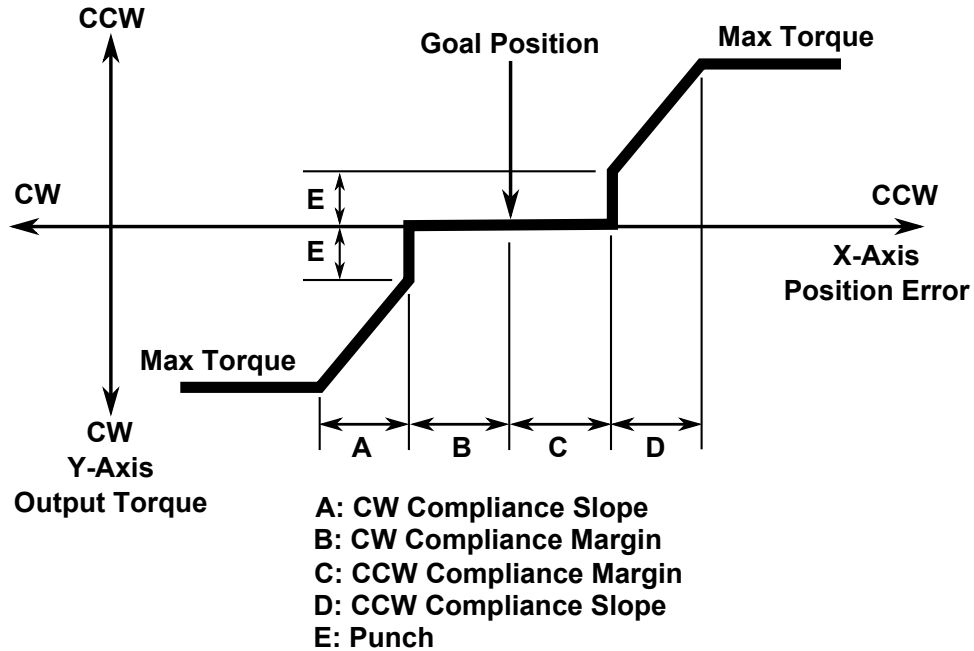
Figure 5.2: Actuator compliance: Actuator compliance governed by compliance slope and margin in the clockwise (CW) and counter-clockwise (CCW) direction. (Adapted from [71]).

Figure 5.2 shows the compliant behavior of the Dynamixel actuators. The output torque of the actuator around the zero position is controlled by the compliance margin and slope values. If the compliance slope of the actuator is set high and the compliance margin is set to a small value, the actuator can be compliant enough to move in clockwise (CW) and counter-clockwise (CCW) directions. An approximate estimation of the force on the actuator can be made by reading the position error.

A compliant joint is added to the hexapod leg structure to detect foot forces corresponding to the leg. The compliant actuator (θ_c) is placed in between the *ThC* joint (θ_1) and the *CTr* joint (θ_2) and is used to detect the foot force in the Z-direction. The position is based on the fact that the *CTr* and *FTi* joints (θ_2 and θ_3) control the foot elevation and depression (Figure 5.1). Figure 5.3

48
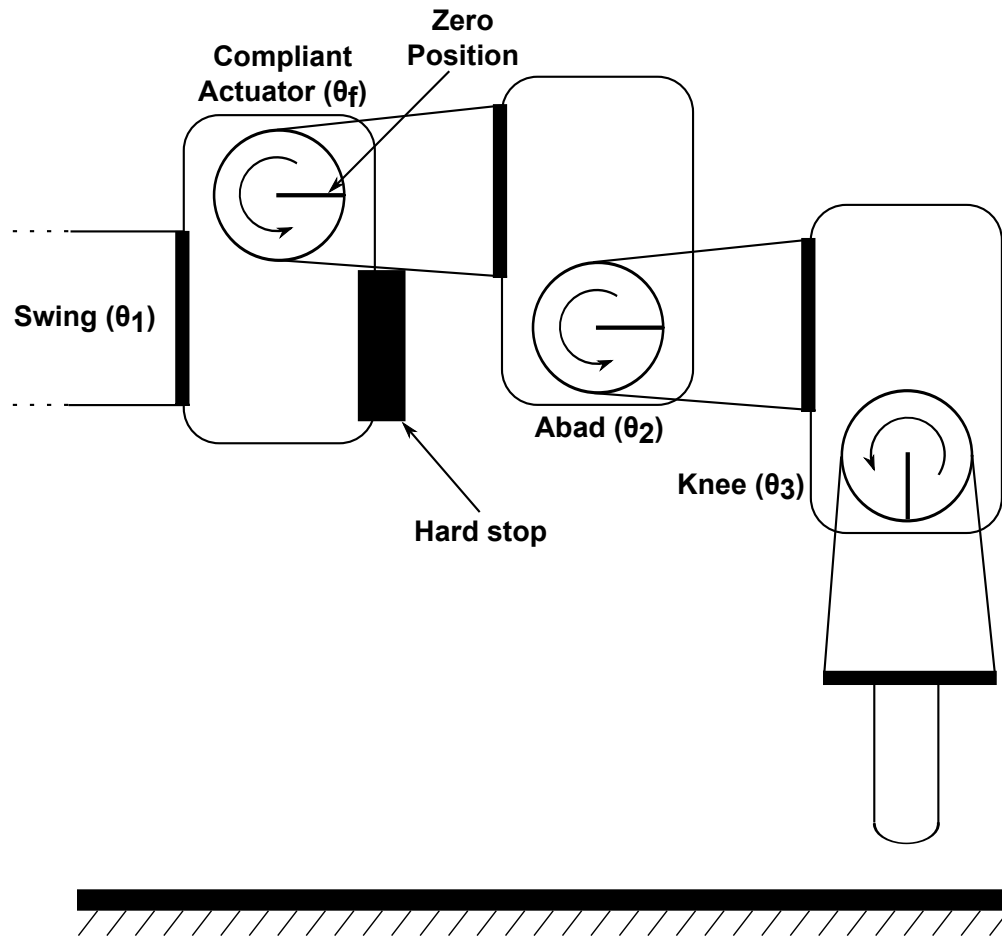
Figure 5.3: Hexapod leg with a compliant actuator.

shows the actuator structure for a single leg. Since the compliant actuator is used to find foot forces during foot touchdown, a hard stop has been placed such that the actuator does not move past zero in the clockwise direction during flight. The compliant actuator is commanded to hold the zero position. When the foot touches the ground, force due to the body weight of the hexapod causes the compliant actuator to deviate from this position. Figure 5.4 shows this scenario in the counter clockwise direction. The change in the actuator position can be read and ground contact can be inferred. Please note that there is some compliance in all the ThC (θ_1), CTr (θ_2) and FTi (θ_3) joints but they are much stiffer than the compliant actuator (θ_c). However, individually or a combination of those joints are not able to accurately predict the foot forces while maintaining the

49

body weight during walking. An additional compliant actuator with a high compliance margin is needed to sense the foot forces while walking upright on the ground.
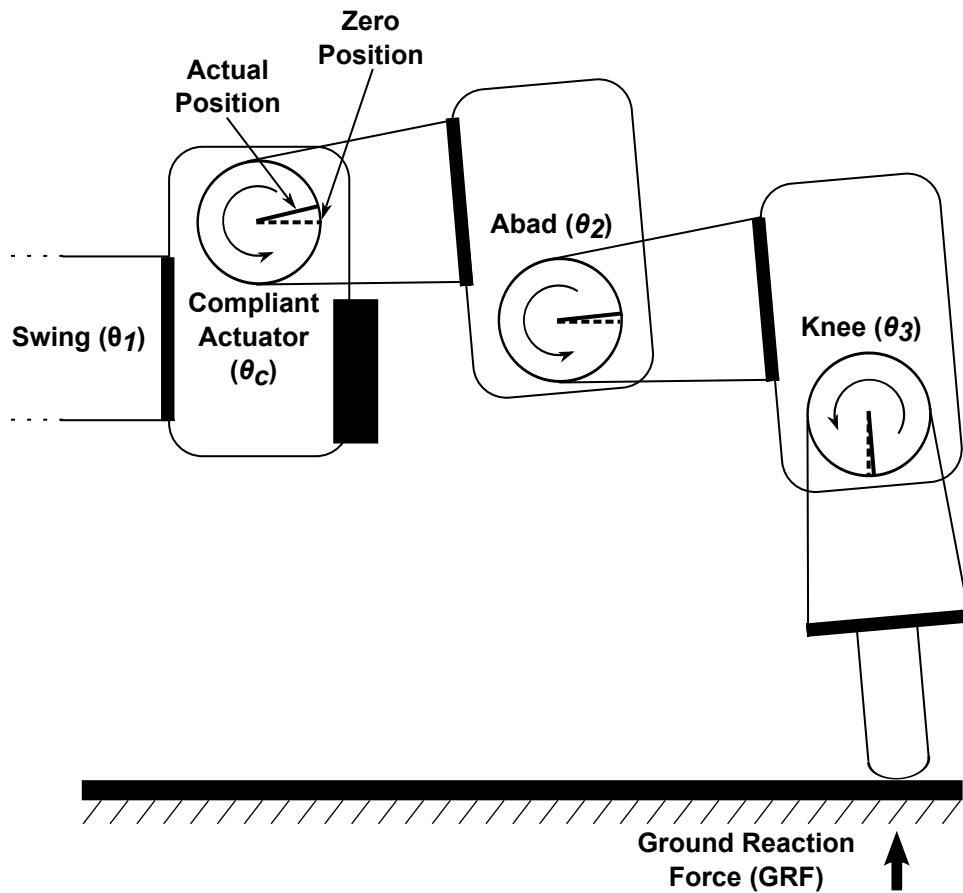
Figure 5.4: Hexapod leg with a compliant actuator: Detecting foot forces. (Adapted from [42])

The relationship between compliance of the actuator and load could be evaluated by using a weighing scale to note the load at the foot corresponding to the position deviation of the compliant actuator. Figure 5.5 shows the load corresponding to the compliant actuator position. For this experiment, one tripod was made to carry the weight of the hexapod and the foot depression of each tripod leg was increased slowly. Additional weights were added to the hexapod to find the load corresponding to the higher position deviations. Each experiment was done multiple times and the mean load was calculated. The figure shows the mean and standard deviation of the load corresponding to the compliant actuator position. The figure also shows the possible torque

50

generated by the actuator at specific actuator positions based on the compliance margin and slope limits set. As can be seen from the figure, the change in the actuator position has an almost linear relationship to the load experienced by the leg and has a slope similar in magnitude to the slope of the actuator torque based on the set compliance margin and slope limits. The compliant actuator position can be used in the forward kinematic calculation of the desired joint angles from the commanded foot depression level.
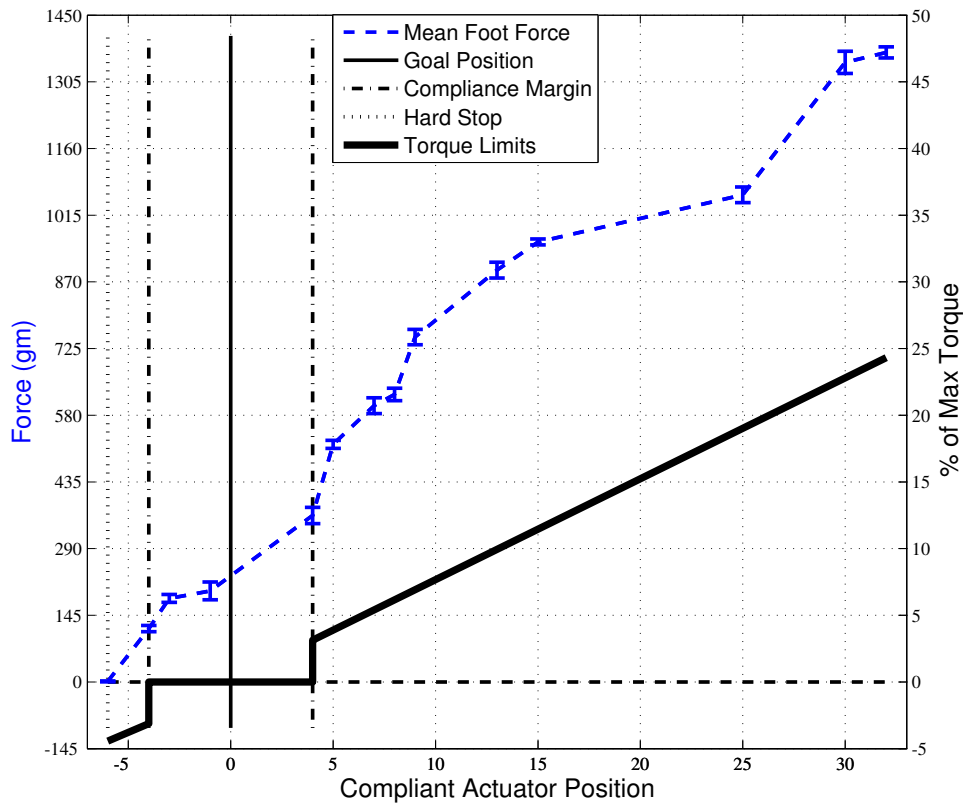
Figure 5.5: Load corresponding to a compliant actuator position. (Adapted from [42])

Even though reading the actuator position through a serial port is far slower than using the force sensitive resistor (FSR) through an analog-to-digital channel, the reads can be done fast enough for the hexapod to walk properly.

51

5.4 Leg Structure with Force Sensing
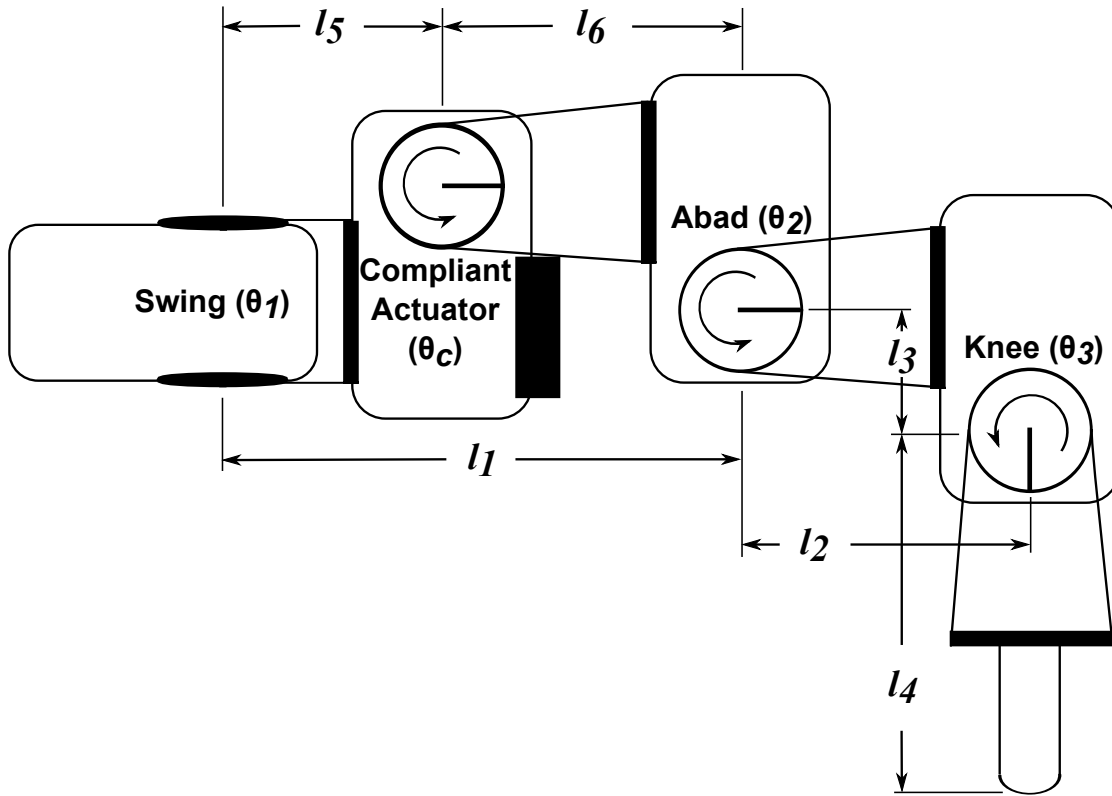
Figure 5.6: Side view of the hexapod leg structure in the zero position. (Adapted from [42])

The whole structure of the hexapod leg along with the compliant actuator is shown in Figure 5.6. Adding the compliant actuator increases the degrees of freedom on each leg to four. The dimensions of the hexapod leg structure are given in Table 5.1. The compliant actuator position can be used in the calculation of the end effector of the leg. As the compliant actuator position changes due to foot touching the ground, the FTP controller can make sure the leg can hold the weight of the body by taking the actuator position in to account. Based on the leg structure (Figure 5.6) and link lengths (Table 5.1), each leg can achieve a foot clearance of 6 *cms* during the swing phase and a maximum foot depression of 18 *cms* during stance phase.

52

Table 5.1: Hexapod dimensions: HexaBull-1.

Product	Centimeters
Body Length: Chassis	44.5
Body Length: Between ThC Joints (θ_1)	52.5
Body Length: Total (Including Leg Stride)	64.5
Body Width: Chassis	7.9
Body Width: Between ThC Joints (θ_1)	10.5
Body Width: Total (Including Contralateral Legs)	43.3
Body Depth	6.8
Leg: Link Length 1 (l_1)	9.3
Leg: Link Length 2 (l_2)	7.1
Leg: Link Length 3 (l_3)	2.4
Leg: Link Length 4 (l_4)	9.2
Leg: Link Length 5 (l_5)	5.1
Leg: Link Length 6 (l_6)	4.2

5.5 Experimental Hexapod: HexaBull-1

Figure 5.7 shows the experimental hexapod, HexaBull-1. The dimensions of the whole hexapod system are given in Table 5.1. The ThC joint (θ_1) is controlled using a Dynamixel RX-28 (Robotis Inc.) [72] servo actuator, while the joints CTr (θ_2), FTi (θ_3) and the compliant joint (θ_c) are controlled using a Dynamixel AX-18A (Robotis Inc.) [71] servo actuator. The Dynamixel AX-18A actuators has a maximum holding torque of 18 $kg.cm$ while the Dynamixel RX-28 has a maximum holding torque of 37.7 $kg.cm$. The RX-28 uses the RS485 asynchronous serial while the AX-18A communicates using the TTL half-duplex asynchronous serial communication. Information about the actuators and their control can be found in the Appendix A.

The CM-700 control board [73] is used to control each contralateral pair of hexapod legs through serial communication with each joint servo. The control board uses the $ATMega2561$ 8-bit AVR RISC-based micro-controller running at $16MHz$ frequency and has $256Kb$ of flash program memory. Three CM-700 boards are used to control the hexapod and are completely separate except for the power supply. The same code is loaded in to three boards and as the boards are powered on,

53

Figure 5.7: Experimental hexapod: HexaBull-1.

the connected legs are recognized by their motor id and the legs are controlled to move in sync and no data communication is needed for smooth walking. Stable walking behavior was implemented on this experimental hexapod over a wide range of frequencies from 20 Hz to 80 Hz. The normal controller frequency used is 40 Hz for most of the experiments on this experimental hexapod. Information about the control board and working can be found in Table A.4.

Figure 5.8 shows the wiring between all the components in the experimental hexapod, HexaBull-1. Since the Dynamixel AX-18A actuator working is limited to 12 V while the Dynamixel RX-28 is able to produce the largest torque when connected to 16 V, two separate batteries are required by the hexapod for operation. The 11.1 V battery powers the Dynamixel AX-18A actuators while the 14.8 V battery powers the CM-700 which, in turn, powers the Dynamixel RX-28. The FTP algorithm sends the desired position to the connected motors and also reads the compliant actuator position to determine foot forces. Please note that for experimental results the position of other actuators are also read but those positions are not required for the operation of the FTP algorithm. The experimental hexapod, HexaBull-1, weighs a total of 2.7 kg without onboard

54
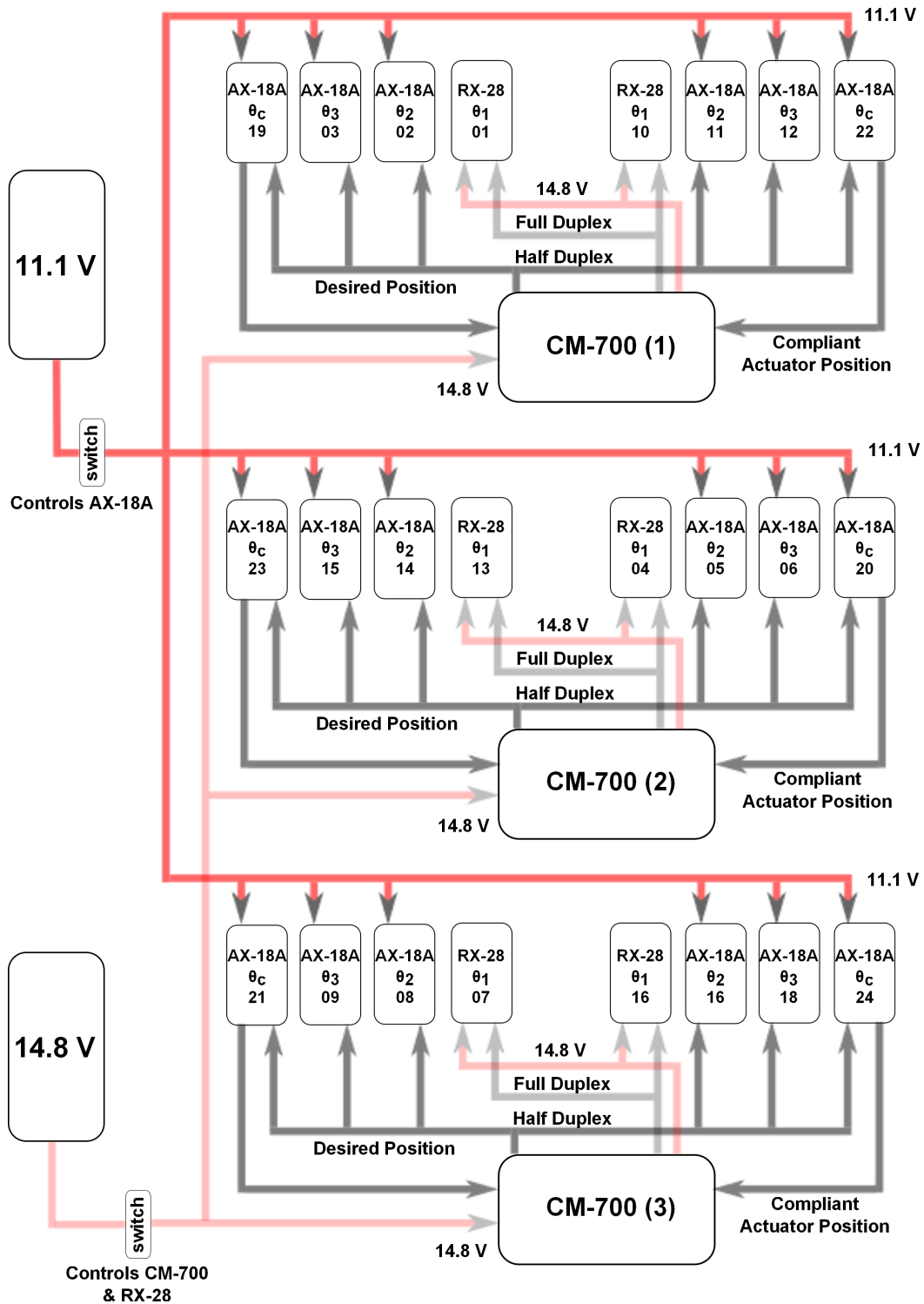
Figure 5.8: Experimental hexapod HexaBull-1 wiring.

power and 3.4 *kg* with the two batteries. Motor IDs are also displayed in Fig. 5.8. The motor IDs for the compliant actuator are from $19 - 24$.

5.6 Hexapod in Simulation
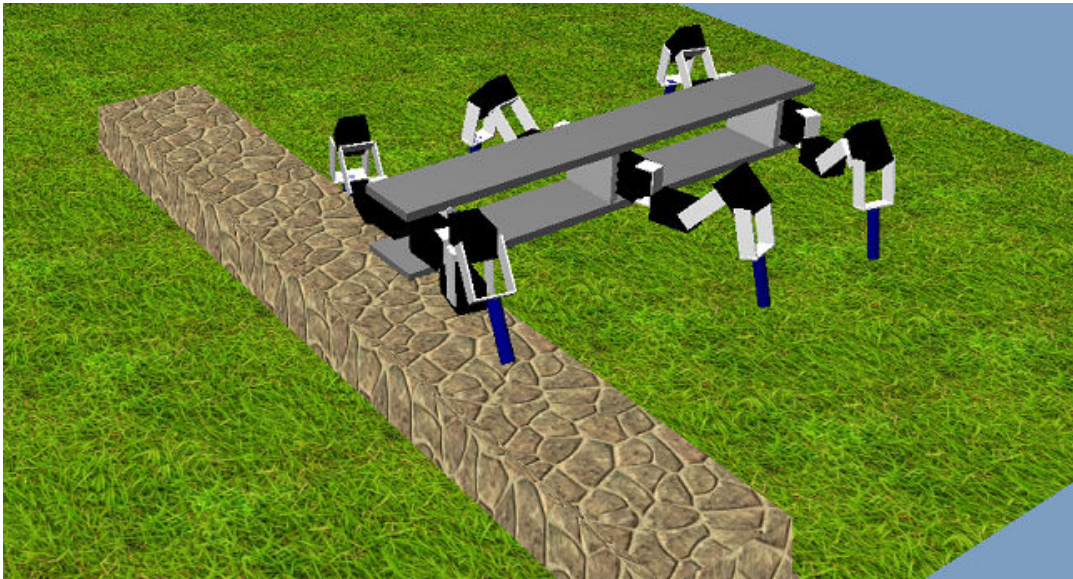
Figure 5.9: Hexapod in simulation negotiating an obstacle.

Simulation of the FTP algorithm (Fig. 5.9) is done using the RobotBuilder simulation environment, which is built upon the DynaMechs [74] software package. System losses are modeled as damping in the compliant ground. Ground spring and damping coefficients are taken as 75 *kN/m* and 2 *kN/m/s* respectively. Ground static and kinetic friction coefficients are 0.75 and 0.6 respectively, matching the properties of rubber on concrete. Each leg link is modeled as a 0.1 *kg* slim rod with geometrically-centered mass. Leg mass combined to make up 59% of the complete system mass, each leg making up approximately 9.8%. The simulated hexapod is modeled similarly to the experimental hexapod, however no compliant actuator is simulated. Joint torques multiplied through a Jacobian are used to compute the foot forces for each leg.

5.7 Experimental Hexapod: HexaBull-2

Due to the placement of the compliant force sensor actuator (θ_c) in between the *ThC* joint (θ_1) and the *CTr* joint (θ_2), the arm length of the hexapod leg in the experimental hexapod HexaBull-1 is high. This requires more torque to be produced by the leg actuators to hold the body at a specific height. This limits the stride area the leg can move during a walking step while still lifting the body off the ground. This also causes the body to sag and the body height to decrease during each step. The resulting walking behavior causes the maintenance of body height to be very difficult and requires a high slow elevate rate (Δ_{SE}). Also, due to the mismatch of voltage between the two Dynamixel actuators, two batteries are required which increases the body weight and exacerbates the problem of maintaining body height.

Dynamixel AX-18A actuators have a coarse resolution in terms of rotation angle and using an AX-18A as a compliant force sensor actuator causes read errors which leads to some unintended body pitches and somewhat unstable walking behavior. Also, using the compliant actuator position in the calculation of the foot position of the leg can lead to some jagged walking behavior. If the compliant actuator position is not used during the calculation of foot position, the leg tends to splay during walking which causes the body to sag further and requires a more higher slow elevate rate (Δ_{SE}) to maintain a specific body height.

To solve the above problems, a newer version of the experimental hexapod has been developed. The Dynamixel AX-18A actuators were replaced by Dynamixel MX-28T (Robotis Inc.) [75] actuators. The Dynamixel MX-28T actuators have a maximum holding torque of 31.6 *kg.cm* (compared to 18 *kg.cm* for Dynamixel AX-18A) and resolution of $0.088°$ (compared to $0.29°$ for Dynamixel AX-18A). The MX-28T also uses a contact-less magnetic encoder instead of a potentiometer. This will provide more accurate readings without deterioration over time. The force sensing mechanism was removed from the hexapod leg and moved to the hip in the hexapod

57
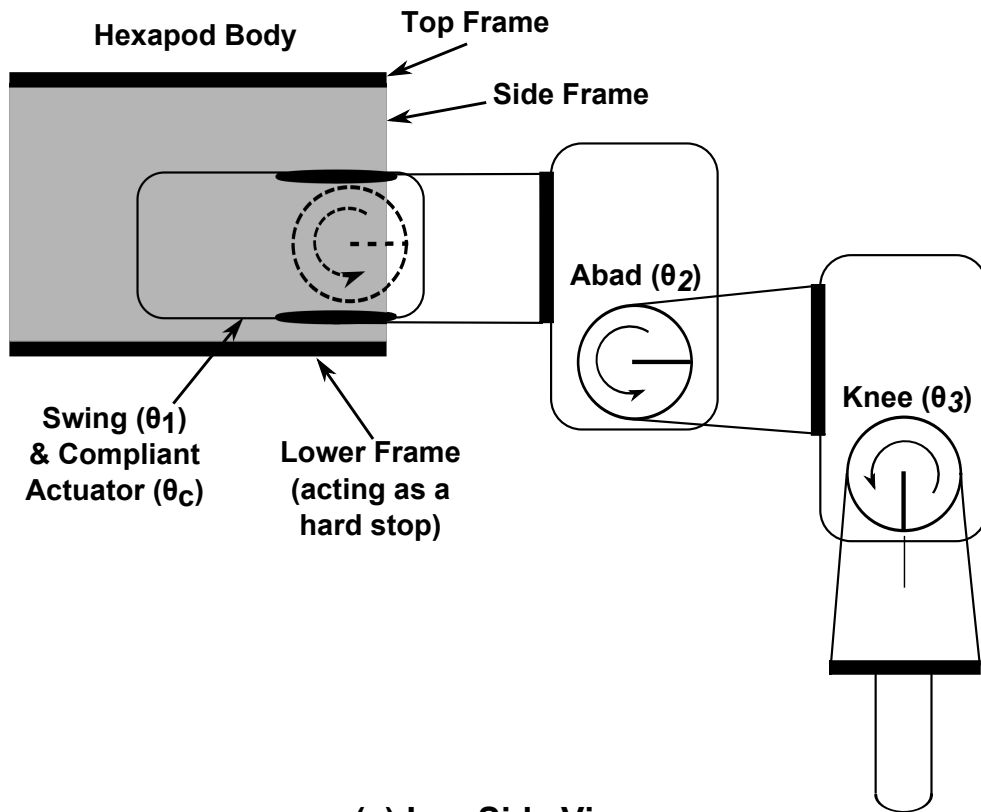
(a) Leg Side View
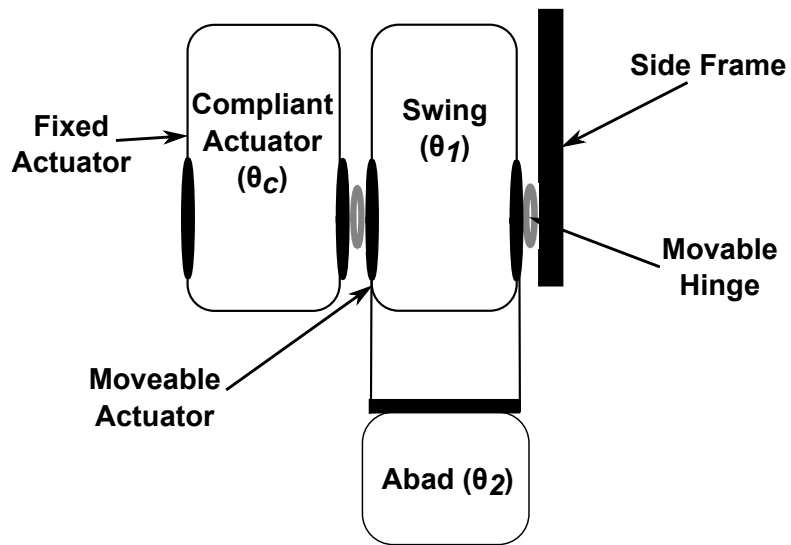
(b) Swing & Compliant Actuator Top View

Figure 5.10: HexaBull-2 leg structure.

58
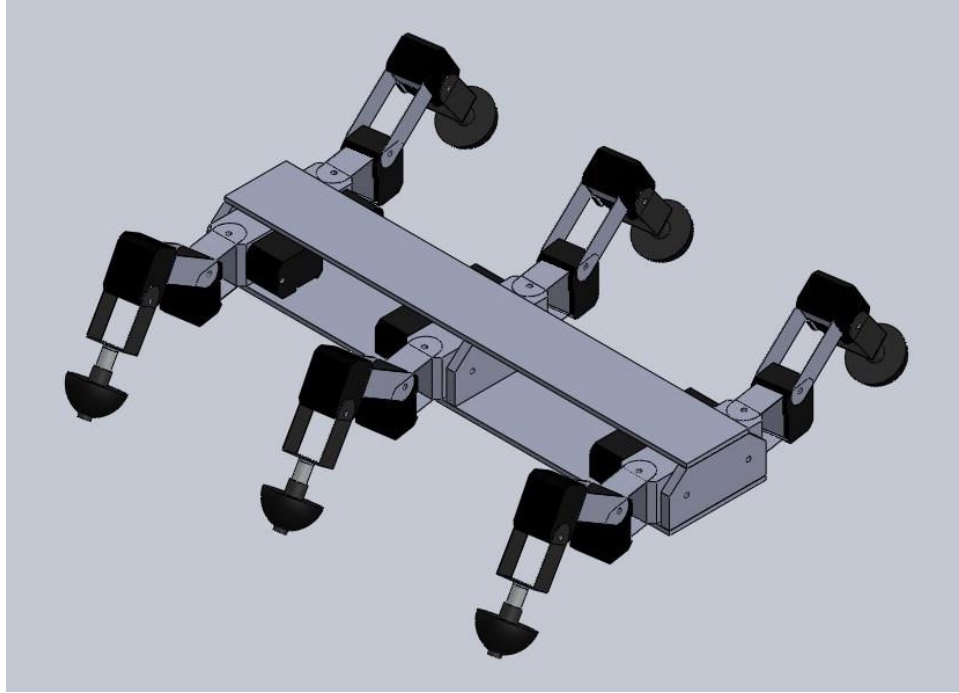
Figure 5.11: SolidWorks model of the HexaBull-2.

body. Figure 5.10 shows the newer version of the hexapod leg. As can be seen in the figure, the hexapod leg (similar to one shown in Figure 5.1) is mounted in between a movable hinge and the compliant actuator. This makes the hexapod leg assembly movable and the compliant actuator can be used to read the position error. As with the last version of the hexapod, a hard stop stops the leg assembly to move below the zero position and the compliant actuator is commanded to hold the zero position. During touchdown, force due to the body weight of the hexapod causes the leg assembly to move upwards causing the compliant actuator to deviate from the zero position.

Figure 5.11 shows the SolidWorks model for the new experimental hexapod while Fig. 5.12 shows the experimental hexapod hardware, HexaBull-2. The dimensions of the whole hexapod system are given in Table 5.2. Since the compliant force sensor actuator assembly is moved inside the hexapod body, the arm length of the hexapod is reduced. This reduction of the arm length and the increased holding torque for the MX-28T actuators, the HexaBull-2 is able to hold the body
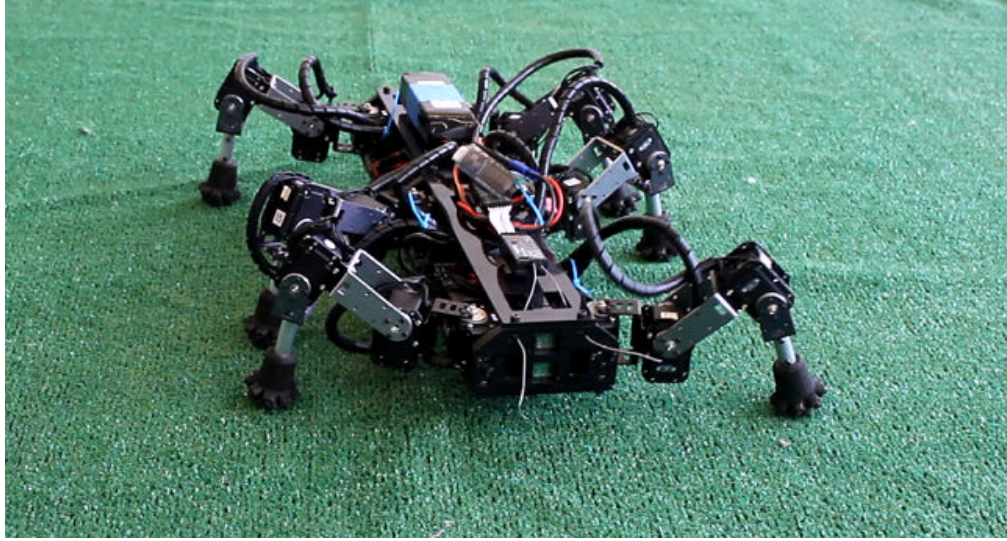
Figure 5.12: Experimental hexapod: HexaBull-2.

Table 5.2: Hexapod dimensions: HexaBull-2.

Product	Centimeters
Body Length: Chassis	52.0
Body Length: Total (Including Leg Stride)	62.0
Body Width: Upper Chassis	6.9
Body Width: Lower Chassis	10.9
Body Width: Between ThC Joints (θ_1)	10.4
Body Width: Total (Including Contralateral Legs)	35.4
Body Depth	6.8
Body Depth: With Battery On Top	10.0
Leg: Link Length 1 (l_1)	5.1
Leg: Link Length 2 (l_2)	7.4
Leg: Link Length 3 (l_3)	2.5
Leg: Link Length 4 (l_4)	11.1

and increase the stride length of the leg compared to HexaBull-1. Due to the increased resolution of the MX-28T actuator position, the compliant actuator can be made much stiffer compared to the AX-18A counterpart while still being able to detect ground contact and measure foot forces. Due to this, the MX-28T compliant actuator is able to function with a small angle error and can produce a stable walking behavior. And this can be done without using the compliant actuator position during calculation of foot position.

الﻤﻨﺎرة ﻟﻼﺳﺘﺸﺎرات

www.manaraa.com

The MX-28T actuators are heavier than the AX-18A counterparts and increase the hexapod body weight. However, as the MX-28T operates at the same voltage levels as the RX-28, only one battery can be used for walking which balances the effect of the heavier actuator. More information about the MX-28T actuator can be found in the Table A.3.

Figure 5.13: Remote control (Futaba $T8FG$ Super) used to control HexaBull-2.

To increase the functionality of HexaBull-2, a wireless remote was added to the configuration and is used to send commands to the hexapod. The Futaba $T8FG$ Super 14 channel 2.4 GHz remote system (Fig. 5.13) along with the Futaba $R6208SB$ 2.4 GHz 8/18 channel receiver is used for that purpose. The wireless receiver is connected to another CM-700 board which constantly reads the remote buttons and sends the commands to the three CM-700 boards running the FTP algorithm when the input on the remote is changed and thus, limiting the communication.

Figure 5.14 shows the wiring between all the components in the experimental hexapod, HexaBull-2. Since both MX-28T and RX-28 operate at the same voltage levels, only one type of battery is used to power the hexapod. One or more batteries could be added in series for walking.
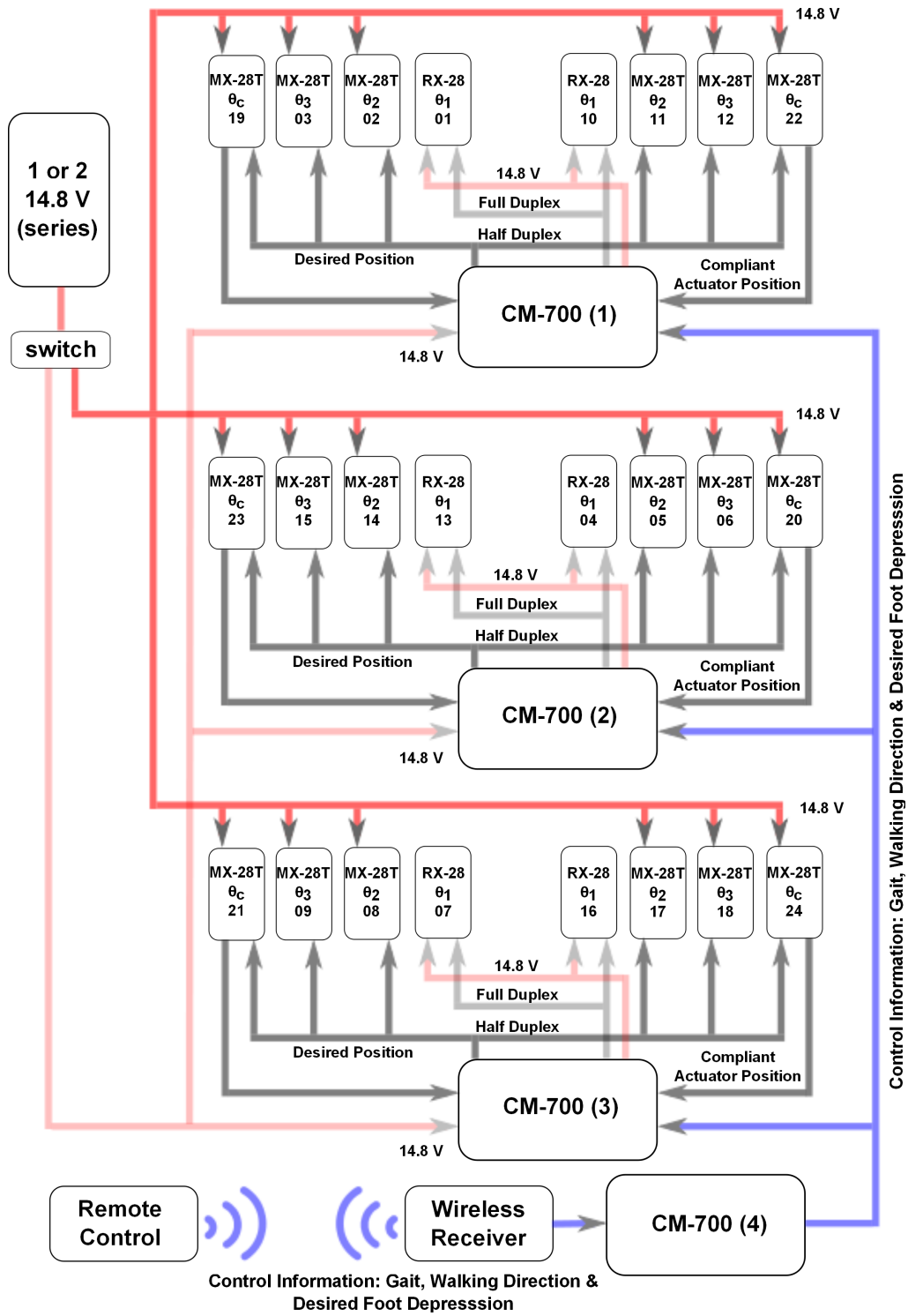
Figure 5.14: Experimental hexapod HexaBull-2 wiring.

Since adding more batteries add more weight to the hexapod, testing on the HexaBull-2 is done using only one battery. The experimental hexapod, HexaBull-2, weighs a total of 4.3 *kg* without onboard power and 4.7 *kg* with a single battery. Motor IDs are also displayed in Fig. 5.8. The figure also shows the fourth board used for communication. This board is connected to a wireless receiver which receives the commands from the remote control in 8-bit packets.

5.8   Summary

This chapter provided a detailed description of the hexapod built for implementing and testing the FTP algorithm. The experimental hexapod uses a novel method to record the foot forces by using a compliant actuator. The chapter gives details of the two versions of the experimental hexapods that have been used with this research. The next chapter provides all the experiments performed in simulation and hardware to test the algorithm.

CHAPTER 6: WALKING ANALYSIS[1]

6.1   Introduction

Since the FTP controller is a local-leg controller operating independently on the six legs of the hexapod, rigorous testing is required to know the effect of the algorithm on the body of the hexapod. Testing is required to check if the legs working individually can maintain body pitch and height while walking on uneven terrain. Also, the effect of each of the Δ rates (Δ_{FD}, Δ_{SD}, and Δ_{SE}) on the walking behavior has to be tested. For the FTP controller to work properly, the force thresholds have to be set for each to provide appropriate support to the body. These thresholds have to be tested to find out the ones for each pair of contralateral legs that work on every terrain. The following sections describe the results obtained from both simulation and hardware.

6.2   Simulation Results

Simulation of the FTP algorithm was done to analyze the algorithm and fix any errors. The foot forces are calculated using the Jacobian and the joint torques. Initially, contact points from the simulation environment were used. Since contact points which provide information about collision, force etc. about a particular point, contact points added to the foot were used to make the simulation more robust. Later, after much testing of the force feedback, the contact points were removed. The following sections describe some of the experiments performed in simulation.

---

[1]Portions of these results have been adapted from previously published publications {[42], [43], [62]}.

6.2.1   Testing Terrains

Different simulation environments were created for testing the algorithm. Terrain A contains a gap of height 6 *cm* (first subplot of Fig. 6.3). The height of the terrain returns to normal after the gap. All the legs of the hexapod have to negotiate the gap. Terrain B contains a 6 *cm* obstacle (Fig. 5.9). The width of obstacle (or gap) in Terrain B (or A) is 17 *cm* such that only one pair of contralateral legs are on the obstacle. Terrain C contains a step of size 6 *cm* which decreases the height of the terrain and the terrain remains at that height (third subplot of Fig. 6.3). Terrain D contains a step of size 6 *cm* which raises the height of the terrain. Terrain E is a randomly generated terrain and consists of square tiles of random elevation with a normal distribution centered at 0 *cm* with a deviation of ±6 *cm*. Terrains F and G are terrains with a smooth incline going down and up respectively with a slope of 15°. Terrains H and I are terrains with series of steps going down and up respectively (Fig. 6.8). The steps are arranged such that the overall angle of the terrain is same as the Terrains F and G with a slope of 15°. For Terrains F to I, a flat platform is added at the start and the end before the incline (and steps) so that the hexapod can transition between the terrains. Also, for Terrains F to I, multiple similar terrains were created for various levels of slopes starting from 2.5° to 30°.

6.2.2   Effects on Body Height

Figure 6.1 shows the body position and angles of the hexapod as it walks on a flat terrain using the alternating tripod gait. The bottom of first subplot shows the stepping pattern for both left and right tripods of the hexapod. The black bar represents the stance period. The upper dashed line represents the stepping pattern for the left tripod while the lower one represents the right. The figure shows three completed steps taken by the legs of the right tripod. The left tripod starts in mid stance phase and only provides support and no forward thrust till the end of the phase (1 *sec*

Figure 6.1: Body position and angles of the hexapod as it walks on a flat terrain using the alternating tripod gait in simulation.

mark). As can be seen in the figure, the hexapod is able to achieve forward movement equal to the body length (Table 5.1) at the end of two completed steps by the right and left tripod (5 *sec* mark). The second subplot shows the body angles (pitch, roll, and yaw). The hexapod body is very stable when walking on a flat terrain.

Figure 6.2 shows the body position and angles of the hexapod as it walks on a Terrain E using the alternating tripod gait. The forward movement achieved by the hexapod is dependent on the terrain. For example, due to a step down on the terrain (3 *sec* mark), the leg requires more time for ground contact and is not able to move the body forward as much compared to a regular step. The body angles (pitch, roll, and yaw) are also dependent on the terrain.
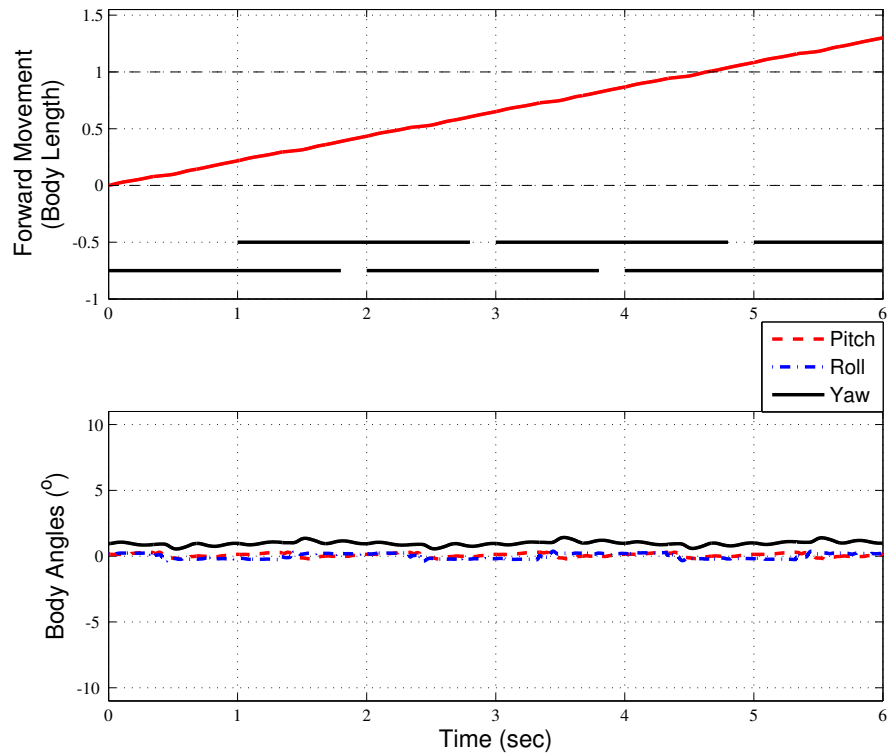
66
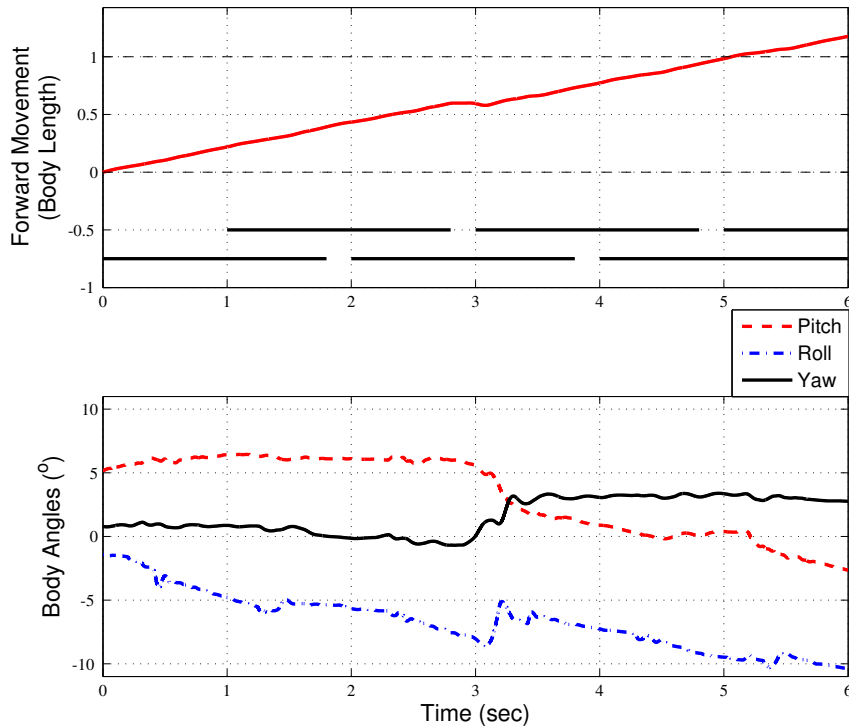
Figure 6.2: Body position and angles of the hexapod as it walks on randomly generated uneven terrain using the alternating tripod gait in simulation.

Figure 6.3 shows the body height of the hexapod walking over Terrains A through D in simulation using the alternating tripod gait. The body height is measured from the geometric center of the hexapod to the terrain. The bottom of each subplot also shows the stepping pattern for both left and right tripods of the hexapod. In the first two subplots, the body height of the hexapod remains fairly stable as each set of contralateral legs passes over the gap or the obstacle. In the latter two subplots, once the hexapod goes over the step up or down, each leg works toward the preferred foot depression D_{PRE}. After several steps, the body height returns to its original walking height with respect to the ground. This is the benefit of FTP algorithm continuing to run during the stance phase. If the foot depression remains constant after ground contact (Force Feedback Control in Section 3.4.3), the body height would not return to normal.

67
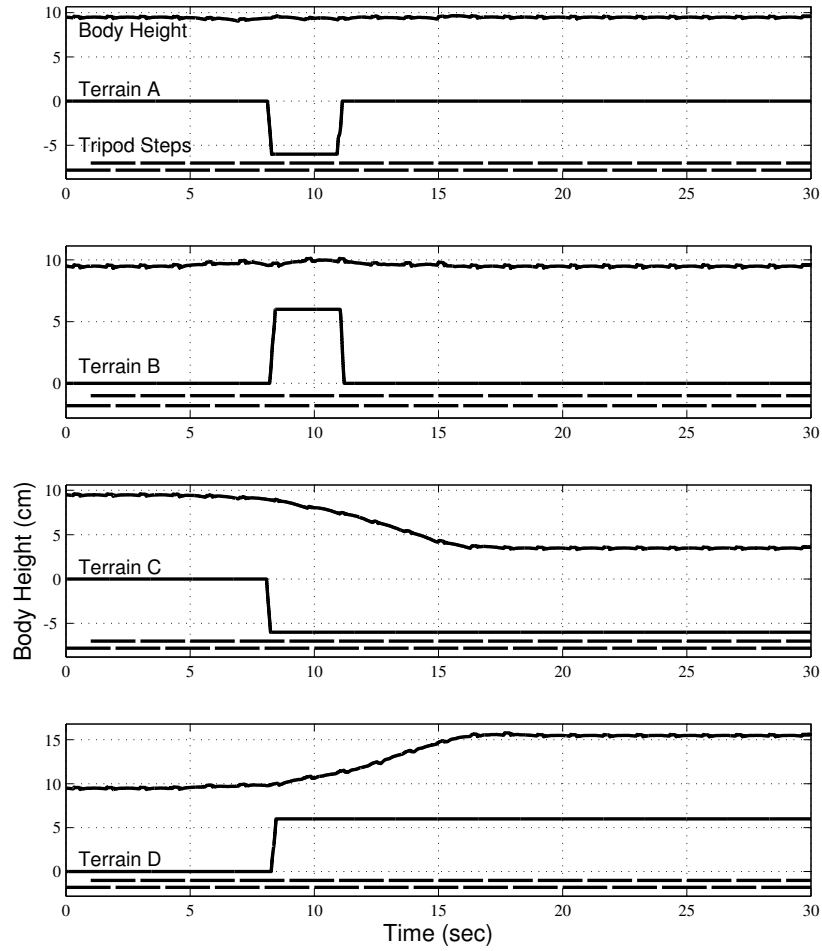
Figure 6.3: Body height of the hexapod walking on different terrains using the alternating tripod gait in simulation. (Adapted from [42])

The rate of slow depression Δ_{SD} and slow elevation Δ_{SE} dictates the number of steps needed by the hexapod to reach D_{PRE} which, in effect, controls the body height. The alternating tripod gait was used by the hexapod in the remaining experiments as well. The Δ_{SD} rate for this experiment was $0.01 * \Delta_{FD}$ while the Δ_{SE} was $0.015 * \Delta_{FD}$ where the Δ_{FD} is 0.4 *mm* per control step. The control step in simulation is 1 *ms* (frequency 1 *KHz*). The same rates have been used for other simulation experiments unless stated.

68

Figure 6.4: Walking over an obstacle: Foot depression and foot force of the front right leg of the hexapod as it passes over an obstacle using the alternating tripod gait in simulation.

Figure 6.4 shows the foot depression and foot force of the front right leg and body height of the hexapod as it walks on Terrain B in simulation. The body height is measured from the geometric center of the hexapod to the terrain. The figure shows three steps taken by the front right leg before, during and after the obstacle. The first and the third steps are on the same height of the terrain. In each of the three steps, the leg enters the $S1$ state and depresses the foot at a constant rate (Δ_{FD}). Around 3 sec, when the leg contacts the ground early, the leg enters the $S4$ state and depresses the foot using Δ_{SD}. The foot depression does not reach D_{PRE} but increases the body height slightly. As the front right leg lifts the body (state $S4$), the middle left leg (not shown in figure) loses ground contact. Due to this, the middle left leg enters the $S1$ state again to depress the foot and regain ground contact. At the next step, the front right leg returns to normal cyclic

69

pattern. This behavior can be verified using the FTP controller states in Fig. 4.2. Please note that the terrain in the third subplot of the Fig. 6.4 does not match the stance phase of the leg in the first subplot. This is because the front leg is further away from the hexapod body at the end of the flight phase.
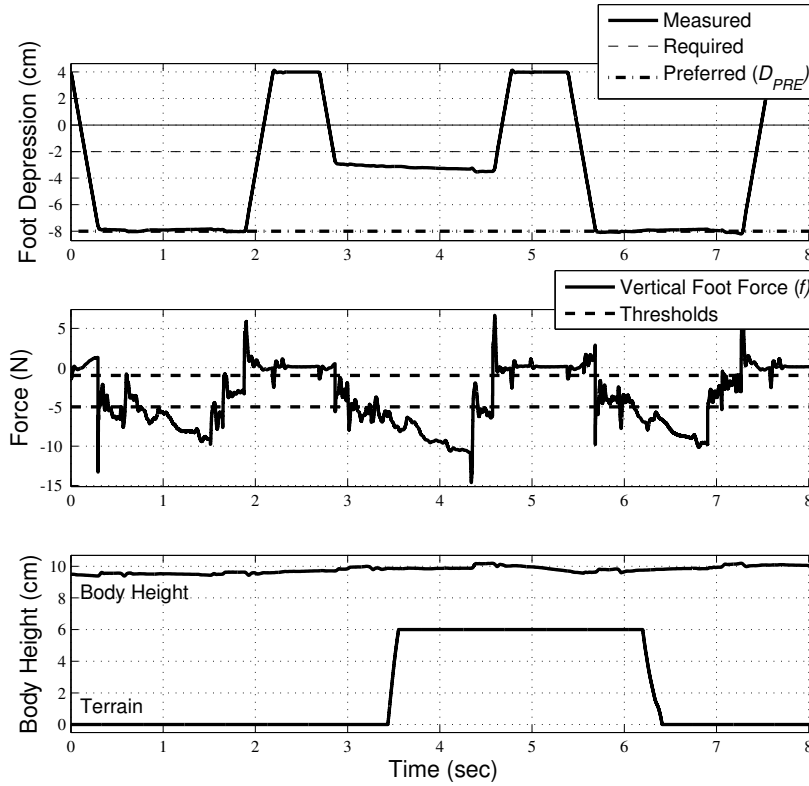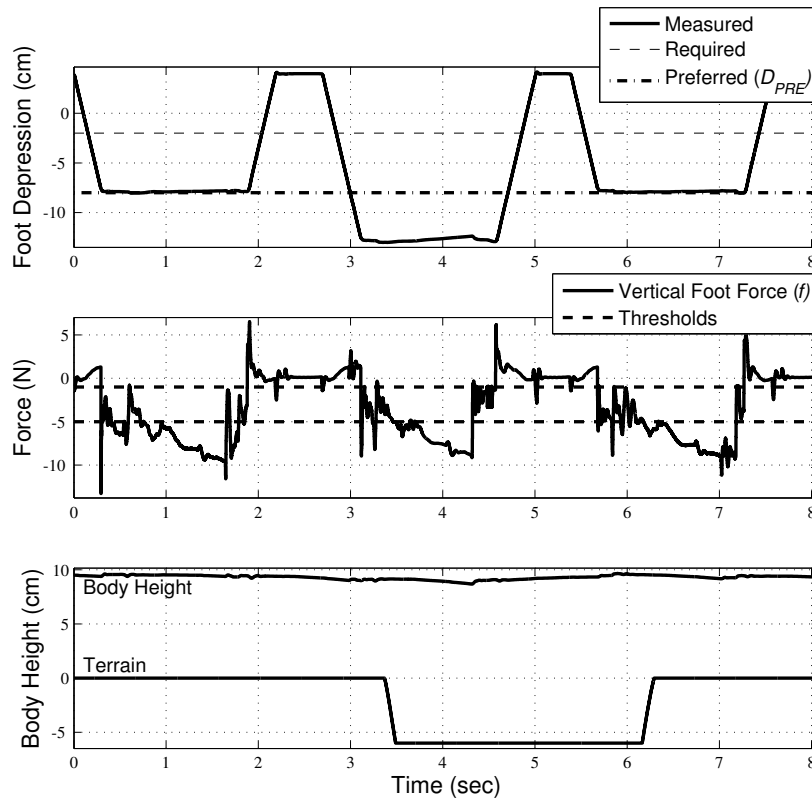

Figure 6.5: Walking over a gap: Foot depression and foot force of the front right leg of the hexapod as it passes over a gap using the alternating tripod gait in simulation.

Figure 6.5 shows the foot depression and foot force of the front right leg and body height of the hexapod as it walks on Terrain A in simulation. The first step is similar to the first step in Fig. 6.4. However, when the leg tries to reach for the ground around the 3 *sec* mark, the leg is unable to do so and continues to depress the foot at a constant rate (Δ_{FD}). After ground contact, the leg enters the $S3$ state and elevates the foot using Δ_{SE}. The foot depression does not reach D_{PRE}

70

but decreases the body height slightly. At the next step, the front right leg returns to normal cyclic pattern.

Figure 6.6: Walking up a step: Foot depression and foot force of the front right leg with body height as the hexapod walks up a step in simulation. (Adapted from [42])

Figure 6.6 shows the foot depression and foot force of the front right leg with body height as the hexapod walks on Terrain D in simulation. At each step, the leg enters the $S1$ state and depresses the foot at a constant rate (Δ_{FD}) until the foot touches down. Around 3 *sec*, the leg contacts the ground early than expected and enters the $S4$ state to slowly depress the foot. The foot depression does not reach D_{PRE} but lifts the body. The same happens during step 3, 4 and 5 and the foot depression increases at each step until it reaches D_{PRE} and the body height reaches back to its original walking height. After step 5, the front right leg returns to normal cyclic pattern and the body height remains consistent as it walks over the flat terrain.
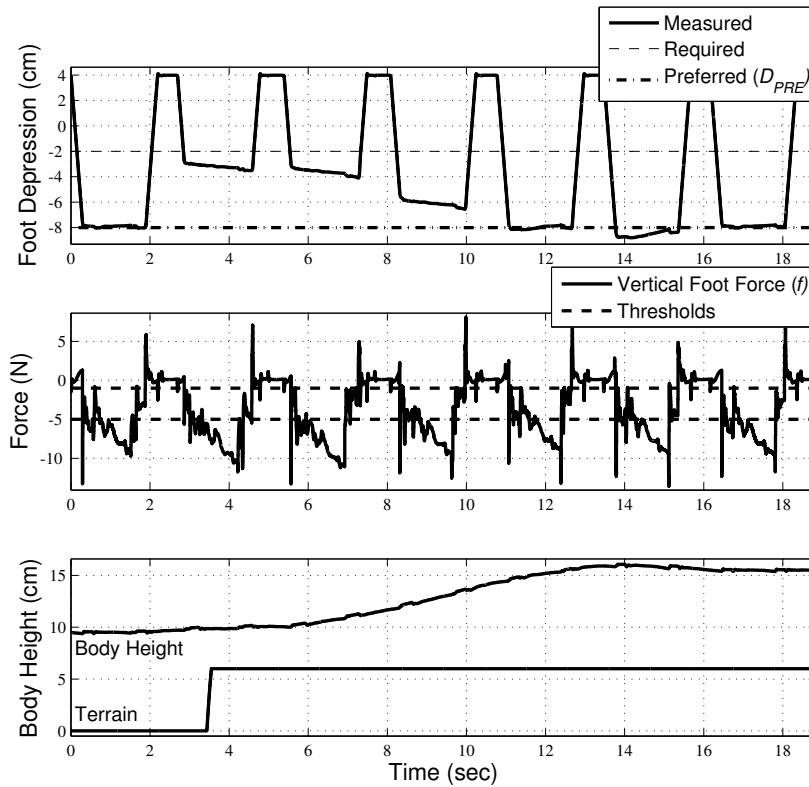
71
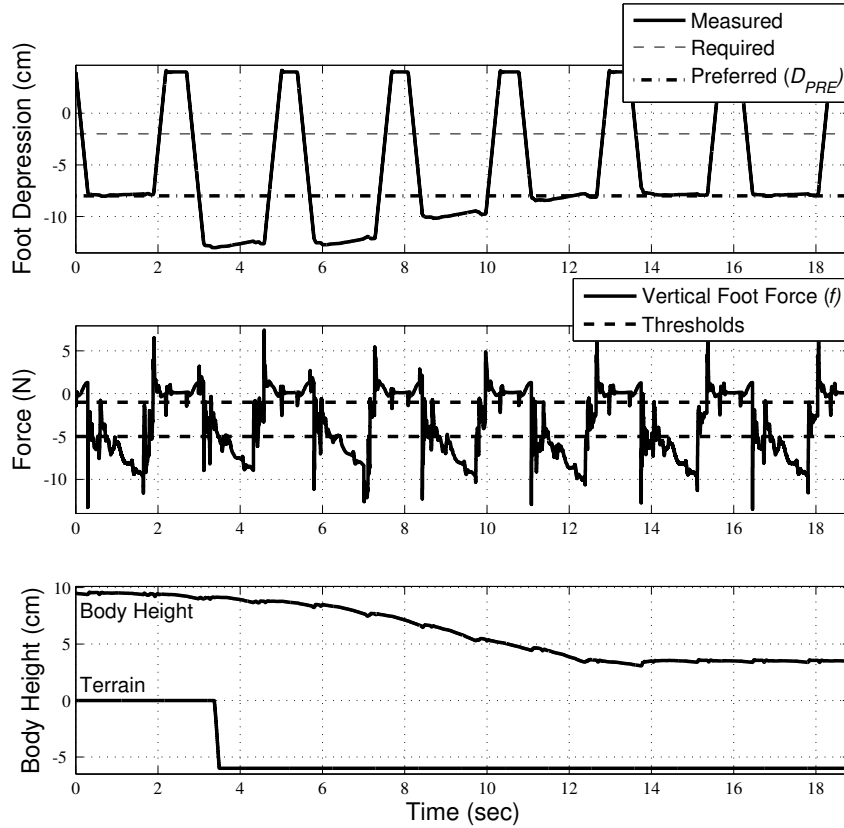
Figure 6.7: Walking down a step: Foot depression and foot force of the front right leg with body height as the hexapod walks down a step in simulation. (Adapted from [42])

Figure 6.7 shows the foot depression and foot force of the front right leg with body height as the hexapod walks on Terrain C in simulation. As the hexapod walks down the step, each leg achieves ground contact using Δ_{FD}. Similar to Fig. 6.6, the leg length works toward the preferred foot depression D_{PRE} which brings the body back to its original walking height. The Figs. 6.6 and 6.7 shows how the states $S3$ and $S4$ help the hexapod regain the preferred foot depression D_{PRE}. The hexapod regains the preferred foot depression D_{PRE} after three steps in these figures.

Figure 6.8 shows the hexapod in simulation walking over a series of steps going up (Terrain I). Figure 6.9 shows the body height (relative to the ground height) of the hexapod walking over Terrains H and I in simulation using the alternating tripod gait. As can be seen in the figure, the

72
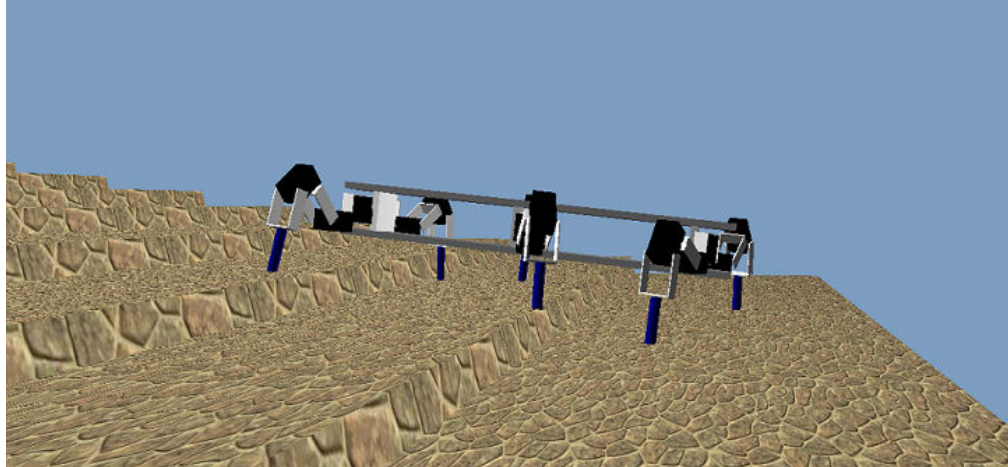
Figure 6.8: Hexapod in simulation walking on a series of steps.
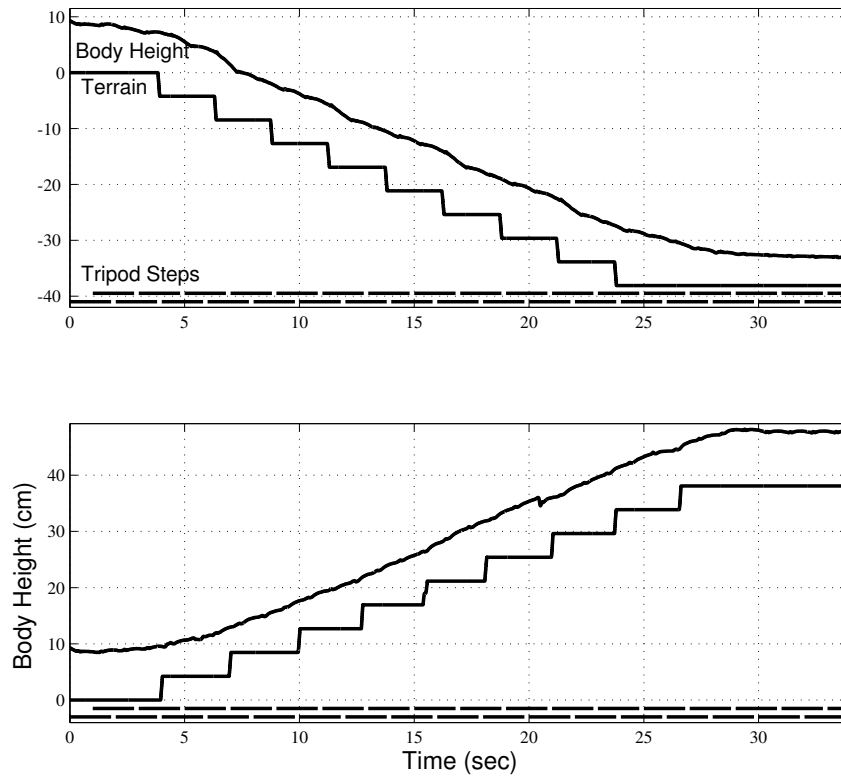
Figure 6.9: Body height of the hexapod walking on a sequence of steps using the alternating tripod gait in simulation.

73

body height remains close to the actual terrain even when some slips are involved (around 20.5 *sec* mark in the bottom subplot). Same Δ rates described previously were used for this experiment.
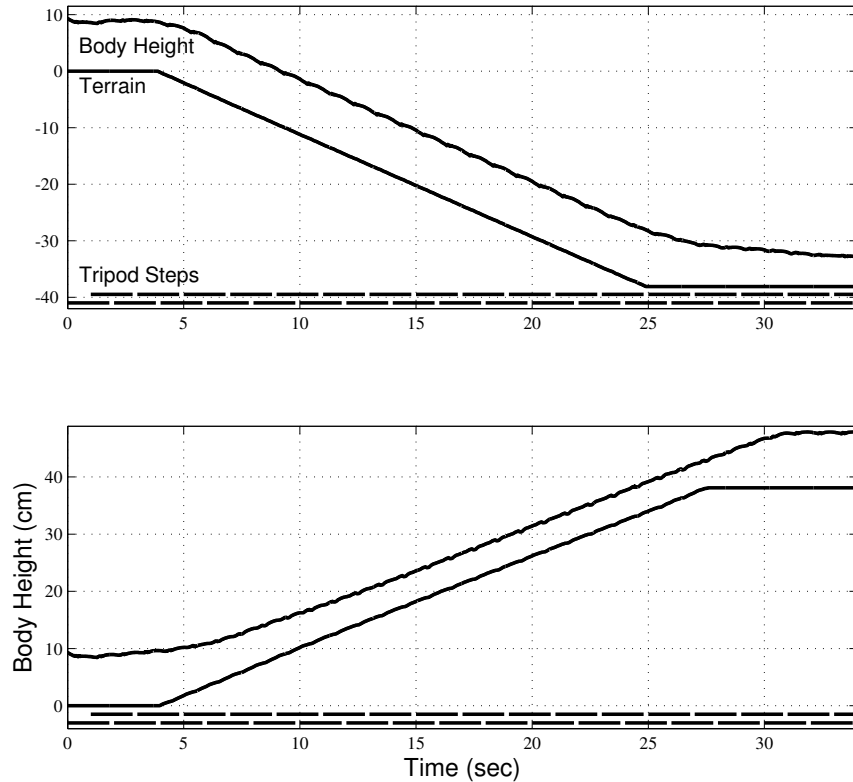
Figure 6.10: Body height of the hexapod walking on a incline using the alternating tripod gait in simulation.

Figure 6.10 shows the body height (relative to the ground height) of the hexapod walking over Terrains F and G in simulation using the alternating tripod gait. In both the subplots, the body height of the hexapod remains fairly stable as it walks down and up the slope. One thing to note is that the body height, even though looks smooth, is not maintained as the hexapod walks up the incline (Terrain G). The body height continues to decrease even though the slow depress rate Δ_{SD} is the same in Fig. 6.9 and 6.10. Even though the Terrain I has greater change in terrain height due to a step compared to Terrain G, the body height remains closer to the desired in Terrain I

74
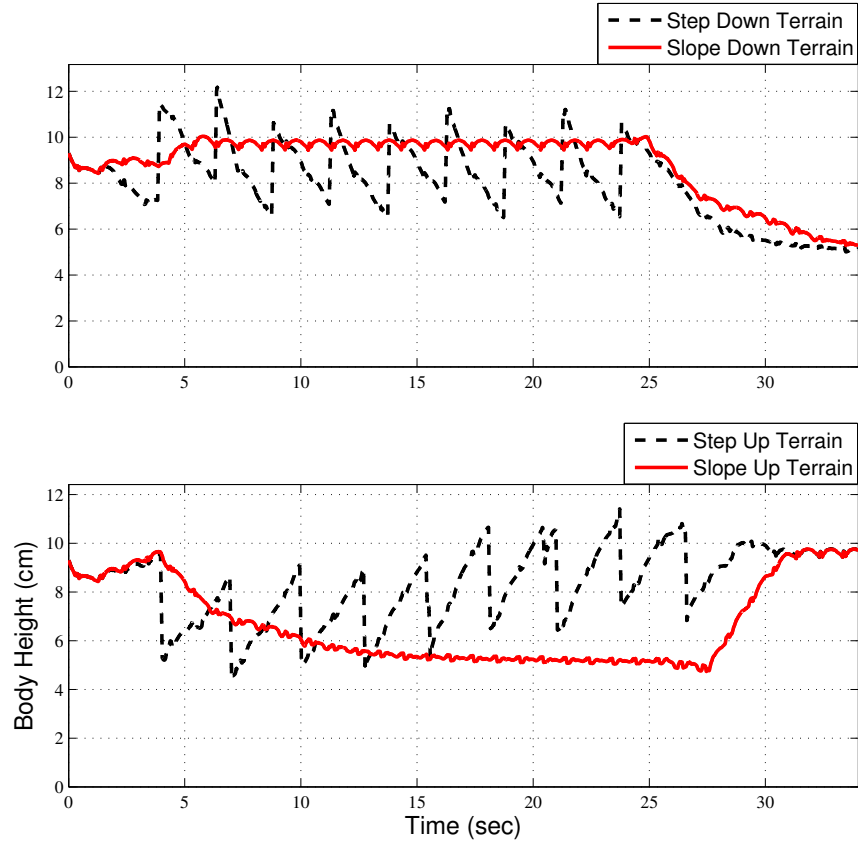
Figure 6.11: Comparison between the absolute body height of the hexapod as the hexapod walks up and down a terrain with steps and an incline.

than in Terrain G. The difference in walking can be more clearly seen in Fig. 6.11 which shows the actual body height of the hexapod. The spikes in the body height when going down or up a terrain with steps are due to the sudden change in terrain height due to the steps. The body height of the hexapod is fairly similar when going down a slope. However, when walking on Terrain I, the hexapod is able to recover due to the presence of flat areas in the terrain which is not the case in Terrain G. A leg walking on Terrain I spends more time in the fast depress mode and is able to maintain the body height. This means that, while walking on Terrain G with the same slope as Terrain I, the slow depress rate Δ_{SD} needs to be higher for the hexapod. This can be verified in Section 6.2.4.

75

6.2.3 Comparison with Position Controller
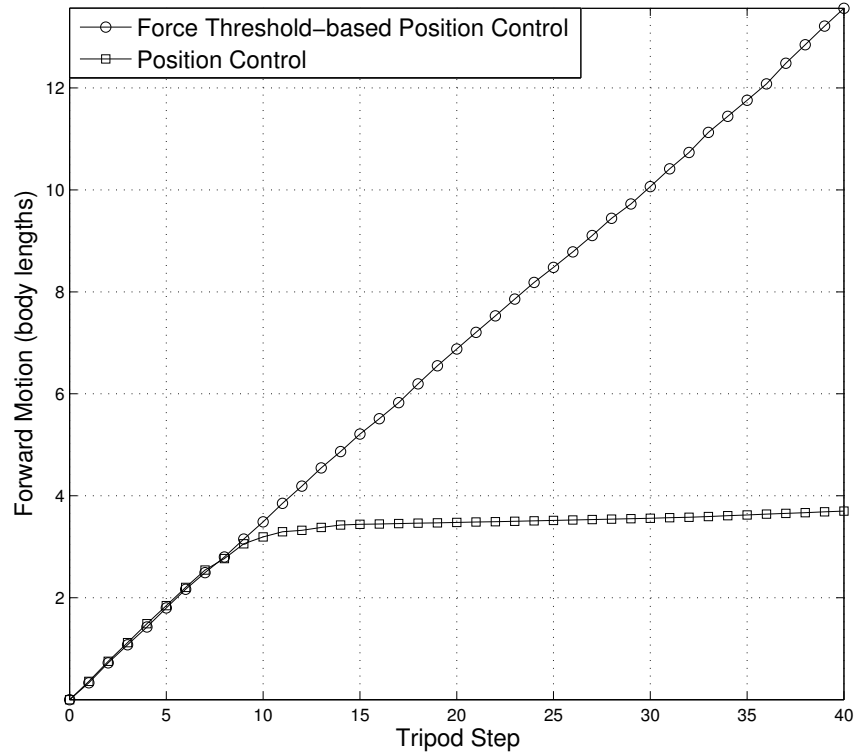
Figure 6.12: Comparison between the FTP controller and a position controller walking over a randomly generated uneven terrain. (Adapted from [43])

Figure 6.12 shows the comparison between the FTP controller and a position controller as the hexapod walks on a random built Terrain E. Although other algorithms exist for legged locomotion on irregular terrain, a pure position control algorithm is the only control algorithm known to the author which does not require 1) vestibular sensing of body state, 2) terrain sensing, or 3) interleg cooperation, and therefore is the only appropriate comparison for the FTP controller at the moment. The figure shows the displacement of the hexapod in terms of body length (Table 5.1). After some steps, the hexapod under position control arrives at a location in which the feet do not

reach the terrain and results in sluggish motion. The FTP controller, however, constantly seeks the ground resulting in forward motion at each step.
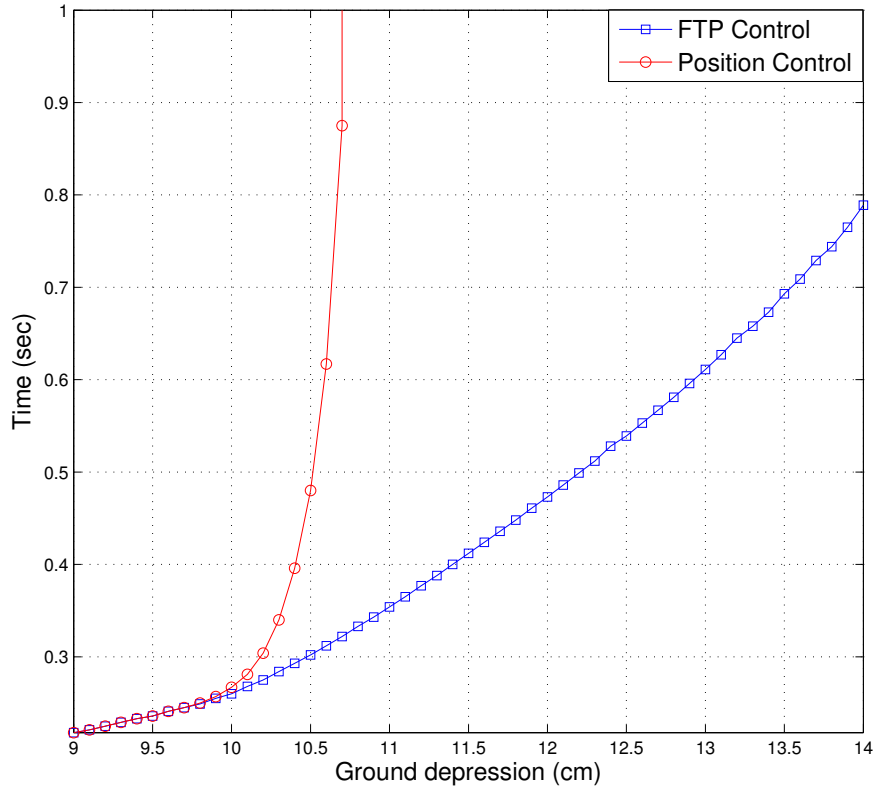
Figure 6.13: Timing comparison between the FTP controller and a position controller for a leg to touch the ground at different depths. Position control of the hexapod leg results in terrain misses after a certain depth of ground depression while the FTP control of the hexapod leg forces the foot to engage the ground. (Adapted from [62])

Figure 6.13 shows the timing comparison between the FTP controller and a position controller. The figure shows the time taken by the foot to touch the ground at different depths. After a certain depth of the ground depression, the leg using feed-forward position controller is unable to touch the ground. Also, when the ground is a little lower than expected, the time taken to touch the ground increases and the leg is not able to produce the force needed for a proper step. On the other

77

side, the FTP controller creates sufficient vertical force to reach the ground and produce enough force for forward motion.

6.2.4   Changing Elevate and Depress Rates
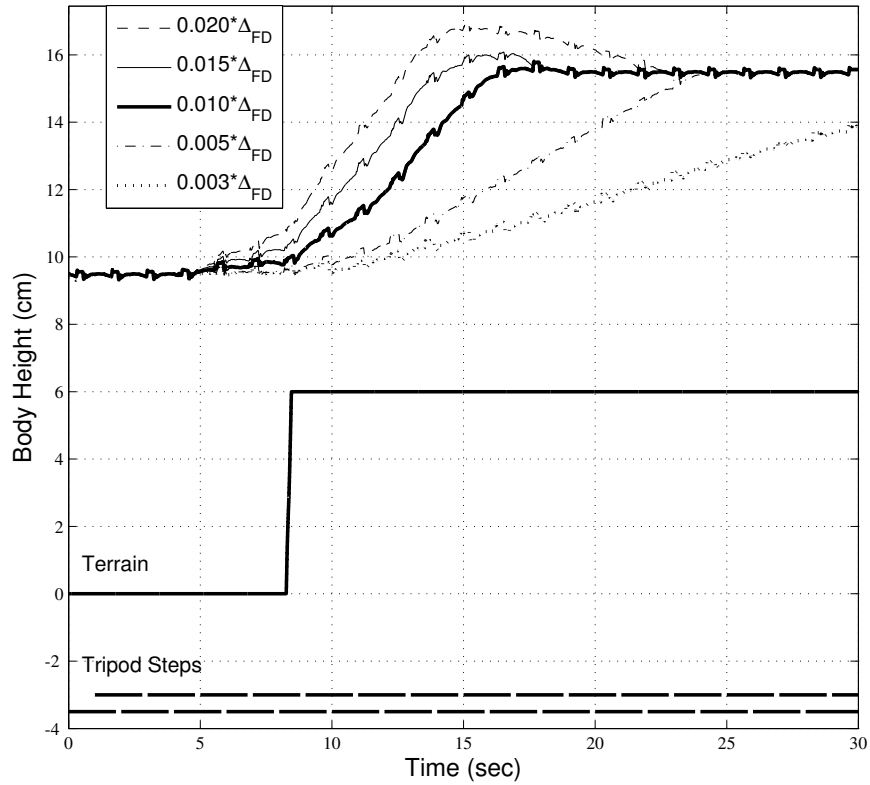
Figure 6.14: Effect of slow foot depression: Body height of the hexapod as it walks up a step using different Δ_{SD} in simulation. The figure shows the time taken by the hexapod to regain the desired body height. (Adapted from [42])

Figure 6.14 shows the body height of the hexapod as it walks on Terrain D in simulation using multiple slow depression (Δ_{SD}) rates (State $S4$ in Fig. 4.2). As can been seen, the time (or number of steps) for the body height to return to the original height depends on the rate. The $\Delta_{SD} =$

$0.010 * \Delta_{FD}$ works very well for the simulated terrains described. As the step size is increased, higher rates are needed for the body height to return to normal in a reasonable number of steps.
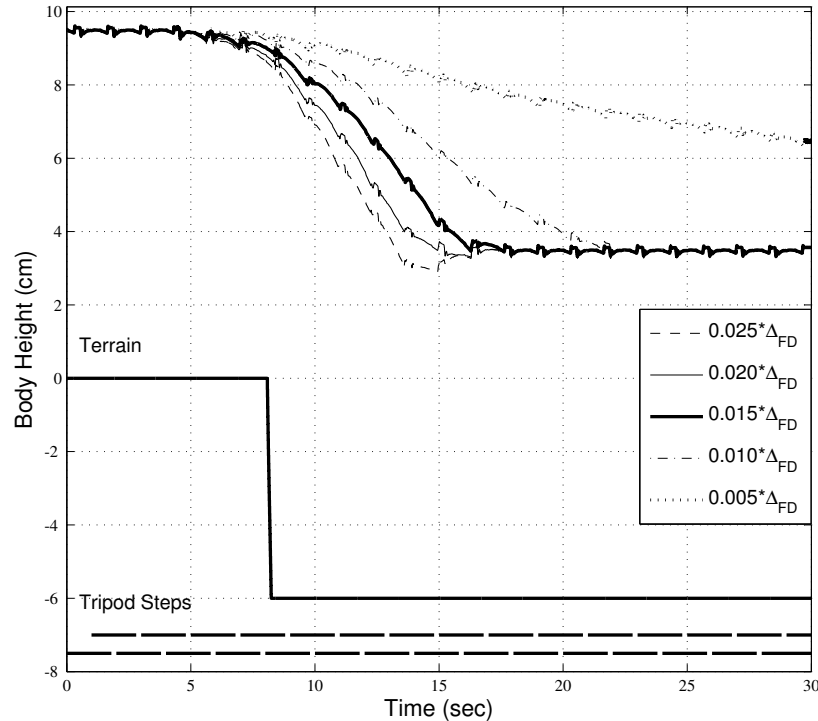
Figure 6.15: Effect of slow foot elevation: Body height of the hexapod as it walks down a step using different Δ_{SE} in simulation. The figure shows the time taken by the hexapod to regain the desired body height.

Figure 6.15 shows the body height of the hexapod as it walks on Terrain C in simulation using multiple slow elevate (Δ_{SE}) rates (State $S3$ in Fig. 4.2). Similar to Fig. 6.14, the time (or number of steps) for the body height to return to the original height depends on the rate. The $\Delta_{SE} = 0.015 * \Delta_{FD}$ works very well for the terrains described. As the step size is increased, higher rates are needed for the body height to return to normal in a reasonable number of steps.

The Fig. 6.14 and 6.15 show the effect of using different Δ rates when transitioning from one surface to the other. The body height has to be regained by the hexapod quickly after the

79

transition but the body height has to be maintained when the terrain is changing continuously. Figure 6.16 shows the body height of the hexapod as it walks up and down a continuous incline (Terrain F and G). As can be seen from the figure, any Δ_{SE} greater than or equal to $0.010 * \Delta_{FD}$ is fairly good for maintaining the body height, while any Δ_{SD} greater than or equal to $0.025 * \Delta_{FD}$. As can be seen in the figure, $\Delta_{SD} = 0.020 * \Delta_{FD}$ used in Fig. 6.10 is not enough to maintain the body height.
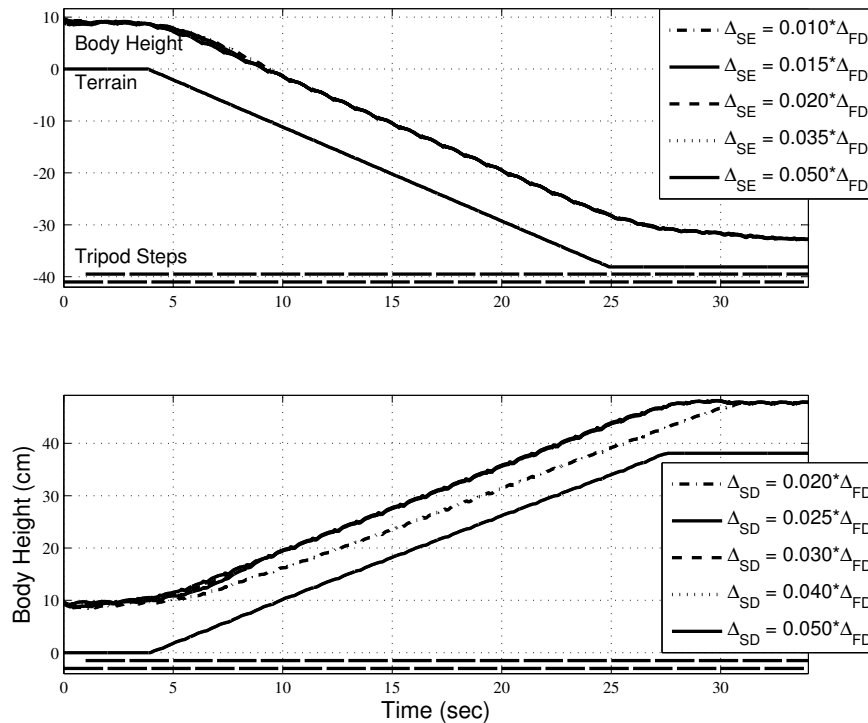
Figure 6.16: Effect of slow foot depression/elevation: Body height of the hexapod as it walks down and up a slope using different Δ_{SE} and Δ_{SD} in simulation.

Figure 6.17 shows the body height of the hexapod as it walks up and down continuous steps (Terrain H and I). Even though most of the Δ rates are acceptable for walking, $\Delta_{SD} = 0.020 * \Delta_{FD}$ is not the optimal solution. Thus, Δ rates describe before ($\Delta_{SE} \geq 0.010 * \Delta_{FD}$ and $\Delta_{SD} \geq 0.025 * \Delta_{FD}$) can be used as the minimum rates that could be used for walking.

80
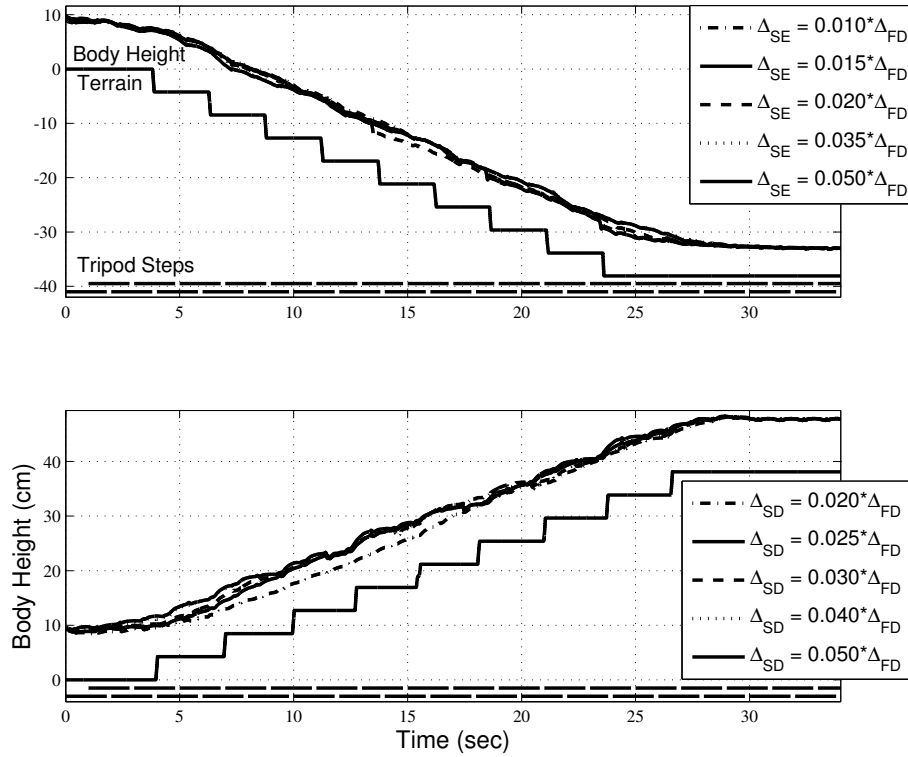
Figure 6.17: Effect of slow foot depression/elevation: Body height of the hexapod as it climbs down and up steps using different Δ_{SE} and Δ_{SD} in simulation.

6.2.5   Relationship between Delta Rates and Terrain

One way to study the impact of the Δ rates on the walking behavior of the hexapod is by checking the stability of the body while walking and whether or not, the required parameters were met. For a hexapod to walk properly, the body has to be lifted above the ground at all times and have some forward motion at each step so as not to get stuck at any terrains. Also, since the input for the FTP algorithm is the preferred foot depression D_{PRE}, which is based on the zero-force height in a stick insect, the body height could also be checked to see if the individual legs are able to achieve the desired body height irrespective of the terrain.

81

Figure 6.18: Relationship between terrain slope and Δ_{SE}: Percentage of the experimental run the body height is within 5% error margin of the actual body height while walking down an incline when the slope of the incline and Δ_{SE} rate are changed.

Since the reason for the choice of the zero-force height in a stick insect is not known, the FTP algorithm can, therefore, be judged only based on how close the body height it maintains to the desired body height while walking on different terrains. The FTP algorithm was run in simulation on Terrains F and G with varying incline angles and with varying Δ rates to check how close the algorithm maintained the body height on different terrains and also to find if there is a specific relation that could be found in between the terrain and the Δ rates such that the walking could be optimized for different terrains using different Δ rates for different terrains.

In each experiment, the body height was recorded and compared with the desired body height. If the body height was within 5% of the desired body height during most of the walking run (for example 90% of the test run), the particular Δ rates could be called a good fit for that particular terrain. The concept of body height with an error percentage (of the desired body height) and

82

Figure 6.19: Relationship between terrain slope and Δ_{SE}: Percentage of the experimental run the body height is within 25% error margin of the actual body height while walking down an incline when the slope of the incline and Δ_{SE} rate are changed.

time that body height is maintained (percentage of run) is used for these experiments because the Terrains F and G have plane transitions in the start and end of the terrain which cause some body height deviation. Also, when walking on uneven platform the body cannot be exactly maintained.

When walking up or down a step or slope there is a possibility that the body hits the ground. When the body hits the ground, the test results are not included. Also, when the hexapod is not able to achieve the goal of finishing the walking experiment either due to toppling or slipping, those results were also not included.

Figure 6.18 shows the percentage of the experimental run the body height remains with the 5% error margin of the actual body height while walking down an incline with different slopes and Δ_{SE} rate are changed. As can be seen from the figure, a Δ_{SE} rate of zero (Force Feedback Control in Section 3.4.3) is never able to achieve the desired height. As the Δ_{SE} rate is increased the body
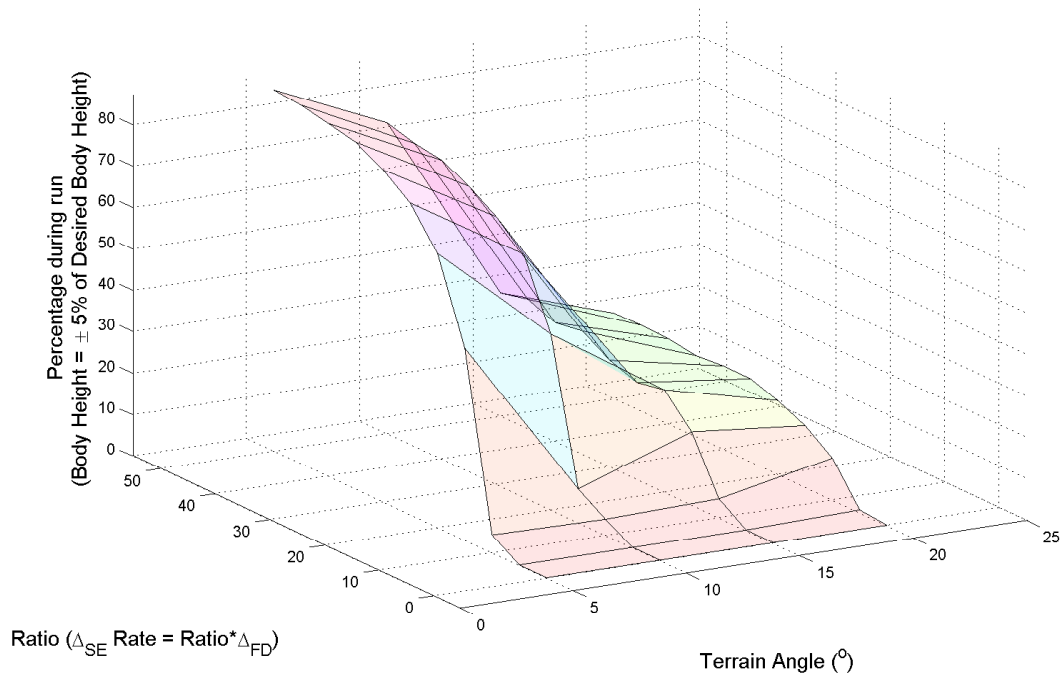
83

Figure 6.20: Relationship between terrain slope and Δ_{SD}: Percentage of the experimental run the body height is within 5% error margin of the actual body height while walking up an incline when the slope of the incline and Δ_{SD} rate are changed.

height is closer to the desired more percentage of the time. Looking at the graph, one can say that $\Delta_{SE} < 0.020 * \Delta_{FD}$ will not result in a smooth walking behavior. The figure also shows that for higher inclines increasing the Δ_{SE} does not make the body height stable.

Figure 6.19 shows the percentage of the experimental run the body height remains with the 25% error margin of the actual body height while walking down an incline with different slopes and different Δ_{SE} rate are changed. Figure 6.19 confirms the notion that $\Delta_{SE} \geq 0.020 * \Delta_{FD}$ is needed when walking down an incline such that the legs are able to lift the body and maintain the body height during the slope and terrain transitions.

Figure 6.20 shows the percentage of the experimental run the body height remains with the 5% error margin of the actual body height while walking down an incline with different slopes and different Δ_{SD} rate are changed. The behavior is similar to the Fig. 6.18. Please note that the
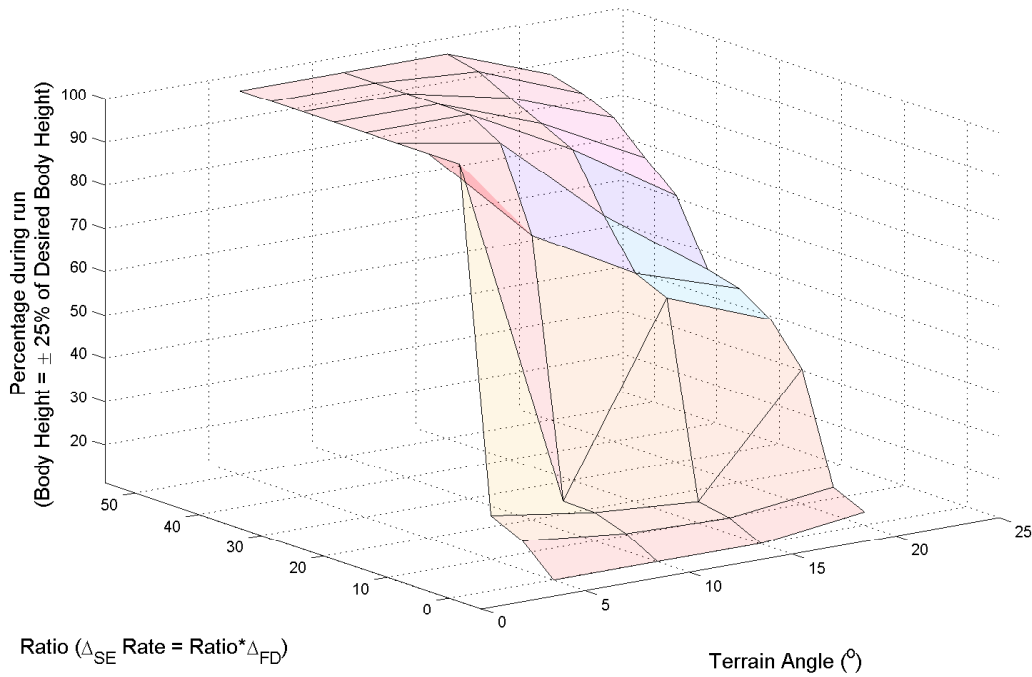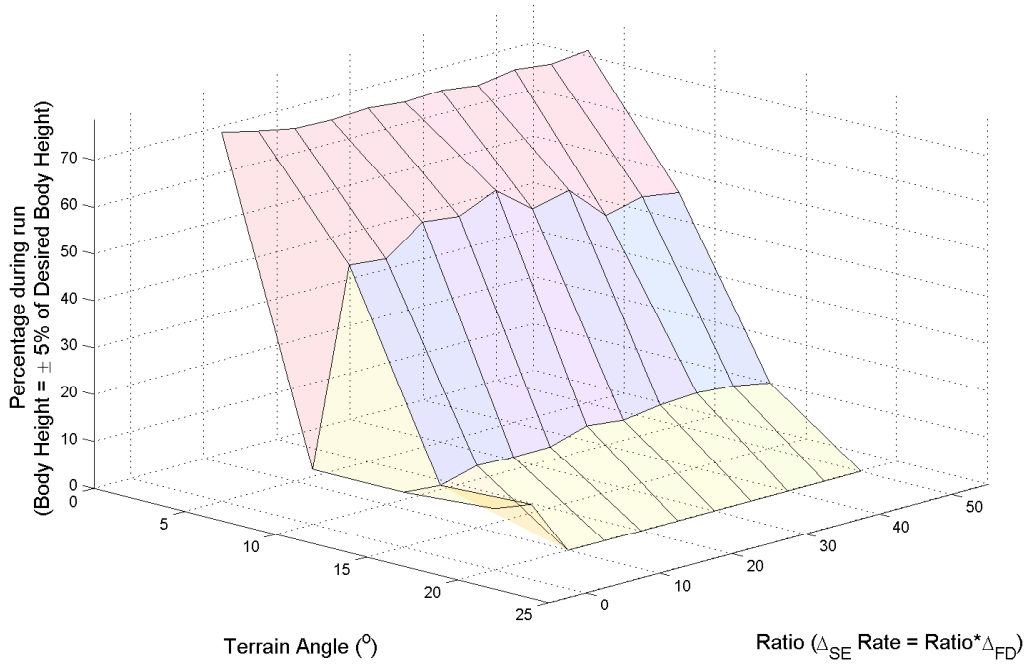
84
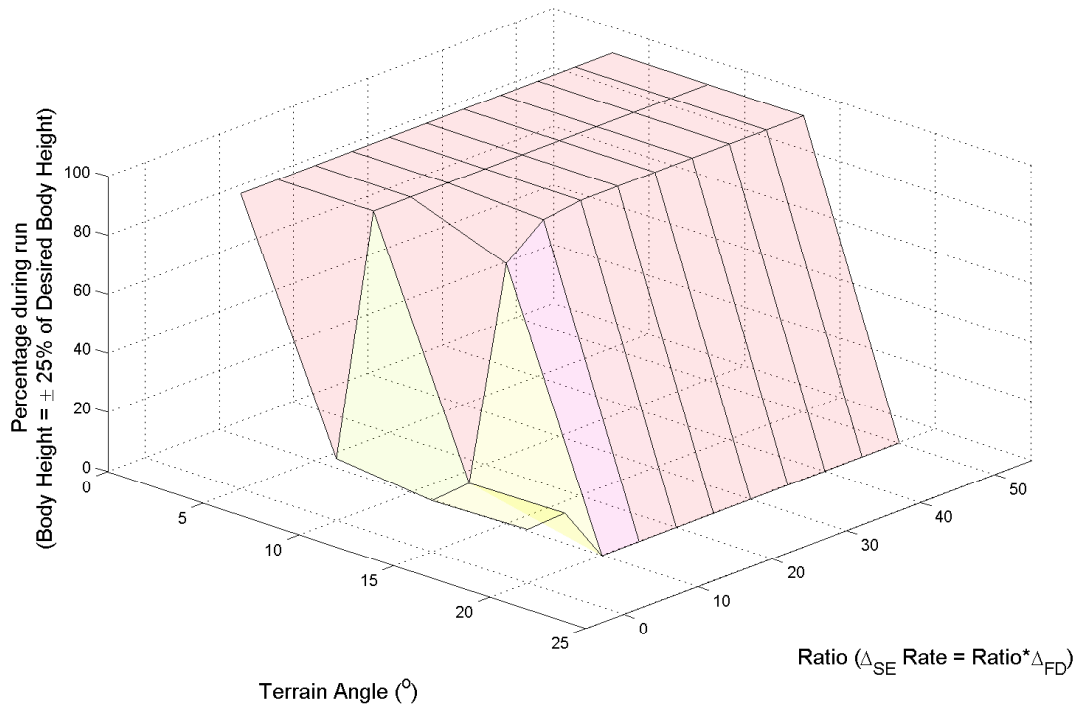
Figure 6.21: Relationship between terrain slope and Δ_{SD}: Percentage of the experimental run the body height is within 25% error margin of the actual body height while walking up an incline when the slope of the incline and Δ_{SD} rate are changed.

figure is reversed compared to Fig. 6.18. Also, note that even if the Δ_{SD} is zero (position control with ground sensing only) the body height is close to the desired some of the time unlike Fig. 6.18. In Fig. 6.20, the hexapod is not able to complete the terrain walking irrespective of the Δ_{SD} rate except in the case of zero where the hexapod completes the test but is not able to maintain the desired body height for most of the experiment.

Figure 6.21 shows the percentage of the experimental run the body height remains with the 25% error margin of the actual body height while walking down an incline with different slopes and different Δ_{SD} rate are changed. By evaluating the Fig. 6.20 and 6.21, one can conclude that when $\Delta_{SD} \geq 0.015 * \Delta_{FD}$ the hexapod is able to maintain the body height to a desired level while walking up an incline with slopes between $0°$ and $15°$.

85

6.3 Hardware Results

Following sections provide the data results from testing the FTP algorithm on the experimental hexapods, HexaBull-1 and HexaBull-2. As explained in the previous chapter, the FTP algorithm running on three CM-700 boards produce the walking behavior in the hexapod robot.

6.3.1 Testing Terrains

Testing environments described in Section 6.2.1 for testing the simulation code were recreated using wooden planks and blocks. Terrains A to E were created to test the hardware platform. Terrains A to D were built with obstacle and steps of height 6.35 *cm* and gaps of height 10.16 *cm*. The randomly generated Terrain E consisted of square blocks of sizes 3.8 *cm*, 7.6 *cm*, 11.4 *cm*, and 15.2 *cm* randomly placed on the ground. Wooden planks and beams of width of multiples of 1.5 *in* were used to create the terrains.

6.3.2 Effects on Body Pitch

Figure 6.22 shows the foot depression, the compliant actuator position of the front right leg and the body pitch as the experimental hexapod, HexaBull-1, walks on Terrain C with a step of height 10.16 *cm*. The body pitch of the hexapod is found using a $SCA121T$ dual axis inclinometer which is configured to record the body pitch of the hexapod. The inclinometer data is not used by the FTP algorithm. The first step taken by the leg is the down the step. The leg enters the $S1$ state and depresses the foot at a constant rate (Δ_{FD}). After foot touchdown, the leg enters the $S3$ state and elevates the foot using Δ_{SE}. This happens for another step as the hexapod walks down the step. After some steps, the body height and body pitch of the hexapod reaches back to the original level. As can be seen in Fig. 6.22, the compliant actuator position has a very similar shape when

86

Figure 6.22: Walking down a step: Foot depression and compliant actuator position of the front right leg along with the body pitch as the experimental hexapod, HexaBull-1, walks down a step. (Adapted from [42])

compared with the foot forces in simulation (Fig. 6.7) validating the use of a compliant actuator for recording foot forces. The Δ_{SD} rate for this experiment was $0.08 * \Delta_{FD}$ while the Δ_{SE} was $0.03 * \Delta_{FD}$ where the Δ_{FD} is 1 *cm* per control step. The control step on the experimental hardware is 25 *ms* (frequency 40 *Hz*). The same rates have been used for other hardware experiments for HexaBull-1 unless stated.

Figure 6.23 shows the foot depression, the compliant actuator position of the front right leg and the body pitch as the experimental hexapod walks on Terrain D with a step of height 6.35 *cm*. The leg takes two steps before the leg reaches the step on the terrain. The body pitch of the hexapod reaches back to the same level after several steps.
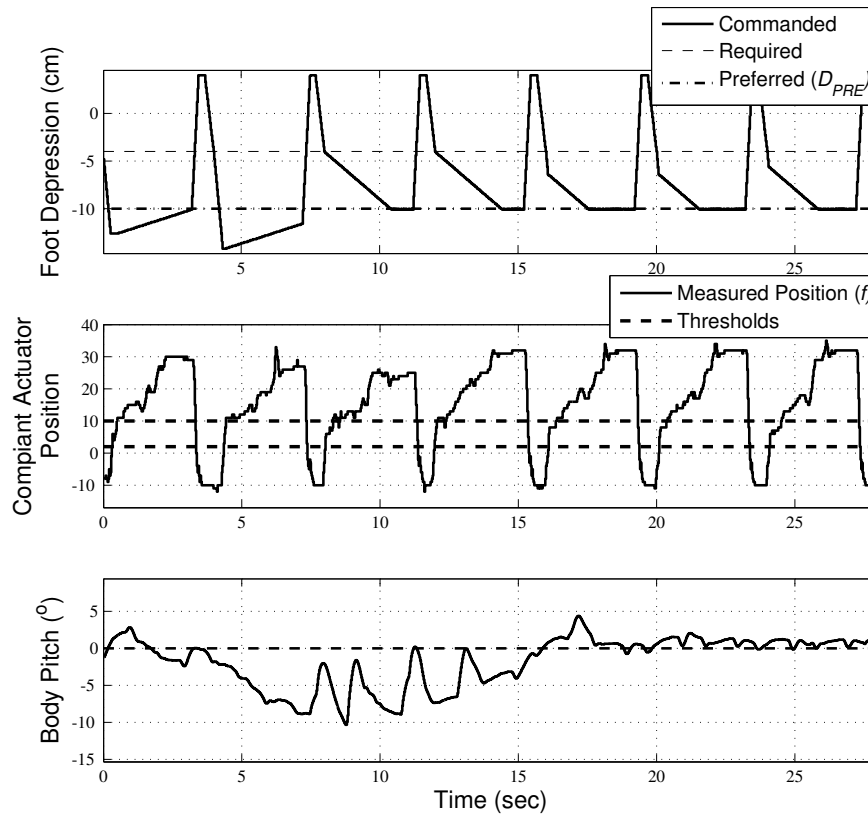
87
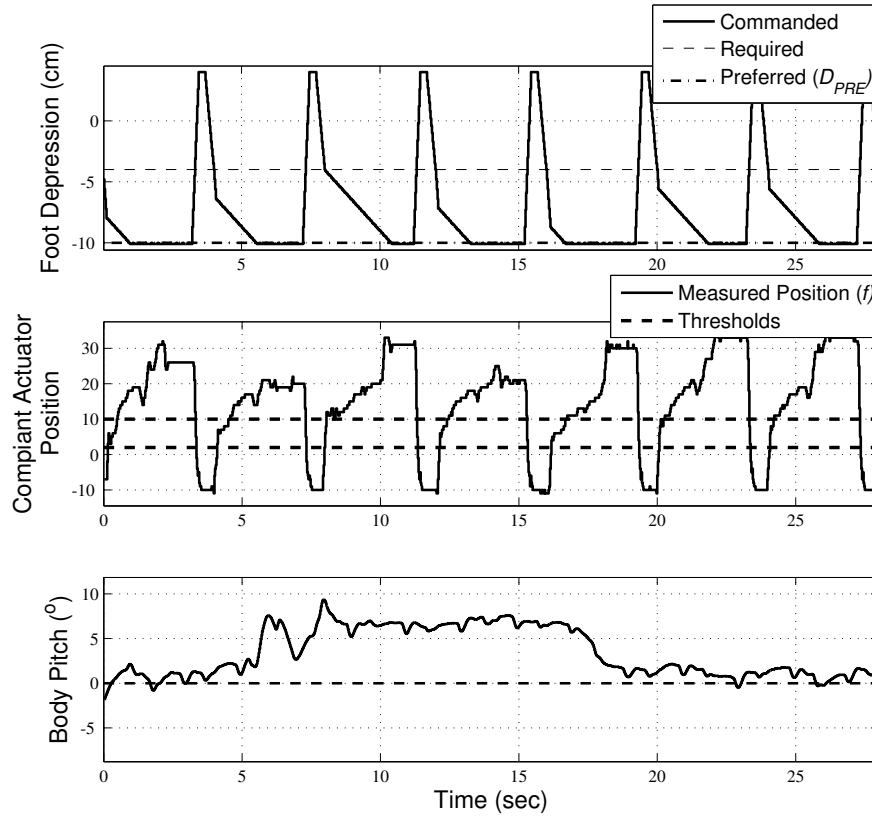
Figure 6.23: Walking up a step: Foot depression and compliant actuator position of the front right leg along with the body pitch as the experimental hexapod, HexaBull-1, walks up a step. (Adapted from [42])

Comparing Fig. 6.23 with Fig. 6.6 and 6.7, it can be seen that the Δ values used in simulation are much different than the ones used with the experimental hexapod, HexaBull-1; especially Δ_{SD}. The reasons for higher Δ values is slippage and body sag. As explained in Section 5.7, a higher Δ_{SD} is needed to lift the body higher after touchdown to compensate for this slippage and to increase the overall body height. This can be clearly observed in Fig. 6.23. After the body pitch returns to normal on completing the step, the hexapod leg touches down earlier than expected in the next few steps. So larger Δ_{SD} is required for the experimental hexapod HexaBull-1 to maintain its body height.

88

6.3.3   Comparison with Position Controller

Figure 6.24: Stuck hexapod: Screenshots of the experimental hexapod, HexaBull-1, as it walks over a gap in the terrain using the position controller.

To compare the working of the FTP controller with the position controller, the experimental hexapod, HexaBull-1, was tested to go over a gap in the terrain. The behavior of the hexapod in position controller and the FTP controller was recorded. The gap in the terrain was around 7.6 *cm*.

Figure 6.24 shows screenshots of the experimental hexapod walking over the gap in the terrain during one of the tests while using the position controller. Since the foot depression of every leg during the walk does not go past the desired height, the front body of the hexapod start to pitch down as the front legs step off the ledge (seen in Fig. 6.24 (II) and (III)). Therefore when the hexapod has to go over the step, the front part of the hexapod body gets stuck (seen in Fig. 6.24
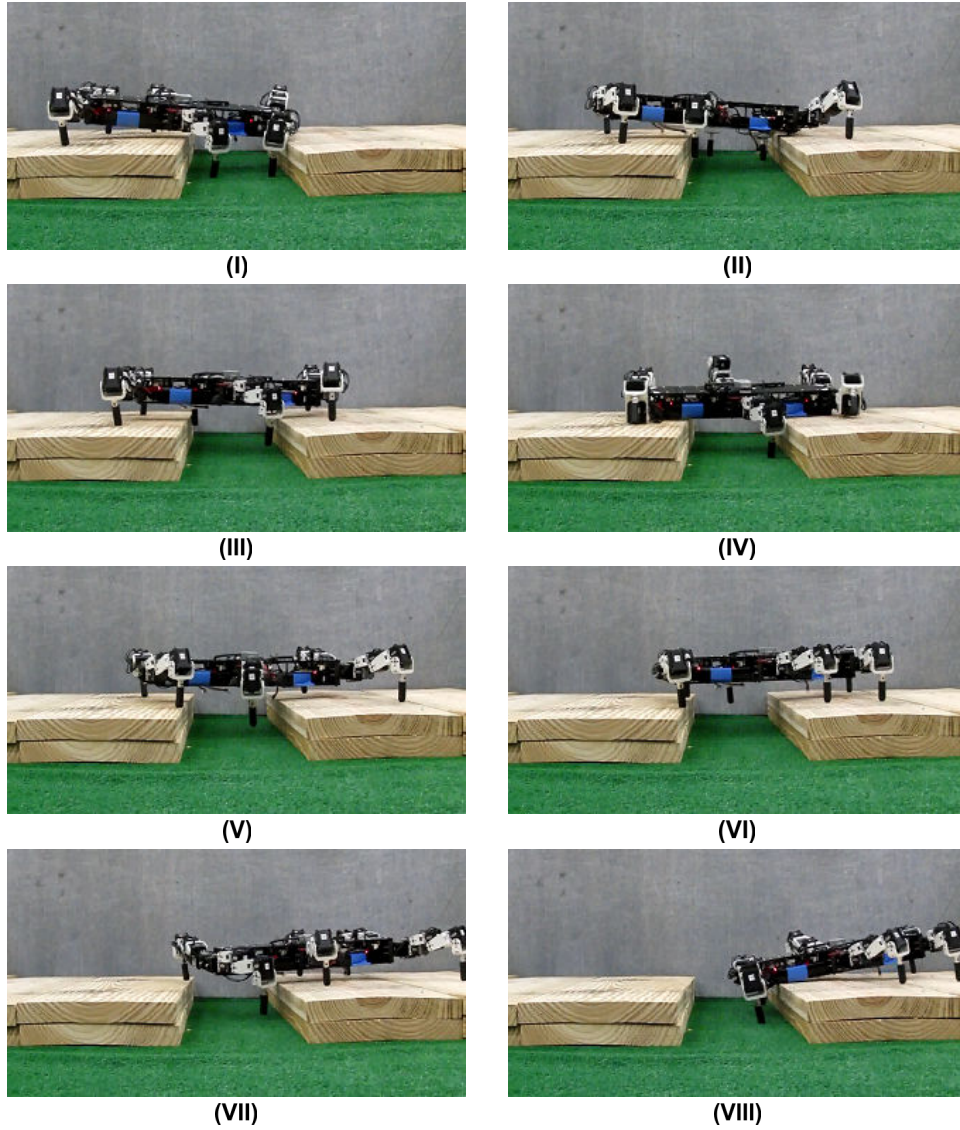
Figure 6.25: Missed ground contacts: Screenshots of the experimental hexapod, HexaBull-1, as it walks over a gap in the terrain using the position controller.

(IV) and (V)). The hexapod gets stuck in that position because the front legs are not able to lift the body as they are limited by the desired height while the middle is not able to make any ground contact during the same time. The hexapod gets stuck and is not able to move from that position.

The main reason the experimental hexapod gets stuck in Fig, 6.24 is because the front legs are not able to lift the body up. However, if the front side of the hexapod contacts the step in

90
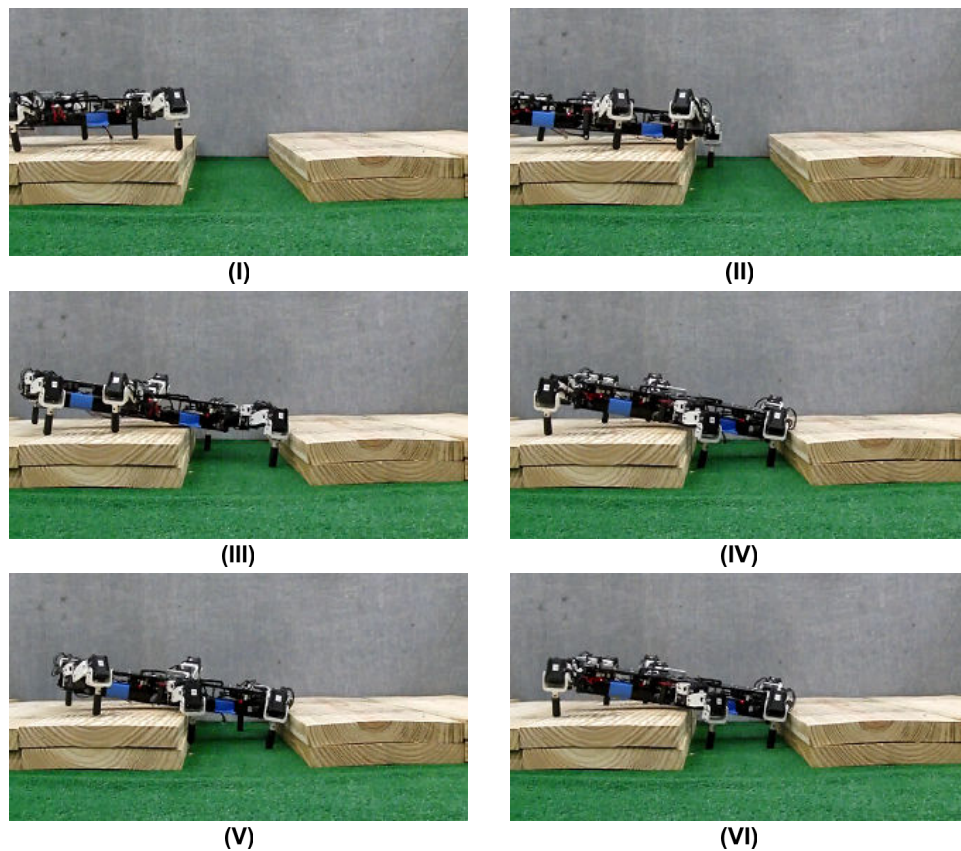
Figure 6.26: Screenshots of the experimental hexapod, HexaBull-1, as it walks over a gap in the terrain using the FTP controller. The gap in the terrain is lower than the terrain by 7.62 *cm*. Subfigures (I) to (X) show the 10 steps taken by the hexapod as it walks over the terrain. The Δ_{SD} and Δ_{SE} are chosen such that the body height remains constant throughout the walking experiment. (Adapted from [42])

such a way that front gets lifted slightly due to friction, front movement is possible. Figure 6.25 shows the experimental hexapod walking over the gap in one such test. However, due to the gap on the terrain, some of the legs are not able to reach the ground resulting in a lot of missed ground contacts. In subplots (III) to (VI) in Fig. 6.25 shows the missed ground contacts by the middle leg. Since the hexapod is walking using the alternating tripod gait where the middle leg holds one side of the hexapod body, the experimental hexapod does fall during such missed ground contacts (subplot (IV) of Fig. 6.25). Same is true from the hind legs in subplots (VII) to (VIII) in Fig. 6.25. Even though the hexapod is able to walk over the terrain, the result is a sluggish walk which causes some wear and tear on the hexapod structure.
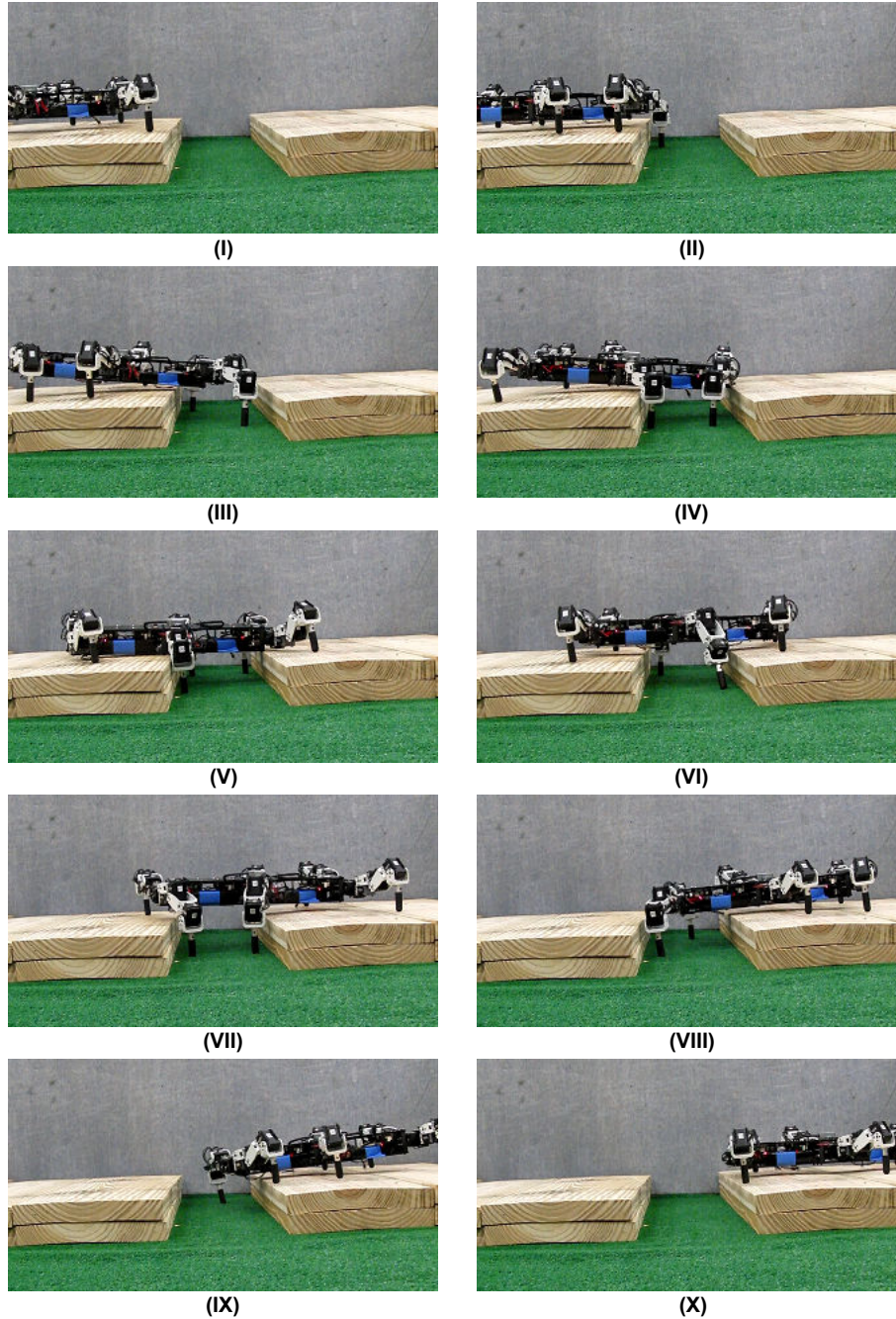
Figure 6.26 shows screenshots of the experimental hexapod, HexaBull-1, as it walks over the gap in the terrain. As can been seen, the body height remains constant throughout the walking experiment. The Δ's used in this experiment are same as the ones given in previous sections. As the legs are able to change length are able to match the terrain, the legs are able to tackle the gap on the terrain without any change in the body height.

6.3.4   Changing Elevate and Depress Rates

Figure 6.27 shows the effect of using different Δ_{SE} as the experimental hexapod, HexaBull-1, walks on Terrain C. As can be seen, the legs returns to the normal stepping pattern faster when larger Δ_{SE} is used. The $\Delta_{SE} = 0.03 * \Delta_{FD}$ works very well for HexaBull-1 walking on hardware terrains described in previous section.

6.3.5   Foot Forces during Multiple Gaits

Figure 6.28 shows the foot depression and compliant actuator position of all the three legs on the right side of the experimental hexapod, HexaBull-2, walking using the alternating tripod

92
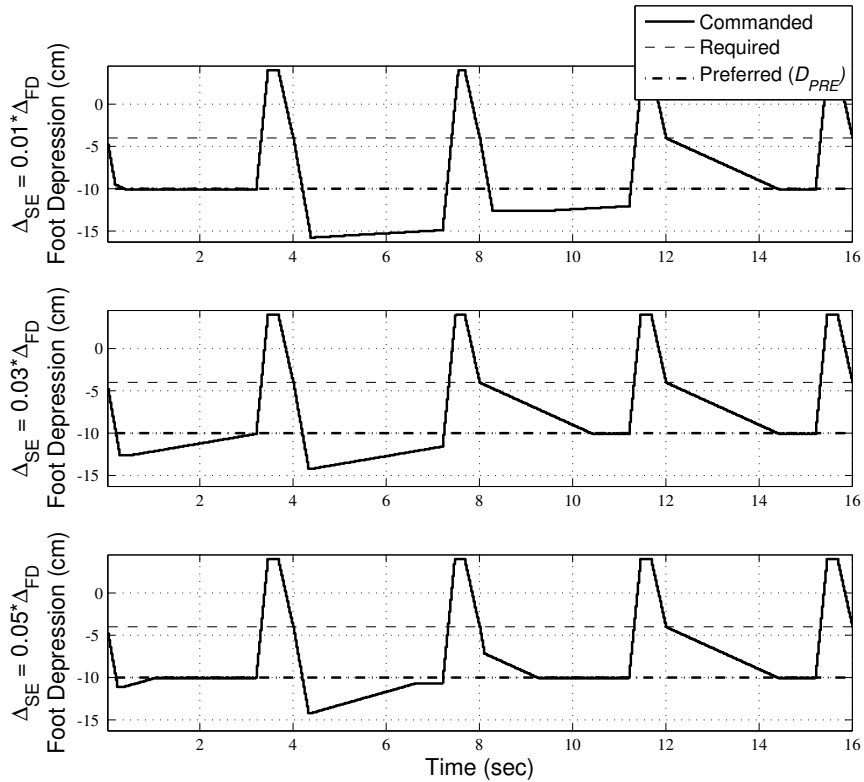
Figure 6.27: Effect of slow foot elevation: Foot depression of the front right leg of the experimental hexapod, HexaBull-1, as it walks down a step using three different Δ_{SE}. (Adapted from [42])

gait on flat terrain. The front and the hind leg are a part of one tripod while the middle is part of another and is phase shifted. As can been seen in the figure, each leg has similar foot force profile based on the actuator position and are quite similar from one step to another. The shapes of the foot force profile for each leg is based on the amount of load on that leg as well as the stepping pattern.

One thing to note is that for the experimental hexapod, HexaBull-2, since only one battery is used and is attached at the lower part of the hexapod body, the weight lifted by the hind legs is more than the weight held by the front. Therefore, at every touchdown, the foot forces for the front leg is smaller compared to the hind legs which hold more weight until the other tripod (middle leg in figure) lifts off the ground.

93

Figure 6.28: Tripod gait: Foot depression and compliant actuator position of all the legs on right side of the experimental hexapod, HexaBull-2, as it walks on flat terrain using the alternating tripod gait.

Comparing the compliant actuator position in HexaBull-1 in Fig. 6.22 and 6.23 with the actuator position in Fig. 6.28, the benefits of using Dynamixel MX-28T can be seen over AX-18A. The position error in much more smooth and has considerably less number of errors compared to AX-18A. Also, the change in the actuator position (in terms of angle) is much smaller in MX-28T compared to the AX-18A. This is because a position error of 30 in AX-18A is $8.7°$ (resolution is $0.29°$ - See Table A.1) while a position error of 40 in MX-28T is $3.52°$ (resolution is $0.088°$ - See Table A.3).

Figure 6.29 and 6.30 shows the foot depression and compliant actuator position of all the three legs on the right side of the experimental hexapod, HexaBull-2, walking using the ripple and

94

Figure 6.29: Ripple gait: Foot depression and compliant actuator position of all the legs on right side of the experimental hexapod, HexaBull-2, as it walks on flat terrain using the alternating ripple gait.

the wave gait on flat terrain. Similar to Fig. 6.28, the shapes of the foot force profile for each leg is not only based on the amount of load on that leg as well as the stepping pattern. The change in gait causes stepping pattern to change causing the foot force profiles to be completely different for all the different gaits.

All the three figures (Fig. 6.28, 6.29 and 6.30) show the uniqueness of the foot force produced by the legs during walking. The force profiles not only are dependent of the body structure but also the gait, timing and foot touchdown of all the legs of the hexapod. The range of force patterns for uneven terrains changes based on the terrain. Trying to replicate all force profiles
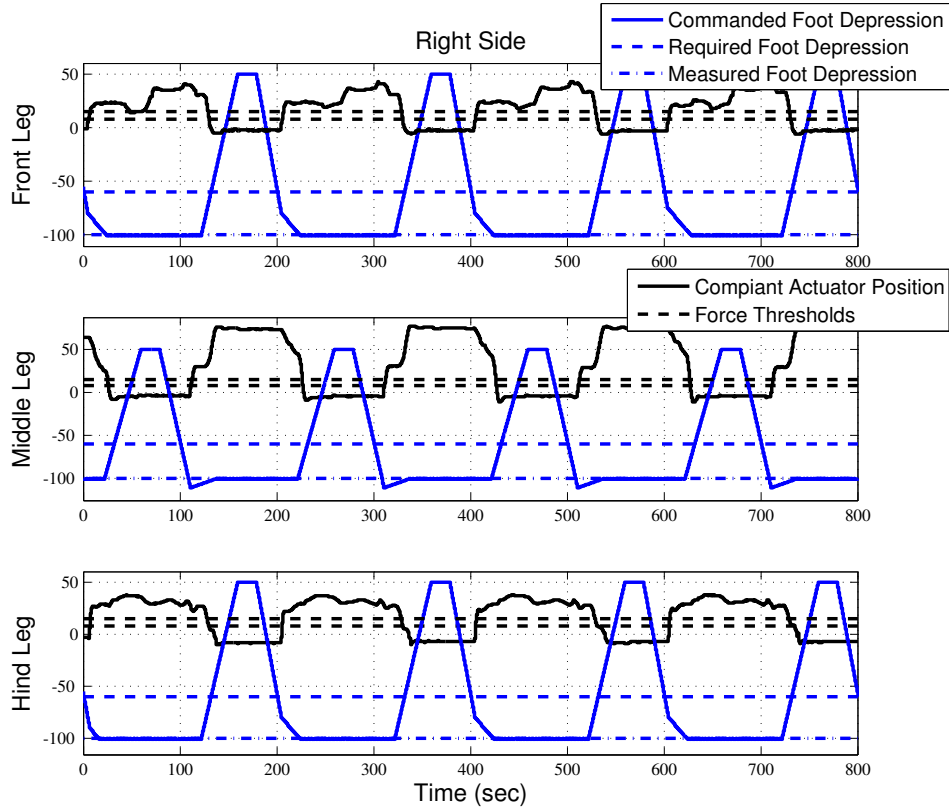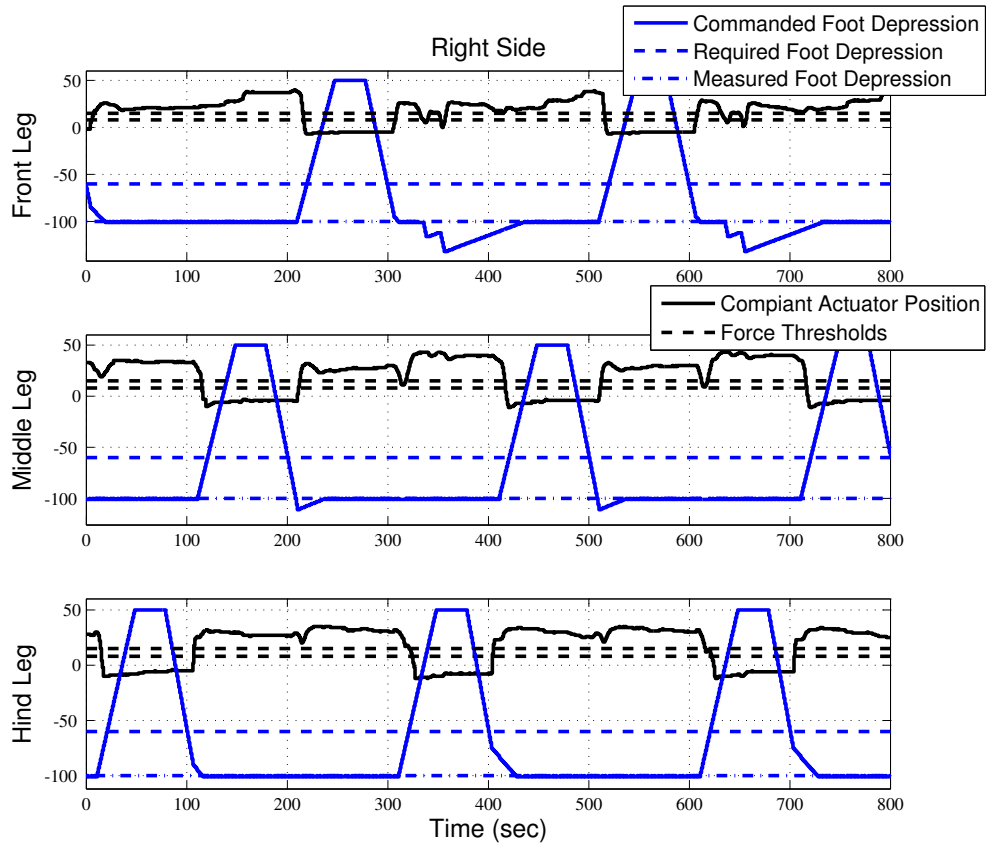
95
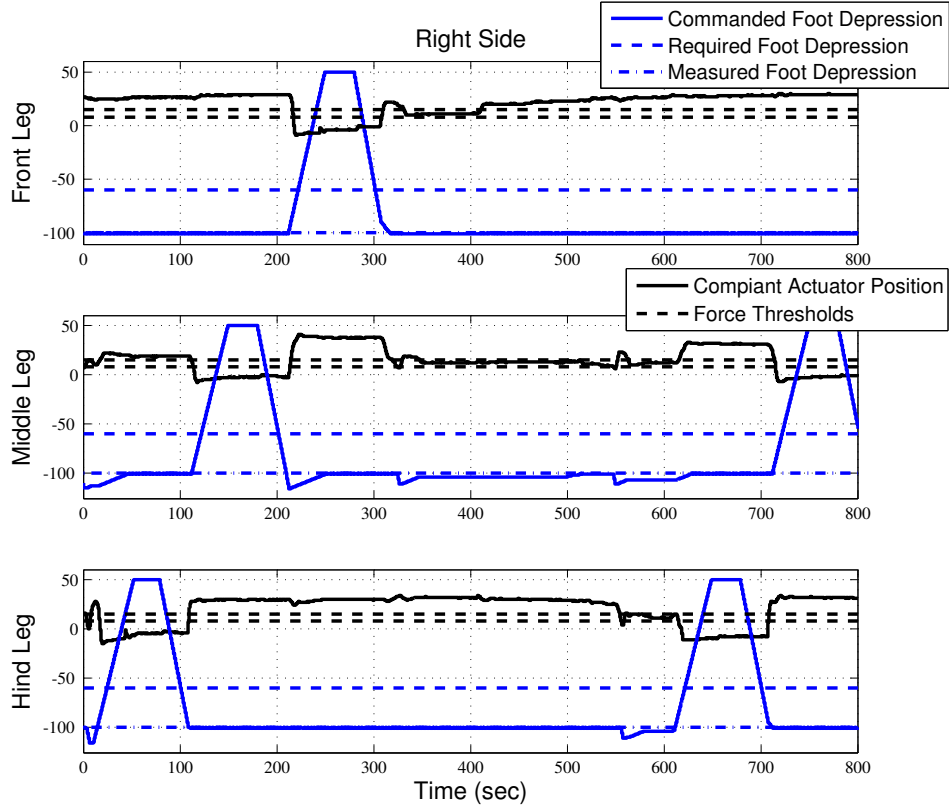
Figure 6.30: Wave gait: Foot depression and compliant actuator position of all the legs on right side of the experimental hexapod, HexaBull-2, as it walks on flat terrain using the alternating wave gait.

to be emulated by each leg for all possible scenarios would be a very tedious task. This would be one more advantage of using force thresholds instead of emulating foot force profiles.

6.4 System Analysis

The experimental hexapod system uses three CM-700 control modules along with 18 Dynamixel MX-28T/AX-18A actuators along with 6 Dynamixel RX-28 actuators. The CM-700 control module uses ATmega2561 8-bit AVR RISC-based micro-controller (16 MHz frequency and 256 Kb flash program memory) while the Dynamixel AX-18A and Dynamixel RX-28 actuators

96

use the ATMega8 8-bit AVR RISC-based micro-controller (16 MHz frequency and 8 Kb flash program memory) and the Dynamixel MX-28T uses the ARM Cortex-M3 32-bit processor (72 MHz frequency). Thus, the hexapod uses 27 micro-controllers for its operation.

The FTP controller code is copies in the three CM-700 control modules. The FTP algorithm HEX file containing the code and associated libraries which runs on the CM-700 boards takes up 19.1 KB program memory while the data memory required for operation is 795 Bytes. Thus, the whole FTP algorithm is run on three 8-bit micro-controllers using 57.3 KB program memory in total and uses 2.3 KB data memory.

6.5   Summary

A number of experiments have been performed, both in simulation and hardware, which shows the working of the FTP controller. The results verify the expected behaviors of the FTP controller. The FTP controller is able to successfully navigate almost all of the terrains that were created. The FTP controller is also able to achieve ground contact at each step and, therefore, forward movement. The FTP controller was successfully able to walk over obstacles and gaps of heights 10.16 *cm*. Apart from walking on uneven terrain, the FTP controller was also able to maintain the desired body height even across uneven terrains.

CHAPTER 7: SIDE STEPPING AND TURNING

7.1 Introduction

So far the working of the FTP algorithm has been done for straight walking on uneven terrain. The foot position of the leg is changed in the X and Z axis such that the leg can achieve forward motion at each step. The foot position in the Y plane is kept constant and chosen such that the leg can achieve the maximum clearance and the maximum depression (Z axis) while being able to hold the body up while walking. The change in the foot position in X axis is based on position control while the change in Z axis is based on the FTP control in stance phase and position control in the swing phase.

For a robot to navigate through uneven terrain, turning and side stepping along with the forward and backward walking have to be implemented. Since force feedback is used to control the foot position of the leg in the Z axis, the foot position in the X and Y axis can be controlled using position control and be made dependent on the motion (walking, turning or side step) that is required to be performed.

7.2 Leg Limitations

For turning and side stepping to be implemented using the FTP algorithm, the maximum reach of the leg has to be found such that the maximum angle and side step distance the hexapod can move be known. For the experiments performed in simulation and on the experimental hardware,

98

the maximum distance in the X direction for forward motion was ± 8 *cm*. The anterior extreme position X_{AEP} was $+8$ *cm* while the posterior extreme position X_{PEP} was -8 *cm* and the position in the X axis changed from anterior to the posterior extreme position in stance phase while walking straight.
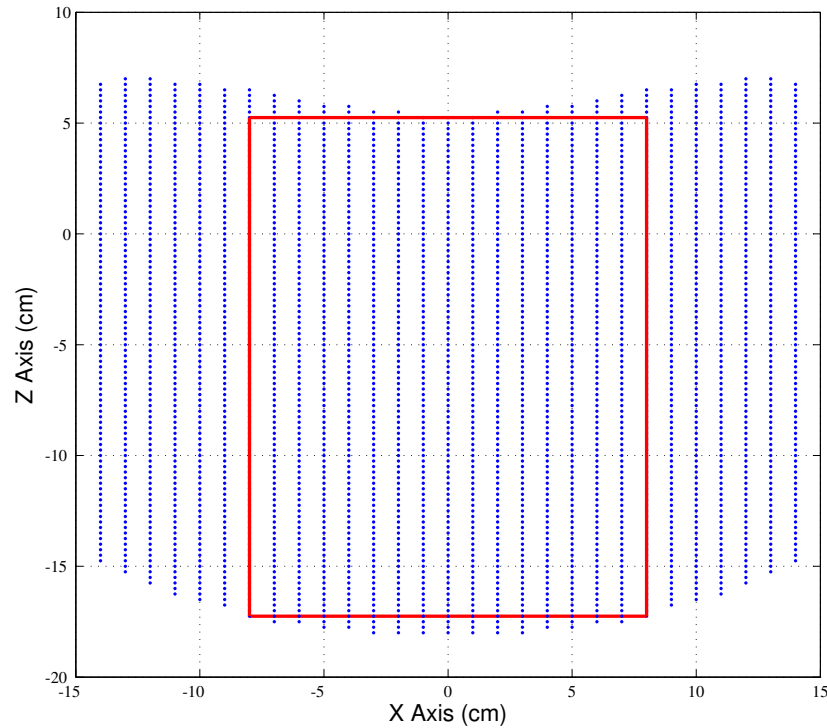
Figure 7.1: Maximum stride of the hexapod leg: Positions in the X and Z plane the foot of the hexapod leg can reach for a single Y value of 14 *cm*. The rectangle shown is the largest rectangle found while maximizing the range in the X and Z axis.

The X_{AEP} and X_{PEP} values were found by using a search algorithm maximizing the range in the X and Z axis while keeping the Y axis constant. Figure 7.1 shows the output of the search algorithm when the position in the Y axis was kept constant at 14 *cm*. The blue dots show the position that could be reached by the foot of the leg. The range is dependent on the link lengths of the leg. The leg links used in the Fig. 7.1 can be seen in Table 5.1. Each point is checked using the

99

inverse kinematics of the leg to find if there is at least one solution (or joint angle values) for the leg such that the point can be reached by the foot. Please note that the positions the foot can reach in the X axis is more than what is shown in the figure but the search has been limited to $\pm$ 14 *cm* because, with a stride $\geq$ 14 *cm*, the legs of the hexapod in hardware are not able to hold the body off the ground. The search algorithm tries to find the best rectangle in the given points such that the area of the rectangle is the largest. The largest rectangle is shown in the figure.
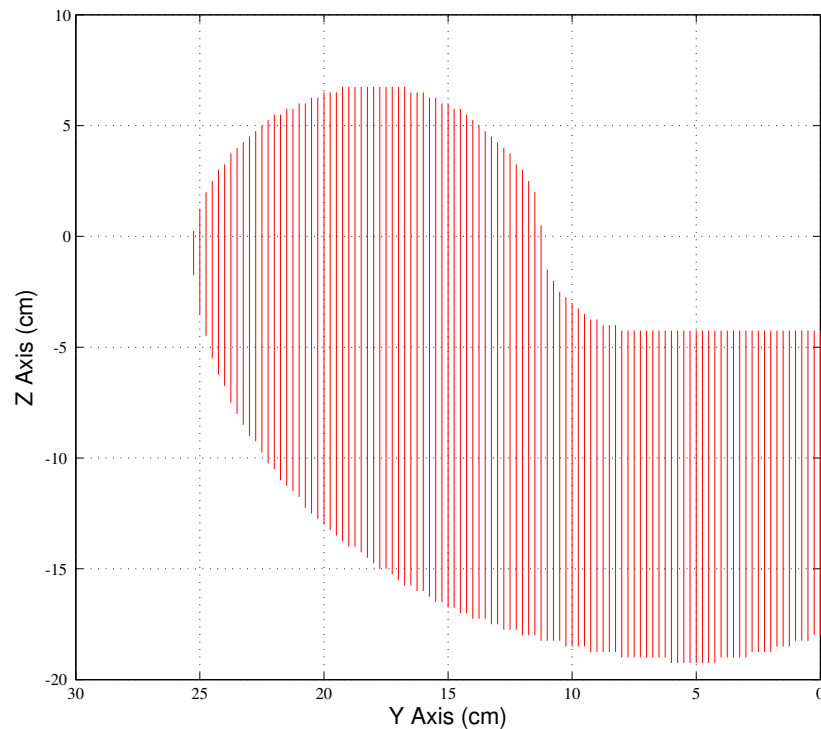
Figure 7.2: Maximum reach of the hexapod leg over the span of reachable Y values. Note that Figure 7.1 is one slice of this figure at a distance of Y = 14 *cm*.

Figure 7.2 shows the range of positions the foot of the hexapod leg can reach in the Y and Z axis. Figure 7.2 shows the largest rectangle for different values of Y. Individual position points are not displayed in the figure. The rectangle is similar, with regards to the X axis, to Fig. 7.1 as all the points between the X_{AEP} and X_{PEP} can be reached for the Y and Z values shown in the figure.

Since the plot in Fig. 7.2 is not uniform, the walking behavior will have to be changed such that turning and side stepping could be done on any terrain without the possibility of the foot reaching singularity.

7.3   Foot Placement
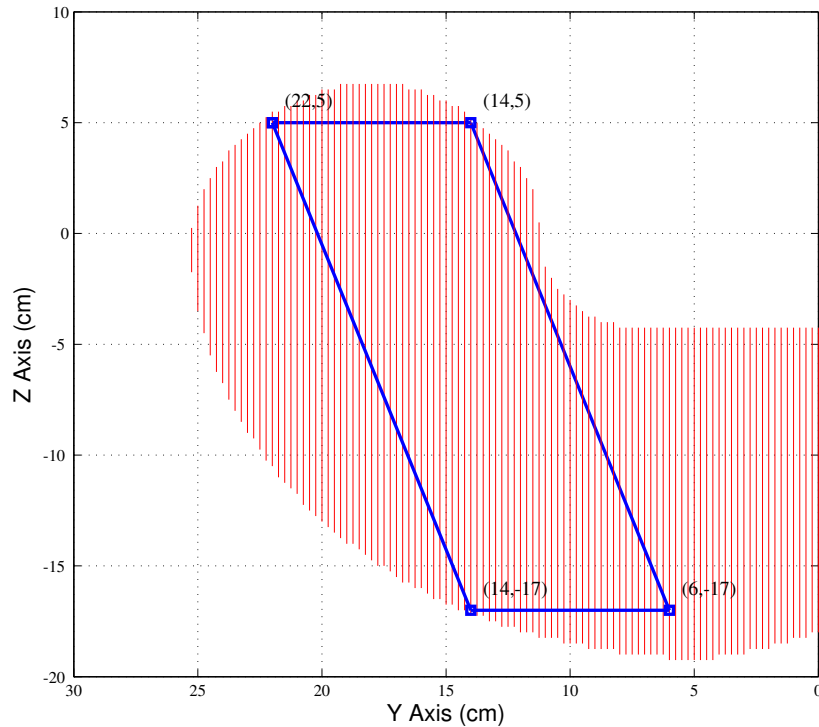
Figure 7.3: Manually selected leg movement range.

To maintain consistency in terms of turning angle and side stepping distance across all terrains, extreme positions need to be found such that the foot is not commanded to move to a singularity. Figure 7.3 shows the manually selected leg movement range in the Z and Y axis. The shape is chosen as a parallelogram such that the leg will be able to achieve turning and side stepping without sacrificing the range of motion in the Z axis. The shape also means that turning and side

101

stepping can be achieved at any terrain height within the Z range. No matter what the height of the terrain (Z value in the figure) is, the range of motion in the Y axis remains same. However, the starting and ending positions of this range is dependent on the Z value. Please note that the range in the Z axis (and also the X axis) have not been changed compared to straight walking.

7.4   Walking and Side Stepping in FTP Control

During straight walking, the foot position in the Y axis was kept constant. This approach could still be used while straight walking. However, to keep the arm length of the hexapod close to the body as possible, the foot position in the Y axis will be changed while walking straight. This is done so that side stepping, turning and straight walking will have similar behaviors which can be changed easily as the walking input changes.

For the hexapod to do side stepping, the foot positions in the Y axis have to change from one extreme point to the other. Figure 7.4 showing the cyclic side stepping behavior used by the FTP controller on flat terrain. The figure shows the hexapod side stepping to the right. The behavior would be mirrored when side stepping to the left. The timing periods, used in this figure, are the same that are used for walking (Fig. 4.4). Retract and protract phase in Y axis, start and end the same time as in the X axis. The retract phase in Y starts at time step *I* and ends at *III* (protract phase in Y goes from time step *III* to *V* and ends at *I*). The same retraction duty factor ($0 < D_R < 1$) in X axis controls the ratio of time between retract and protract phase during a single step.

For walking straight, during the retract phase, the position in Y has to bring the leg inward until the foot touches the ground while during the protract phase, the position of the leg has to go outward to go to the original position. Please note that based on the side the leg is attached to the body the Y value would be positive or negative. But the direction with respect to the body will remain same. For side stepping, the legs have to move in the direction the side step has to be done. Figure 7.4 shows the change in position in the Y and Z axis when side stepping to the right.

102
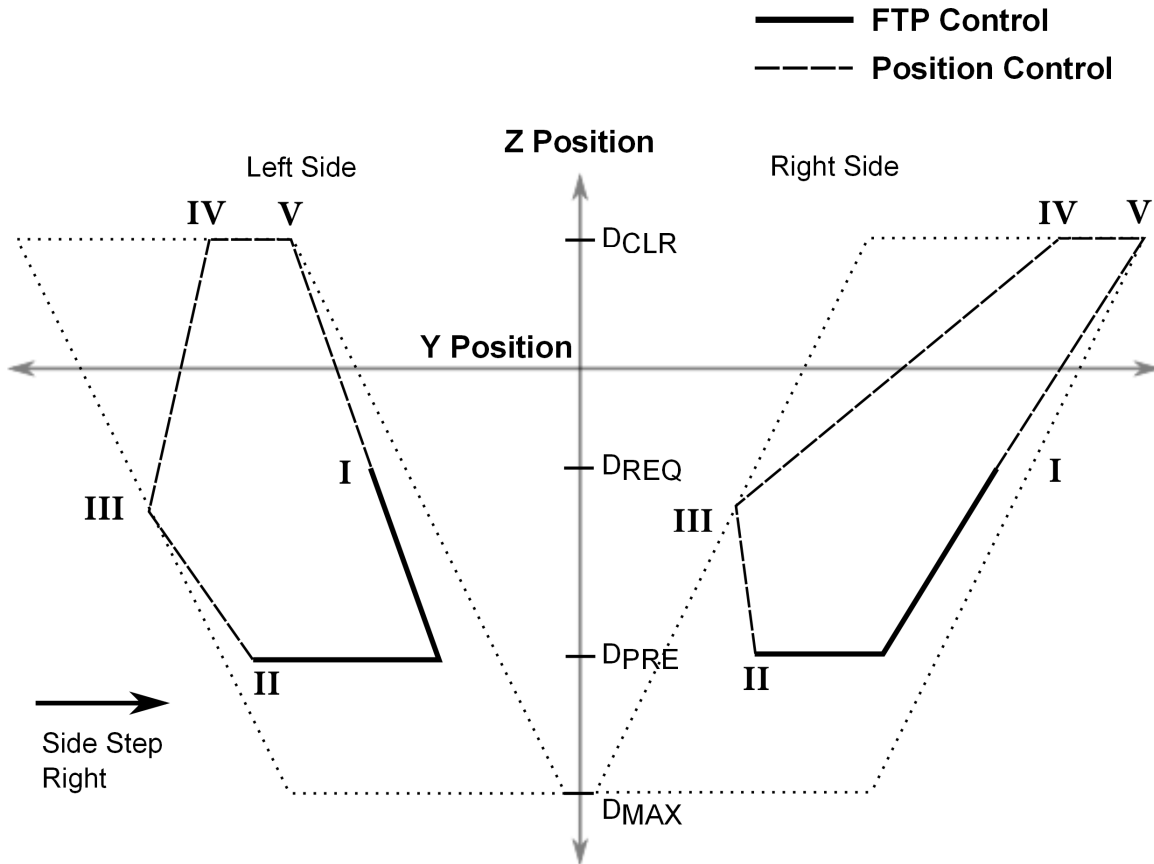
Figure 7.4: Cyclic behavior for side stepping to the right using the FTP algorithm on flat terrain. D_{CLR} is the preferred clearance while D_{REQ}, D_{PRE}, and D_{MAX} are the required, preferred, and maximum depression in the Z axis.

The position of Y is changed with respect to the Z axis such that the value of Y remains inside the parallelogram at all times. The FTP algorithm uses two rates to deal with walking and side stepping; Δ_{Search} and Δ_{Step}. Δ_{Search} is dependent on the change in the Z axis and dependent on the slope of the parallelogram. Thus, $\Delta_{Search} = slope * \Delta_Z$ (Please note that Δ_Z could be either Δ_{FD}, Δ_{SD}, Δ_{FE}, Δ_{SE}, or zero). Δ_{Step} is the stepping rate and is dependent on either the maximum distance the hexapod can side step or the turning distance and when walking straight, Δ_{Step} is equal to zero.

Therefore, when walking straight, Δ_{Search} changes according to Δ_Z and follows the slope of the parallelogram. When side stepping, Δ_{Search} and Δ_{Step} are added. The behavior is shown in Fig. 7.4. From time step *I* to *III*, Δ_{Step} is constant and is calculated based on the maximum stepping distance. In the figure, Δ_Z is Δ_{FD} until touchdown and zero until time step *II*. After time step *II* the foot is lifted off the ground in the swing phase using Δ_{FE}. Since the change in Y is dependent on the Z axis, the value of Y remains inside the parallelogram.

Figure 7.5: Commanded and measured foot positions of contralateral pair of hexapod legs as the hexapod walks straight in simulation suspended in air.

Figure 7.5 shows the commanded and measured foot position of a contralateral pair of legs as the hexapod walks straight in simulation suspended in air. The contralateral pair of legs are the front two legs of the hexapod. The hexapod is suspended by fixing the body to a specific location in air and not allowing the body to move as the legs move to walk forward. The body is suspended such that the legs do not touch the ground while walking. This experiment is done to

104

see the behavior of the walking algorithm in the extreme condition. Since the foot never touches the ground, the leg depressed using the fast depress rate Δ_{FD} and elevated using the fast elevate rate Δ_{FE}. The figure shows three steps completed by the legs and as can be seen from the figure, expected behavior results from the experiment.
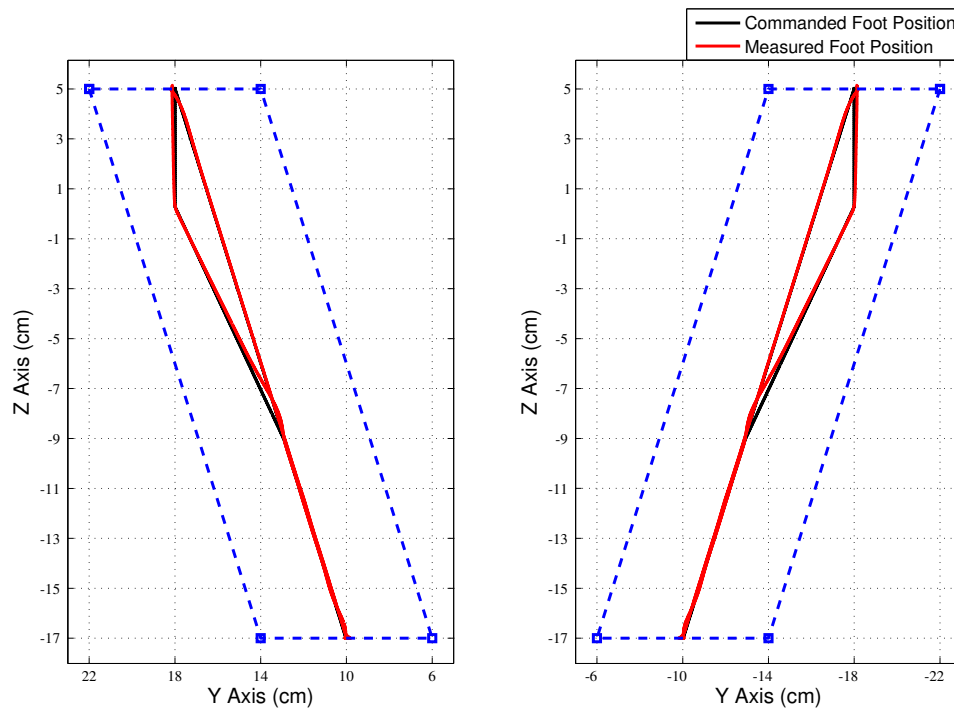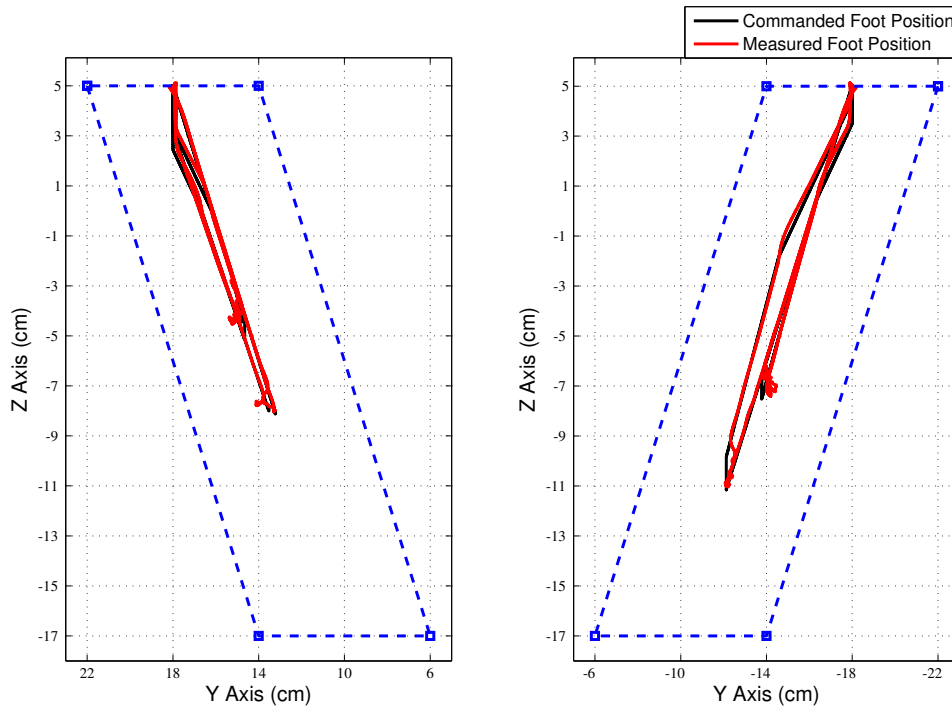

Figure 7.6: Commanded and measured foot positions of contralateral pair of hexapod legs as the hexapod walks straight on an uneven terrain in simulation.

Figure 7.6 shows the commanded and measured foot position of a contralateral pair of legs as the hexapod walks straight on an uneven terrain in simulation. The figure shows three steps completed by the legs on a terrain with different heights.

Figure 7.7 shows the commanded and measured foot position of a contralateral pair of legs as the hexapod side steps to the right suspended in air in simulation. The figure shows three steps completed by the legs. At each step, the position of the foot in the Y axis changes based on the $\Delta_{Search} + \Delta_{Step}$ rates which continues till the foot touches the ground or in this case, the
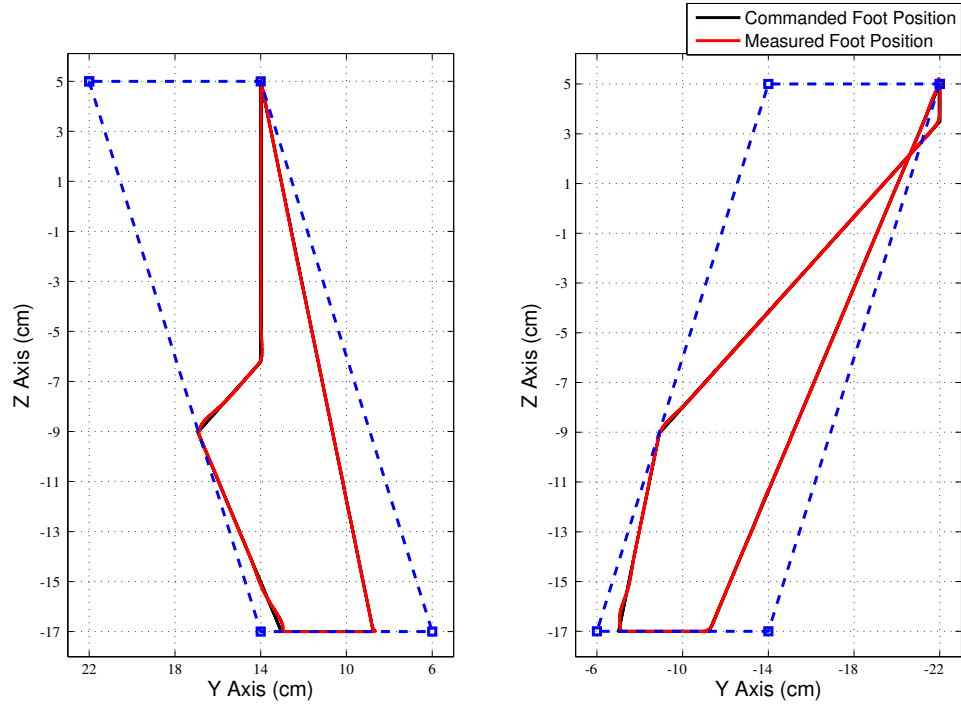
105

Figure 7.7: Commanded and measured foot positions of contralateral pair of hexapod legs as the hexapod side steps to the right suspended in air in simulation.

maximum depression that could be achieved is reached. After which the leg completes the side step using the Δ_{Step} till the end of retraction phase. Since the change in the Y position depends on the Z position, the Y position is able to move within the boundaries of the parallelogram without explicitly checking the boundaries.

Figure 7.8 shows the body position and angles of the hexapod side stepping to the right on flat terrain in simulation. The figure shows three completed steps taken by the legs of the right tripod. The left tripod starts in mid stance phase and only provides support and side movement occurs till the end of the phase (1 *sec* mark). As can be seen in the figure, the hexapod is able to achieve side movement equal to the twice the body width (Table 5.1) at the end of two completed steps by the right and left tripod (5 *sec* mark). The second subplot shows the body angles (pitch, roll, and yaw). The hexapod body is very stable when side stepping on a flat terrain.

106

Figure 7.8: Body position and body angles of the hexapod as it side steps to the right on flat terrain in simulation.

Figure 7.9 shows the body position and angles of the hexapod side stepping to the right on Terrain E in simulation. The side movement achieved by the hexapod is dependent on the terrain. For example, due to a step up on the terrain (3.5 and 5.5 *sec* mark), the leg is not able to climb over the step sideways as quickly. The body angles (pitch, roll, and yaw) are also dependent on the terrain.

Figure 7.10 shows the commanded and measured foot position of a contralateral pair of legs as the hexapod side steps to the right on uneven terrain in simulation. The figure shows two
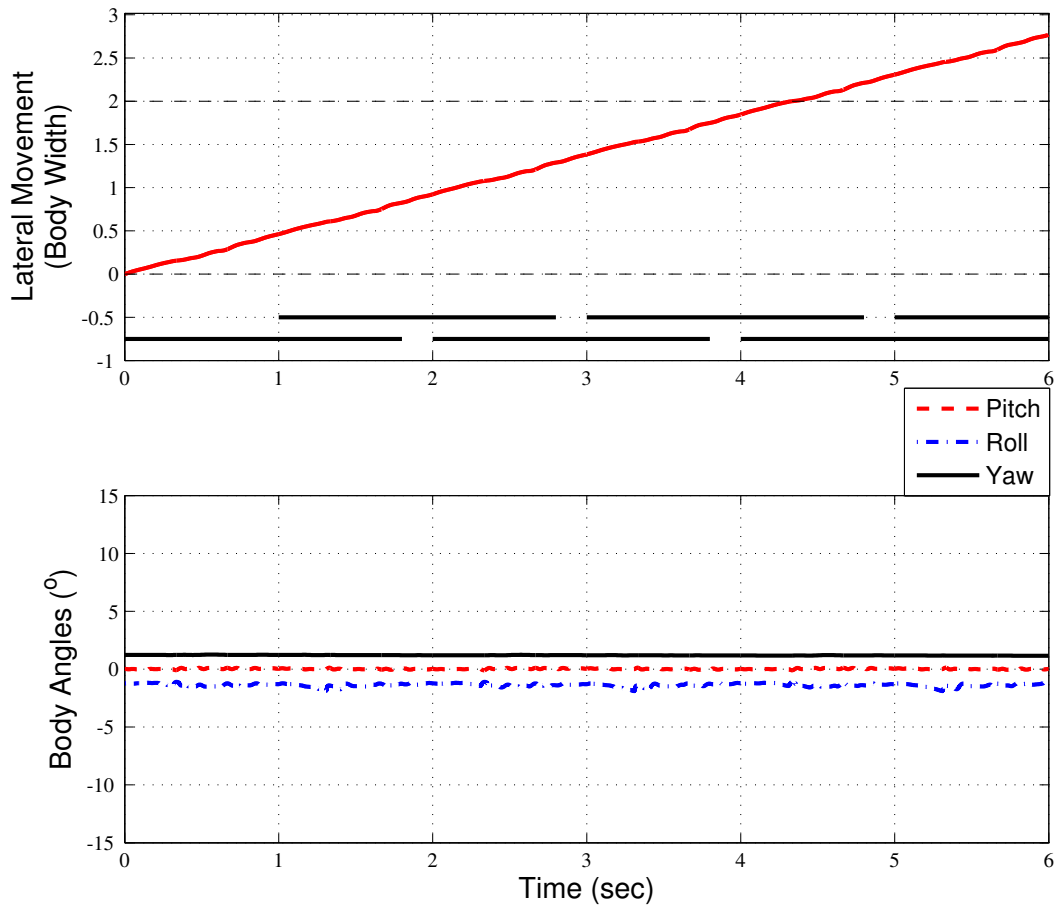
107
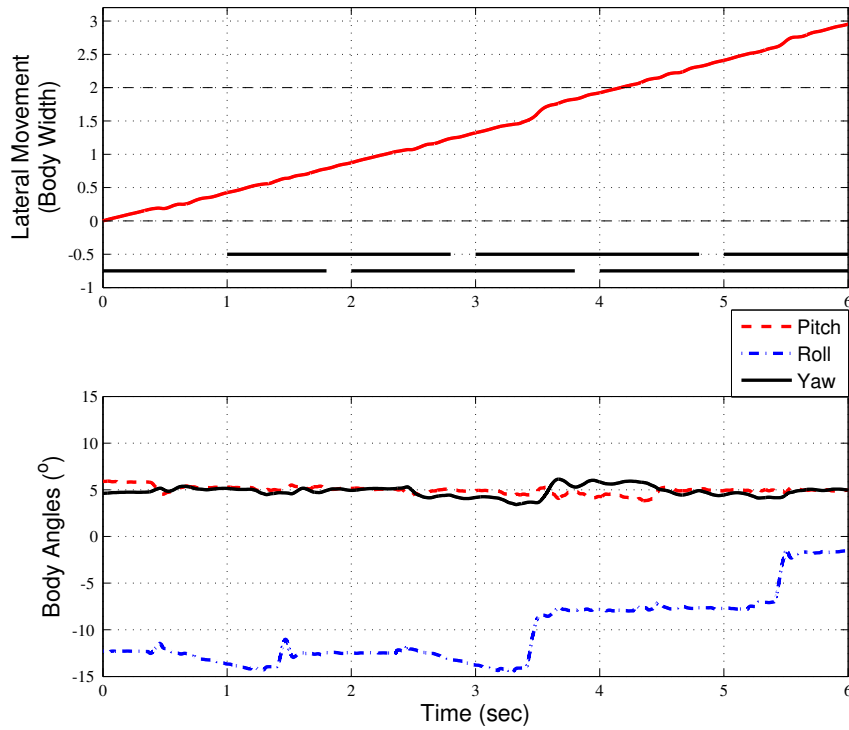
Figure 7.9: Body position and body angles of the hexapod as it side steps to the right on uneven terrain in simulation.

steps completed by the legs. Even on uneven terrain, the Y position is able to move within the boundaries of the parallelogram without explicitly checking the boundaries.

7.5 Turning in FTP Control

To add turning in the FTP controller, the maximum angle that could be turned in the limits imposed by the parallelogram was computed. Using inverse kinematics, the position of the body and leg were found to make a turn of specific angle. Using this search, the maximum turn that could be done in the limits of the parallelogram (Fig. 7.3) was found to be $22.5°$. Figure 7.11 shows the foot and hexapod body positions before and after taking a turn of $20°$. In this figure, the

www.manaraa.com

Figure 7.10: Commanded and measured foot positions of contralateral pair of hexapod legs as the hexapod side steps to the right on uneven terrain in simulation.
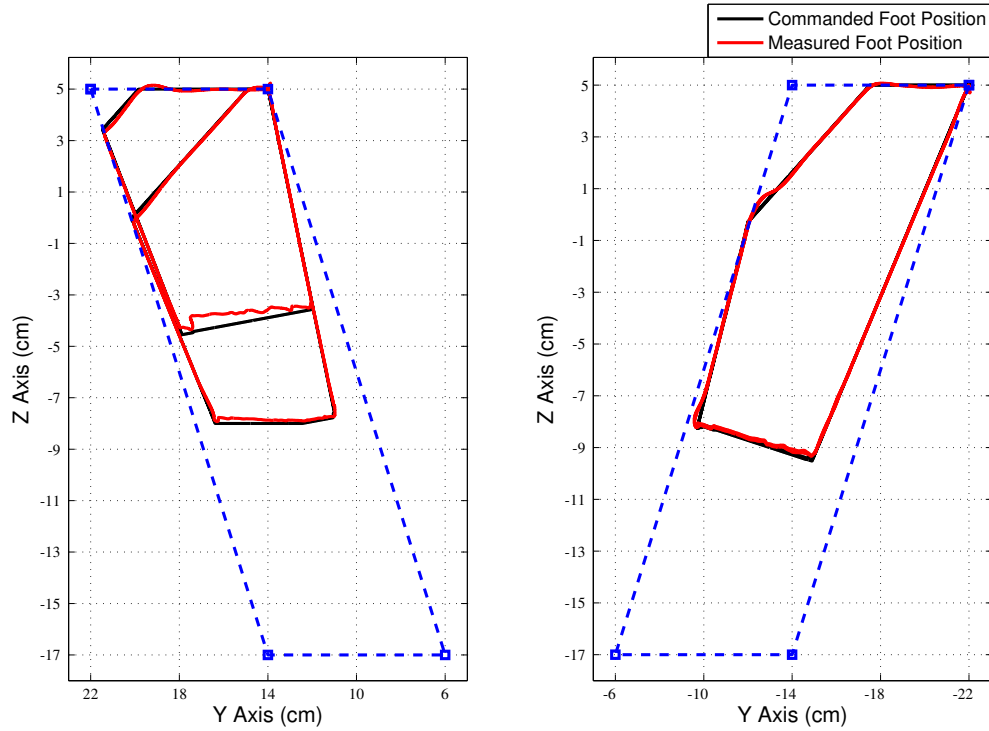
left tripod takes a left turn of 20° while in place. The solid lines show the hexapod and the left tripod legs before taking the turn while the dashed lines show the position after taking the turn. The shaded position shows the maximum reach of this leg.

To make the implementation simple, only one angle was chosen for a turn step. Thus, if a turn is commanded, a specific angle turn will be executed during the tripod step. The angle was chosen as 15° as the angle is within the limits and also the greatest common divisor for higher angles (30°, 45° and 90°). So a 90° or 180° turn could be done within some steps. The initial and final position of the tripod feet are used to implement the turn. Since each leg has a different behavior during turning, the X and Y positions for one tripod (either left or right) is stored and altered, in real time, based on the direction of turn and the tripod (left or right).
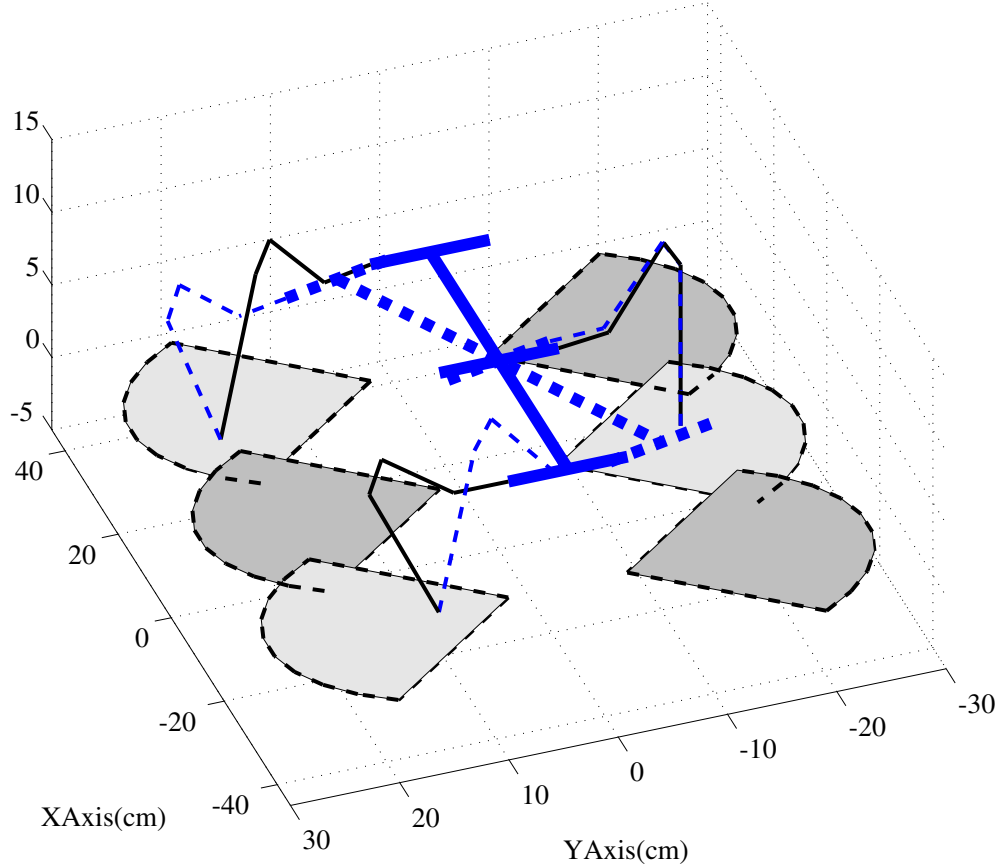
Figure 7.11: Initial (solid) and final (dashed) body and leg positions of the left tripod to execute a 20° left stationary turn in one step. Shaded areas represent the range of motion for each leg for a Z value of 8 *cm*.

The implementation of turning is done the same way as side stepping and a turn rate is used Δ_{Turn} (Δ_{Step}) to implement the turn. This rate is constant and dependent on the angle. Also, while turning the rate in the X axis changes based on the positions stored.

Figure 7.12 shows the commanded and measured foot position of a contralateral pair of legs as the hexapod side turns right in place on flat terrain in simulation. The figure shows three steps completed by the legs. At each step, the position of the foot in the Y axis changes based on the $\Delta_{Search} + \Delta_{Turn}$ rates which continues till the foot touches the ground. After touchdown the leg

110

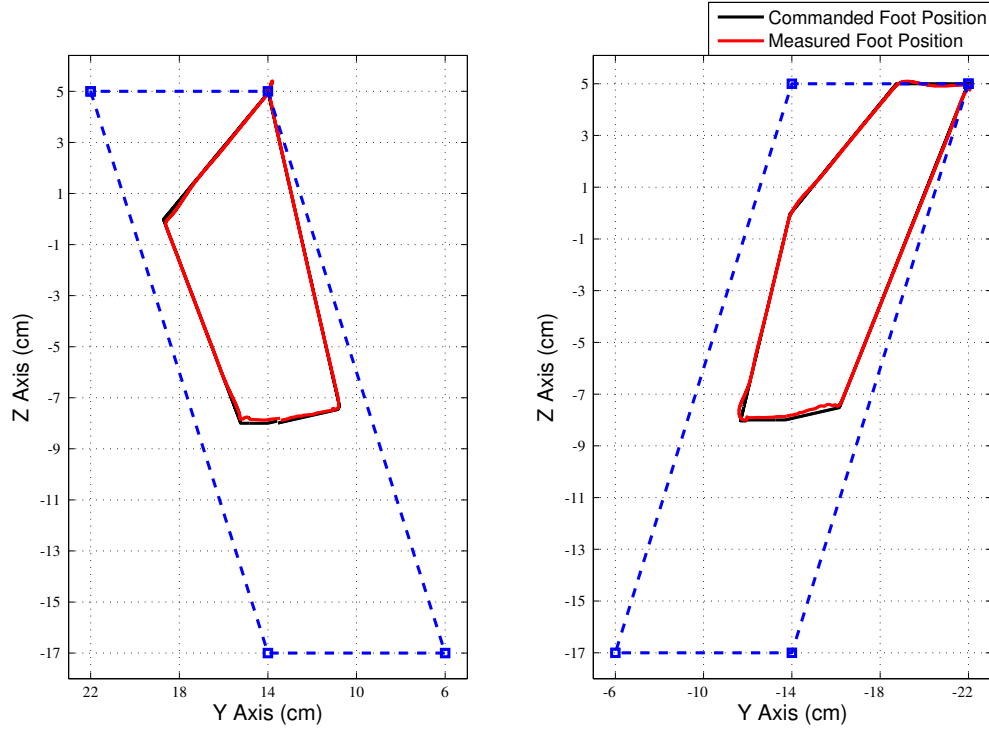Figure 7.12: Commanded and measured foot positions of contralateral pair of hexapod legs as the hexapod turns right in place on flat terrain in simulation.

finishes the turn using the Δ_{Turn} till the end of retraction phase. Since the change in the Y position due to turn angle depends on the Z position (as in the case of side stepping), the Y position is able to move within the boundaries of the parallelogram without explicitly checking the boundaries. However, as the turn angle does not utilize the full Y range and only turns $15°$ in a single step, the Y position is well inside the parallelogram.

Figure 7.13 shows the body position and angles of the hexapod turning right on flat terrain in simulation. The figure shows three completed steps taken by the legs of the right tripod. The left tripod starts in mid stance phase and only provides support and side movement occurs till the end of the phase (1 *sec* mark). As can be seen in the figure, the hexapod is able to achieve turn angle of $15°$ at most steps resulting in a turn of almost $50°$ at the end of two completed steps by the right and left tripod (5 *sec* mark). The second subplot shows the body angles (pitch, roll, and
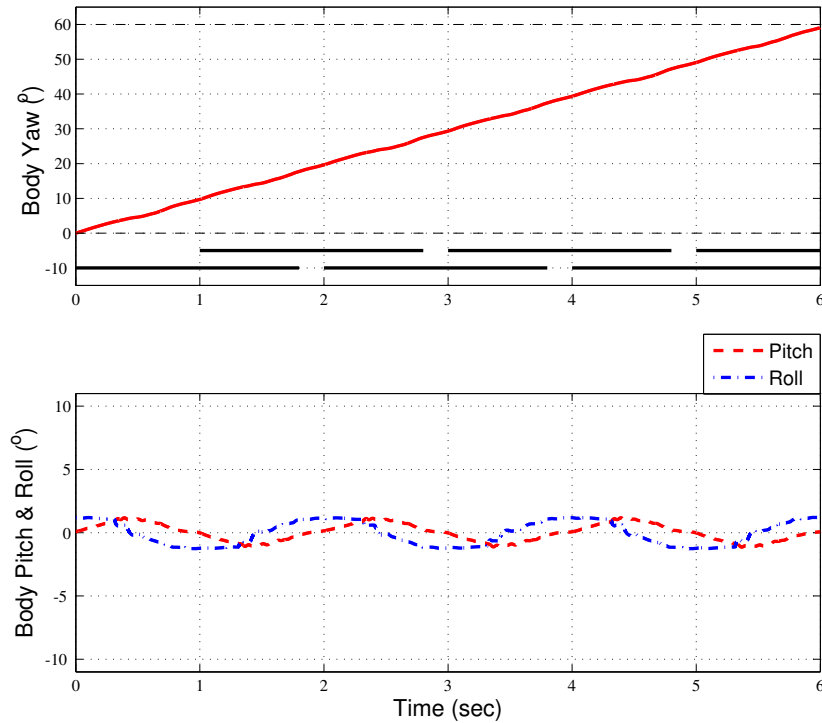
111

Figure 7.13: Body position and body angles of the hexapod as it turns right in place on flat terrain in simulation.

yaw). The hexapod body is very stable when turning on a flat terrain. The oscillating behavior of the body angles is expected while turning in place.

Figure 7.14 shows the commanded and measured foot position of a contralateral pair of legs as the hexapod turns right on uneven terrain in simulation. The figure shows three steps completed by the legs. Even on uneven terrain, the Y position is able to move within the boundaries of the parallelogram without explicitly checking the boundaries. As can be seen in Fig. 7.15, the hexapod is able to achieve turn angle of $15°$ at most steps resulting in a turn of almost $50°$ at the end of two completed steps by the right and left tripod (5 *sec* mark). The oscillating behavior of the body angles is more pronounced during this experiment but the hexapod is able to achieve the turn angle even on uneven terrain with a lot of ease.
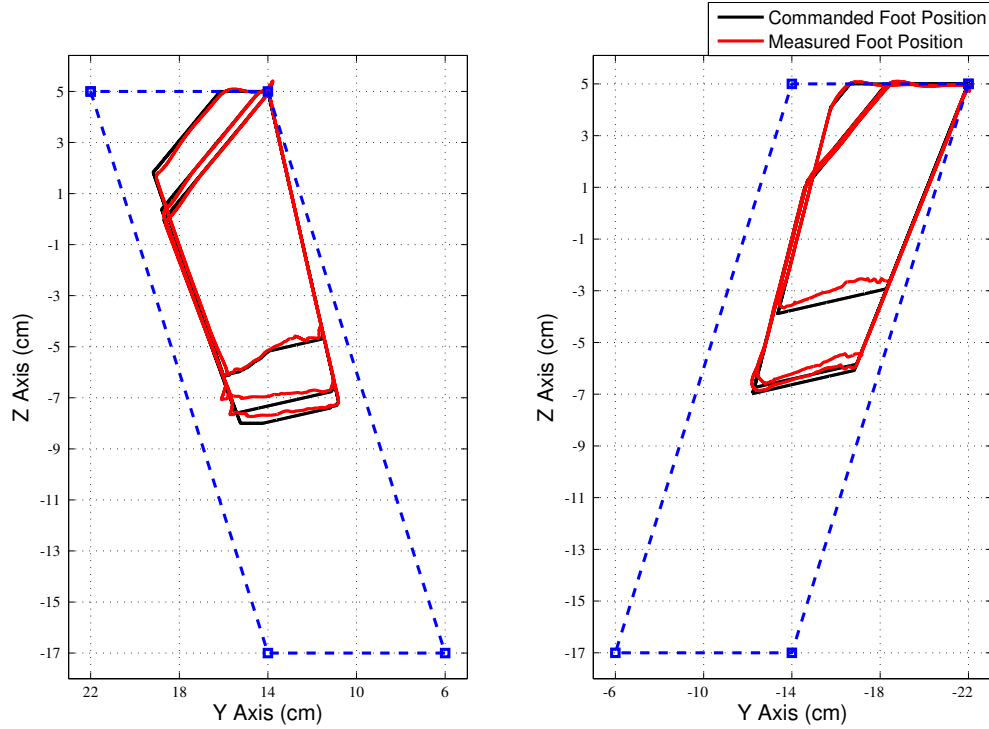
112

Figure 7.14: Commanded and measured foot positions of contralateral pair of hexapod legs as the hexapod turns right in place on uneven terrain in simulation.

7.6 Hardware Results

Figure 7.16 shows the commanded foot position of a contralateral pair of legs as the hexapod, HexaBull-2, walking straight on flat terrain. The position in Y axis is changed based on the Z axis. The behavior is similar to the one seen in simulation. As the rates in the experimental hardware are different, the starting and ending positions are different compared to simulation. The rates are changed to such that the experimental hexapod is faster and more responsive to the terrain.

Figure 7.16 shows the commanded foot position of a contralateral pair of legs as the hexapod, HexaBull-2, side stepping on uneven terrain. Due to the increased rates, the Y position goes beyond the parallelogram boundaries but is able to achieve the side step distance. Please

113
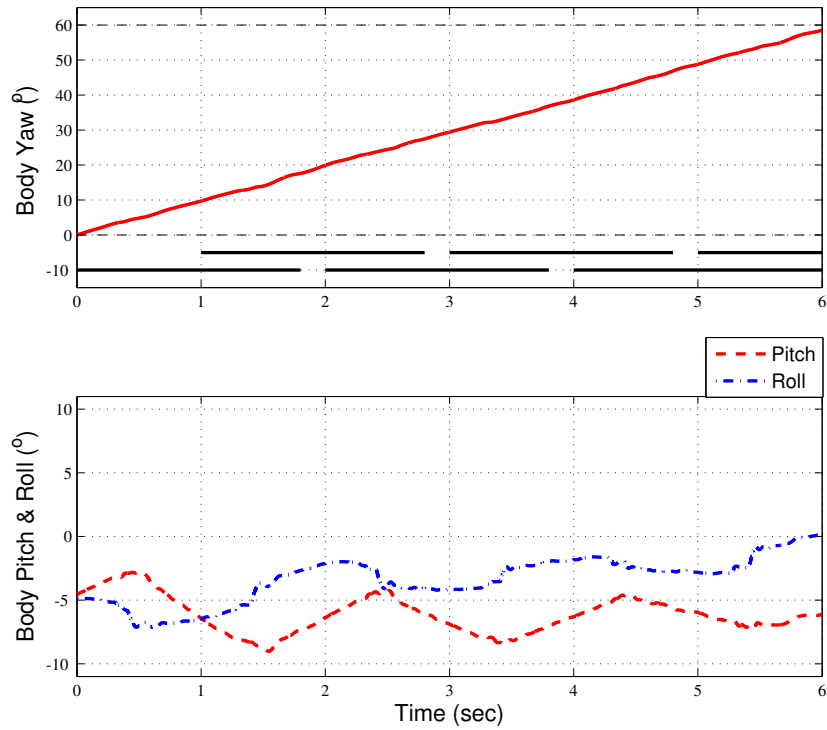
Figure 7.15: Body position and body angles of the hexapod as it turns to the right on uneven terrain in simulation.

note that the parallelogram boundaries in Fig. 7.16 and 7.16 are different than in simulation as the boundaries are based on HexaBull-2 (Table 5.1).

7.7 Summary

This chapter gives a brief description of the implementation of side step and turning behavior in the FTP controller. Few results showing the implementation of the behaviors in simulation and hardware are provided. The individual behaviors can also be combined to give more complicated maneuvers. For example, while doing side stepping, the FTP controller changes the Z position based on the terrain while the position controller changes the Y position based on side

114

Figure 7.16: Foot positions of contralateral pair of hexapod legs as the hexapod, HexaBull-2, walks on flat terrain.

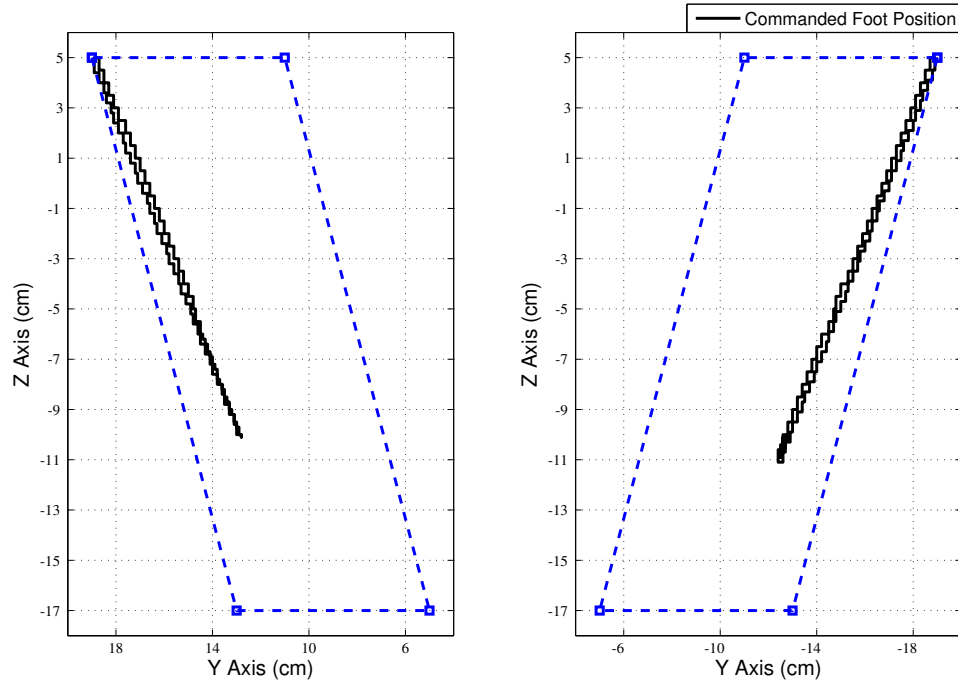step direction. Also, the same is true for walking; the FTP controller changes the Z position while the position controller changes the X position based on walking direction (front or back). Thus side stepping can be combined with walking such that the hexapod is able to side step and walk at the same time; resulting in four maneuvers based on the direction of walking and side stepping.

Also, while turning, the X position changes based on the turn angle and this angle is smaller than the limits imposed by the X_{AEP} and X_{PEP} values. If the maximum value in X direction (walking motion) is used during turning, the hexapod can walk and turn at the same time resulting in four more advanced maneuvers.

Due to this implementation, the hexapod can be commanded to move in 14 different ways while walking on flat or uneven terrain. Due to the robust nature of the FTP algorithm, all the maneuvers can be done on uneven terrain without the loss of stability. The combination of such
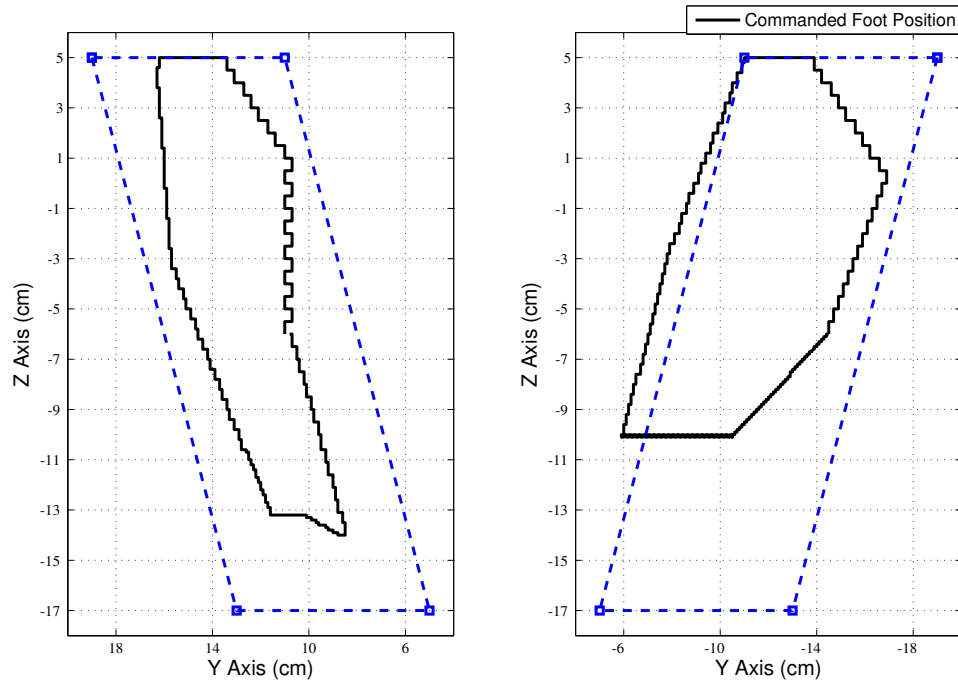
115

Figure 7.17: Foot positions of contralateral pair of hexapod legs as the hexapod, HexaBull-2, walks sideways to the right on uneven terrain.

maneuvers while walking on uneven ground using local-leg control in a single system is, to the best knowledge of the author, the first of its kind.

116

CHAPTER 8: SUMMARY AND FUTURE WORK

8.1   Summary

A Force Threshold-based Position (FTP) algorithm to assist with legged locomotion over irregular terrain has been presented along with simulation and hardware results of its implementation on a hexapod system. The hexapod is able to maneuver over uneven terrain without the use of visual sensors to model the terrain, a priori information about the terrain, inertial or inter-leg feedback for controlling the joints. The algorithm decouples the control of each leg, resulting in increased responsiveness to the terrain, and stabilizes the body using only local leg feedback. The local leg controller is inspired from multiple biological observations of legged animals.

The FTP algorithm was applied to multiple hexapod gaits without significant modification, and could be applied to other hexapod morphologies. Threshold values, a preferred depression level, and depression rates could be found based on the leg design and body weight. However, the process of finding the optimum thresholds for different morphologies has not been generalized and is currently resolved using a trial and error approach.

Due to the nature of the FTP algorithm, turning and side stepping functionality was added with relative ease to the walking behavior. Experimental results, both in simulation and hardware, have been provided. A wireless remote control has been added to show the functionality of the FTP algorithm.

Individual behaviors of walking, side stepping, and turning have been combined to produce advanced maneuvers while moving over uneven terrain. Based on the direction of walking, turning

117

and side stepping, the hexapod can be commanded to move in 14 different ways while walking on flat or uneven terrain. Also, these maneuvers could be done in any of the three gaits implemented allowing a lot of flexibility to the hexapod system. The combination of all these maneuvers implemented on a single system using local-leg controller for walking on uneven terrains is a major achievement of this research work.

8.2 Contributions

The main contribution of this research work is the development of the distributed local-leg controller, called the Force Threshold-based Position controller, and its implementation in simulation and hardware. Biological hypotheses, generated from insect and animal walking studies, have been implemented with this controller. The experimental hardware built for implementing the FTP controller uses a novel way to approximate the foot forces needed for feedback. Another contribution of this research work is the distributed nature of the hardware and the control algorithm which makes the system more responsive, enabling the hexapod to achieve multiple gaits along with maneuvering capabilities while using local leg controller to walk on uneven terrain. The combination of all these features, to the best knowledge of the author, has not been implemented in a single system. This system can form a basic platform on which more biological hypothesis could be tested and verified. Lastly, this system can give more insight on the underlying control system used by insects and animals for walking.

The FTP controller is built as a low-level reflexive system which is guided by a high level controller overseeing its operation. An example of such coordination could be the working of a search and rescue robot using the FTP controller to negotiate the uneven terrain while visual sensors can intermittently pass the rough terrain information along with directional commands to the FTP controller. This makes the walking behavior practically a background process while vision sensors could be used for their main purpose of search and rescue, which is locating survivors

118

or other artifacts of interest. If operated remotely, the operator could potentially focus more on mission objectives rather than terrain modeling for optimal stepping of the legs.

8.3 Future Work

Further work on this algorithm will seek automated ways to generate the force thresholds based on the weight, structure, and dimensions of the robot while also considering the walking gait and timing parameters. Additional work is also required to tune the Δ rates reactively based on the terrain that is being sensed. Communication between legs might be needed to achieve this. Also, research is required so that the timing and the gait can be reactively selected by the robot based on the terrain.

Passive compliant elements can be added to the hexapod to check their effect on the walking behavior. Many animal legs include compliance in their leg assembly which has been well studied. Also, the legs of the hexapod could be changed to match those of the stick insect, in which, each leg serves a different purpose while walking and has different structure and ranges.

The distribution of the control effort could be taken a step further by implementing a distributed controller at the joint level. In the current implementation, the forward and inverse kinematics must be computed at each control step. Instead of using foot force and position as feedback terms, joint torque and angle may be adequate for robust walking. In addition to this, other biological hypotheses can be tested using the FTP algorithm. As stated in the Introduction, curiosity exists about the role of central pattern generators (CPGs) during walking. It has been noted that posterior cockroach legs touch down very closely to the ground position of its anterior neighbor [76]. When the posterior leg assumes support of the body, the anterior leg sees a decrease in foot force which may trigger the end of its stance phase. This would indicate that leg phasing can be achieved only through local leg controllers instead of a CPG. Testing the effectiveness of this controller on a robotic system is well suited for the FTP algorithm, which is one of few leg

119

control algorithms that can operate over rough terrain using only local leg controllers. Cruse also puts forward a hypothesized model of leg coordination in which gait synchronization is achieved through communication between neighboring legs [77]. The FTP algorithm can be augmented to test the usefulness of these hypotheses on robotic systems negotiating complex terrain.

The FTP controller has potential for leg damage compensation in case of hardware faults by changing the gait phasing and walking pattern of other legs after a fault is detected. The FTP controller can be adapted to biped, quadruped, octopod, etc. locomotion. Currently, the algorithm is being implemented on an upright quadruped system in simulation [78]. The basic operation of both the quadruped and hexapod algorithms is similar with some minor changes to account for the different general morphology. There are also pathways to running and climbing using the FTP algorithm.

8.4   Conclusion

In conclusion, this dissertation has developed a distributed local force feedback control algorithm for walking on flat and uneven terrains. The control algorithm can generate walking behaviors using multiple gaits. Complex maneuvers like turning and side stepping have been implemented. The FTP algorithm is not system dependent, and can be extended for implementation on robots with different morphology and leg configurations. The FTP controller is built as a low-level reflexive system and could be used as a black box system by high level controllers. Hopefully, this dissertation will lay the foundation for future implementation for local-leg feedback algorithms on legged systems in order to solve mobility issues facing legged robots.

LIST OF REFERENCES

[1] Anonymous, "Logistical vehicle off-road mobility," U.S. Army Transportation Combat Developments Agency, Fort Eustis, VA., Tech. Rep., February 1967.

[2] P. Holmes, R. J. Full, D. Koditschek, and J. Guckenheimer, "The dynamics of legged locomotion: Models, analyses, and challenges," *SIAM Rev.*, vol. 48, no. 2, pp. 207–304, February 2006.

[3] A. A. Biewener and M. A. Daley, "Unsteady locomotion: integrating muscle function with whole body dynamics and neuromuscular control," *Journal of Experimental Biology*, vol. 210, no. 17, pp. 2949–2960, 2007.

[4] M. Kawato, K. Furukawa, and R. Suzuki, "A hierarchical neural-network model for control and learning of voluntary movement," *Biological Cybernetics*, vol. 57, pp. 169–185, 1987.

[5] P. Whelan, "Control of locomotion in the decerebrate cat," *Progress in Neurobiology*, vol. 49, pp. 481–515, 1996.

[6] M. Berkemeier, "Approximate return maps for quadrupedal running," in *Proceedings of the IEEE International Conference on Robotics and Automation*, vol. 1, April 1997, pp. 805–810.

[7] R. Kurazume, S. Hirose, and K. Yoneda, "Feedforward and feedback dynamic trot gait control for a quadruped walking vehicle," in *Proceedings of the IEEE International Conference on Robotics and Automation*, vol. 3, 2001, pp. 3172–3180.

[8] K. N. Murphy and M. H. Raibert, "Trotting and bounding in a planar two-legged model," in *In Theory and Practice of Robots and Manipulators, Proceedings of RoManSy'84*, A. Morecki, G. Bianchi, and K. Kedzior, Eds. Cambridge: MIT Press, 1985, pp. 411–420.

[9] H. M. Herr and T. A. McMahon, "A trotting horse model," *International Journal of Robotics Research*, vol. 19, no. 6, pp. 566–581, June 2000.

[10] ——, "A galloping horse model," *International Journal of Robotics Research*, vol. 20, no. 1, pp. 26–37, January 2001.

121

[11] K. Autumn, M. Buehler, M. Cutkosky, R. Fearing, R. J. Full, D. Goldman, R. Groff, W. Provancher, A. A. Rizzi, U. Saranli, A. Saunders, and D. E. Koditschek, "Robots in scansorial environments," in *Proceedings of SPIE*, G. Gerhart, C. Shoemaker, and D. Gage, Eds., vol. 5804, Bellingham, WA, 2005, pp. 291–302.

[12] R. Niiyama, A. Nagakubo, and Y. Kuniyoshi, "Mowgli: A bipedal jumping and landing robot with an artificial musculoskeletal system," in *Proceedings of the IEEE International Conference on Robotics and Automation*, April 2007, pp. 2546–2551.

[13] M. Buehler, R. Playter, and M. Raibert, "Robots step outside," in *Proceedings of the International Symposium on Adaptive Motion in Animals and Machines (AMAM)*, Ilmenau, Germany, September 2005.

[14] M. Habib, K. Watanabe, and K. Izumi, "Biped locomotion using cpg with sensory interaction," in *Proceedings of the International Symposium on Industrial Electronics*, July 2009, pp. 1452–1457.

[15] Y. Fukuoka, H. Kimura, and A. Cohen, "Adaptive dynamic walking of a quadruped robot on irregular terrain based on biological concepts," *International Journal of Robotics Research*, vol. 22, no. 3, pp. 187–202, 2003.

[16] J. Hrr, J. Pratt, C.-M. Chew, H. Herr, and G. Pratt, "Adaptive virtual model control of a bipedal walking robot," in *Proceedings of IEEE International Joint Symposia on Intelligence and Systems*, May 1998, pp. 245–251.

[17] M. Kovac, M. Fuchs, A. Guignard, J.-C. Zufferey, and D. Floreano, "A miniature 7g jumping robot," in *Proceedings of the IEEE International Conference on Robotics and Automation*, May 2008, pp. 373–378.

[18] T. Allen, R. Quinn, R. Bachmann, and R. Ritzmann, "Abstracted biological principles applied with reduced actuation improve mobility of legged vehicles," in *Proceedings of the IEEE/RSJ International Conference on Intelligent Robots and Systems*, October 2003, pp. 1370–1375.

[19] N. Neville, M. Buehler, and I. Sharf, "A bipedal running robot with one actuator per leg," in *Proceedings of the IEEE International Conference on Robotics and Automation*, May 2006, pp. 848–853.

[20] U. Saranli, M. Buehler, and D. Koditschek, "Design, modeling and preliminary control of a compliant hexapod robot," in *Proceedings of the IEEE International Conference on Robotics and Automation*, 2000, pp. 2589–2596.

[21] P. Vernaza, M. Likhachev, S. Bhattacharya, S. Chitta, A. Kushleyev, and D. Lee, "Search-based planning for a legged robot over rough terrain," in *Proceedings of the IEEE International Conference on Robotics and Automation*, May 2009, pp. 2380–2387.

[22] D. Pongas, M. Mistry, and S. Schaal, "A robust quadruped walking gait for traversing rough terrain," in *Proceedings of the IEEE International Conference on Robotics and Automation*, April 2007, pp. 1474–1479.

[23] J. Rebula, P. Neuhaus, B. Bonnlander, M. Johnson, and J. Pratt, "A controller for the littledog quadruped walking on rough terrain," in *Proceedings of the IEEE International Conference on Robotics and Automation*, April 2007, pp. 1474–1479.

[24] J. Kolter and A. Y. Ng, "The stanford littledog: A learning and rapid replanning approach to quadruped locomotion," *The International Journal of Robotics Research*, vol. 30, no. 2, pp. 150–174, 2011.

[25] U. Saranli, M. Buehler, and D. E. Koditschek, "Rhex: A simple and highly mobile hexapod robot," *The International Journal of Robotics Research*, vol. 20, no. 7, pp. 616–631, 2001.

[26] R. Altendorfer, N. Moore, H. Komsuoglu, M. Buehler, J. Brown, H.B., D. McMordie, U. Saranli, R. Full, and D. Koditschek, "Rhex: A biologically inspired hexapod runner," *Autonomous Robots*, vol. 11, pp. 207–213, 2001.

[27] E. Moore, D. Campbell, F. Grimminger, and M. Buehler, "Reliable stair climbing in the simple hexapod 'rhex'," in *Proceedings of the IEEE International Conference on Robotics and Automation*, 2002, pp. 2222–2227.

[28] X. Liang, M. Xu, L. Xu, P. Liu, X. Ren, Z. Kong, J. Yang, and S. Zhang, "The amphihex: A novel amphibious robot with transformable leg-flipper composite propulsion mechanism," in *Proceedings of the IEEE/RSJ International Conference on Intelligent Robots and Systems*, October 2012, pp. 3667–3672.

[29] R. Schroer, M. Boggess, R. Bachmann, R. Quinn, and R. Ritzmann, "Comparing cockroach and whegs robot body motions," in *Proceedings of the IEEE International Conference on Robotics and Automation*, 2004, pp. 3288–3293.

[30] D. Goldschmidt, F. Hesse, F. Worgotter, and P. Manoonpong, "Biologically inspired reactive climbing behavior of hexapod robots," in *Proceedings of the IEEE International Conference on Intelligent Robots and Systems, IROS '12*, October 2012, pp. 4632–4637.

[31] W. Lewinger, B. Rutter, M. Blümel, A. Büschges, and R. Quinn, "Sensory coupled action switching modules (SCASM) generate robust, adaptive stepping in legged robots," in *Proceedings of 9th International Conference on Climbing and Walking Robots*, 2006.

[32] O. Ekeberg, M. Blumel, and A. Buschges, "Dynamic simulation of insect walking," *Arthropod Structure and Development*, vol. 33, no. 3, pp. 287–300, 2004.

[33] W. A. Lewinger and R. D. Quinn, "Neurobiologically-based control system for an adaptively walking hexapod," *Industrial Robot: An International Journal*, vol. 38, no. 3, pp. 258–263, 2011.

[34] M. Hutter, C. Gehring, M. Bloesch, M. Hoepflinger, C. Remy, and R. Siegwart, "StarlETH: A compliant quadrupedal robot for fast, efficient, and versatile locomotion," in *Proceedings of the 15th International Conference on Climbing and Walking Robot - CLAWAR 2012*, 2012.

[35] D. I. Goldman, T. S. Chen, D. M. Dudek, and R. J. Full, "Dynamics of rapid vertical climbing in cockroaches reveals a template," *Journal of Experimental Biology*, vol. 209, pp. 2990–3000, 2006.

[36] D. E. Koditschek, R. J. Full, and M. Buehler, "Mechanical aspects of legged locomotion control," 2004.

[37] M. Raibert, K. Blankespoor, G. Nelson, R. Playter, *et al.*, "Bigdog, the rough–terrain quadruped robot," in *Proceedings of the 17th World Congress*, 2008, pp. 10 823–10 825.

[38] Boston Dynamics, "LS3: Legged Squad Support System," http://www.bostondynamics.com/robot_ls3.html, 2012, [Online; accessed 02 February 2013].

[39] M. Kalakrishnan, J. Buchli, P. Pastor, M. Mistry, and S. Schaal, "Learning, planning, and control for quadruped locomotion over challenging terrain," *International Journal of Robotics Research*, vol. 30, pp. 236–258, 2010.

[40] M. P. Murphy, A. Saunders, C. Moreira, A. A. Rizzi, and M. Raibert, "The littledog robot," *The International Journal of Robotics Research*, vol. 30, no. 2, pp. 145–149, 2011.

[41] W. A. Lewinger and R. Quinn, "A hexapod walks over irregular terrain using a controller adapted from an insect's nervous system," in *IEEE/RSJ International Conference on 2010 IEEE/RSJ International Conference on Intelligent Robots and Systems (IROS)*, 2010, pp. 3386–3391.

[42] M. Palankar and L. R. Palmer III, "A force threshold-based position controller for legged locomotion," *Autonomous Robots*, in press.

[43] ——, "Toward innate leg stability on unmodeled and natural terrain: Hexapod walking," in *Proceedings of the IEEE International Conference on Intelligent Robots and Systems*, 2012, pp. 526–531.

[44] ——, "A force threshold-based position controller for legged locomotion over irregular terrain," in *Proceedings of the Fifteenth International Conference on Climbing and Walking Robots and the Support Technologies for Mobile Machines*, 2012, pp. 563–570.

[45] R. J. Full, "Mechanics and energetics of terrestrial locomotion: From bipeds to polypeds," *Energy Transformation in Cells and Animals*, pp. 175–182, 1989.

[46] ——, "Concepts of efficiency and economy in land locomotion," *Energy Transformation in Cells and Animals*, pp. 175–182, 1990.

[47] R. J. Full and M. Tu, "The mechanics of six-legged runners," *Journal of Experimental Biology*, vol. 148, pp. 129–146, 1990.

[48] ——, "Mechanics of rapid running insects: two-, four-, and sixlegged locomotion," *Journal of Experimental Biology*, vol. 156, pp. 215–231, 1991.

[49] R. J. Full and D. E. Koditschek, "Templates and anchors: neuromechanical hypotheses of legged locomotion on land," *Journal of Experimental Biology*, vol. 202, pp. 3325–3332, 1999.

[50] R. J. Full, R. Blickhan, and M. Tu, "Leg design in hexapedal runners," *Journal of Experimental Biology*, vol. 158, pp. 369–390, 1991.

[51] H. Cruse, "Which parameters control the leg movement of a walking insect?: I. velocity control during the stance phase," *Journal of Experimental Biology*, pp. 343–355, 1985.

[52] S. Kaliyamoorthy, S. N. Zill, R. D. Quinn, R. E. Ritzmann, and J. Choi, "Finite element analysis of strains in a blaberus cockroach leg during climbing," in *Proceedings of the IEEE/RSJ International Conference on Intelligent Robots and Systems (IROS)*, 2001, pp. 833–838.

[53] A. Prochazka, D. Gillard, and D. J. Bennett, "Implications of positive feedback in the control of movement," *Journal of Neurophysiology*, vol. 77, pp. 3237–3251, 1997.

[54] J. Bender, E. Simpson, B. Tietz, K. Daltorio, R. Quinn, and R. Ritzmann, "Kinematic and behavioral evidence for a distinction between trotting and ambling gaits in the cockroach blaberus discoidalis," *Journal of Experimental Biology*, vol. 214, pp. 2057–2064, 2011.

[55] H. Cruse, D. Riemenschneider, and W. Stammer, "Control of body position of a stick insect standing on uneven surfaces," *Biological Cybernetics*, vol. 61, no. 1, pp. 71–77, 1989.

[56] H. Cruse, K. Dautenhahn, and H. Schreiner, "Coactivation of leg reflexes in the stick insect," *Biological cybernetics*, vol. 67, no. 4, pp. 369–375, 1992.

125

[57] H. Cruse, "The control of body position in the stick insect (carausius morosus), when walking over uneven surfaces," *Biological Cybernetics*, vol. 24, pp. 25–33, 1976.

[58] H. Cruse, J. Schmitz, U. Braun, and A. Schweins, "Control of body height in a stick insect walking on a treadwheel," *Journal of Experimental Biology*, vol. 181, no. 1, pp. 141–155, 1993.

[59] J. T. Watson, R. E. Ritzmann, S. N. Zill, and A. J. Pollack, "Control of obstacle climbing in the cockroach, Blaberus discoidalis. I. Kinematics," *Journal of Comparative Physiology A: Neuroethology, Sensory, Neural, and Behavioral Physiology*, vol. 188, no. 1, pp. 39–53, February 2002.

[60] L. H. Ting, R. Blickhan, and R. J. Full, "Dynamic and static stability in hexapedal runners," *Journal of Experimental Biology*, vol. 197, no. 1, pp. 251–269, 1994.

[61] T. M. Kubow and R. J. Full, "The role of the mechanical system in control: a hypothesis of self-stabilization in hexapedal runners," *Philosophical Transactions of the Royal Society of London. Series B: Biological Sciences*, vol. 354, no. 1385, pp. 849–861, 1999.

[62] L. R. Palmer III and M. Palankar, "Blind hexapod walking over uneven terrain using only local feedback," in *Proceedings of the IEEE International Conference on Robotics and Biomimetics*, 2011, pp. 1603–1608.

[63] ——, "Blind hexapod walking over uneven terrain using only local feedback," in *Proceedings of the International Conference on Climbing and Walking Robots*, 2011, pp. 623–630.

[64] D. E. Orin, "Supervisory control of a multilegged robot," *International Journal of Robotics Research*, vol. 1, no. 4, pp. 79–91, 1982.

[65] S. M. Song and K. J. Waldron, *Machines that Walk*.   Cambridge, MA: MIT Press, 1989.

[66] S. Hirose, "A study of design and control of a quadruped walking vehicle," *The International Journal of Robotics Research*, vol. 3, no. 2, pp. 113–133, 1984.

[67] W. Lee and D. Orin, "The kinematics of motion planning for multilegged vehicles over uneven terrain," *IEEE Journal of Robotics and Automation*, vol. 4, no. 2, pp. 204–212, 1988.

[68] D. M. Wilson, "Insect walking," *Annual Review of Entomology*, vol. 11, no. 1, pp. 103–122, 1966.

[69] C. Ferrell, "Robust and adaptive locomotion of an autonomous hexapod," in *Proceedings of the From Perception to Action Conference*, September 1994, pp. 66–77.

[70] V. Dürr and W. Ebeling, "The behavioural transition from straight to curve walking: kinetics of leg movement parameters and the initiation of turning," *Journal of Experimental Biology*, vol. 208, no. 12, pp. 2237–2252, 2005.

[71] ROBOTIS, "ROBOTIS AX-18 Actuator e-Manual v1.11," http://support.robotis.com/en/product/dynamixel/ax_series/ax-18f.htm, 2010, [Online; accessed 28 January 2013].

[72] ——, "ROBOTIS RX-28 Actuator e-Manual v1.12," http://support.robotis.com/en/product/dynamixel/rx_series/rx-28.htm, 2010, [Online; accessed 28 January 2013].

[73] ——, "ROBOTIS CM-700 Control Board e-Manual," http://support.robotis.com/en/product/auxdevice/controller/cm700_manual.htm, 2010, [Online; accessed 28 January 2013].

[74] S. McMillan, D. E. Orin, and R. B. McGhee, "DynaMechs: an object oriented software package for efficient dynamic simulation of underwater robotic vehicles," in *Underwater Robotic Vehicles: Design and Control*, J. Yuh, Ed.   Albuquerque, NM: TSI Press, 1995, pp. 73–98.

[75] ROBOTIS, "ROBOTIS MX-28 Actuator e-Manual v1.12," http://support.robotis.com/en/product/dynamixel/mx_series/mx-28.htm, 2010, [Online; accessed 28 January 2013].

[76] S. Zill, B. Keller, S. Chaudhry, E. Duke, D. Neff, R. Quinn, and C. Flannigan, "Detecting substrate engagement: responses of tarsal campaniform sensilla in cockroaches," *Journal of Comparative Physiology A*, vol. 196, pp. 407–420, 2010.

[77] H. Cruse, T. Kindermann, M. Schumm, J. Dean, and J. Schmitz, "Walknet - a biologically inspired network to control six-legged walking," *Neural Networks*, vol. 11, no. 7–8, pp. 1435–1447, 1998.

[78] L. R. Palmer III and C. Eaton, "Toward innate leg stability on unmodeled and natural terrain: Quadruped walking," in *Proceedings of the IEEE/RSJ International Conference on Intelligent Robots and Systems*, October 2012.

APPENDICES

Appendix A: Hardware Specification

Hardware specifications for the hexapod components are given below.

Table A.1: Dynamixel AX-18A servo actuator statistics.

AX-18A Stats	
Operating Voltage	12 *V*
Holding Torque	18 *kg·cm* 250 *oz·in*
No-load Speed	0.103 *sec*/60°
Weight	54.5 *g*
Size	50 *x* 32 *x* 38 *mm*
Resolution	0.29°
Reduction Ratio	1/254
Operating Angle	300° or Continuous Turn
Max Current	2200 *mA*
Standby Current	50 *mA*
Operating Temp	$-5°C \sim 85°C$
Protocol	TTL Half Duplex Async Serial
Module Limit	254 valid addresses
Com Speed	7343 *bps* $\sim$ 1 *Mbps*
Position Feedback	Yes
Temp Feedback	Yes
Load Voltage Feedback	Yes
Input Voltage Feedback	Yes
Compliance/PID	Yes
Material	Plastic Gears and Body
Motor	Cored Motor

Table A.2: Dynamixel RX-28 servo actuator statistics.

RX-28 Stats		
Operating Voltage	16 *V*	12 *V*
Holding Torque	37.7 *kg·cm* 523.55 *oz·in*	28.3 *kg·cm* 393 *oz·in*
No-load Speed	0.126 *sec*/60°	0.167 *sec*/60°
Weight	72 *g*	
Size	50.6 *x* 35.6 *x* 35.5 *mm*	
Resolution	0.29°	
Reduction Ratio	1/193	
Operating Angle	300° or Continuous Turn	
Max Current	1200 *mA*	
Standby Current	50 *mA*	
Operating Temp	$-5°C \sim 85°C$	
Protocol	RS485 Asynchronous Serial	
Module Limit	254 valid addresses	
Com Speed	7343 *bps* $\sim$ 1 *Mbps*	
Position Feedback	Yes	
Temp Feedback	Yes	
Load Voltage Feedback	Yes	
Input Voltage Feedback	Yes	
Compliance/PID	Yes	
Material	Metal Gears & Engineering Plastic Body	
Motor	Maxon RE-MAX	

130

Table A.3: Dynamixel MX-28T servo actuator statistics.

MX-28T Stats		
Operating Voltage	14.8 *V*	12 *V*
Holding Torque	31.6 *kg·cm*	25.5 *kg·cm*
	439 *oz·in*	354 *oz·in*
	3.1 *N·m*	2.5 *N·m*
No-load Speed	67 *RPM*	55 *RPM*
Weight	72 *g*	
Size	35.6 *x* 50.6 *x* 35.5 *mm*	
Resolution	$0.088°$	
Reduction Ratio	$1/193$	
Operating Angle	$360°$ or Continuous Turn	
Max Current	1.4*A* @ 12*V*	
Standby Current	100 *mA*	
Operating Temp	$-5°C \sim 85°C$	
Protocol	TTL Asynchronous Serial	
Module Limit	254 valid addresses	
Com Speed	8000 *bps* $\sim$ 3 *Mbps*	
Position Feedback	Yes	
Temp Feedback	Yes	
Load Voltage Feedback	Yes	
Input Voltage Feedback	Yes	
Compliance/PID	Yes	
Material	Metal Gears & Engineering Plastic Body	
Motor	Maxon RE-MAX	

Table A.4: Dynamixel CM-700 controller statistics.

CM-700 Stats	
Operating Voltage	7 *V* - 35 *V*
Weight	37.3 *g*
Size	50 *x* 32 *x* 38 *mm*
Max Current	10 *A*
Idle Current	40 *mA*
Operating Temp	$-5°C \sim 70°C$
Protocol	TTL/RS485 Communication

131

Appendix B: Permissions

B.1   Journal of Experimental Biology (Figure 1.1, 2.1 and 2.3)

Rights and permissions

Author rights

(these rights are retained when publishing an Open Access article)

Authors remain the owners of the copyright to the article and retain the following non-exclusive rights (for further details, please refer to the licence agreement that accompanies article proofs):

(1) authors may reproduce the article, in whole or in part, in any printed book (including thesis) of which they are author, provided the original article is properly and fully attributed;
(2) authors and any academic institution where they are employed may reproduce the article, in whole or in part, for the purpose of teaching students;
(3) authors may post a copy of the article on their website, provided that it has already been published by the journal and is linked to the journal's website at http://jeb.biologists.org;
(4) authors may use data contained in the article in other works they create;

Disclaimer

Responsibility for:
(1) the accuracy of statements of fact;
(2) the authenticity of scientific findings or observations;
(3) expressions of scientific or other opinion;
(4) any other material published in the journal rests solely with the author(s) of the article in which such statements, etc., appear. No responsibility for such matters is assumed by the journal, its owners, publishers, referees or staff.

Reader and librarian rights

Readers and librarians are free to make copies of articles without seeking specific permission in the following circumstances, providing they are for free distribution and are not sold:
(1) for private study, copying must be done by the individual who wishes to use the article, or an employee at the institution to which he/she belongs, without any charge beyond the cost of the copying;
(2) in the case of production of multiple copies, these must be used for bona fide teaching purposes, and copying must be done by a member of staff of the university, school or comparable institution, without any charge beyond the cost of the copying.

Open Access rights

Articles published under the JEB Open Access model will be made freely available online via the Company's website immediately following publication, deposited in PMC for immediate release and can be distributed under the terms of the Creative Commons Attribution (CC-BY) Licence (the terms of which are set out at http://creativecommons.org/licenses/by/3.0/legalcode). Authors retain ownership of the copyright for their article, but undertake to allow anyone to download, reuse, reprint, modify, distribute, and/or copy articles, including for commercial purposes, provided that:
(i) the original authorship is properly and fully attributed and JEB is attributed as the original place of publication with correct citation details given;
(ii) if an original work is subsequently reproduced or disseminated not in its entirety but only in part or as a derivative work this is clearly indicated.

132

Appendix B: (continued)

No permission is required from the authors or the publishers under the CC-BY licence.

Authors who pay the Open Access fee are permitted to post the final, published PDF of their article on a website, institutional repository or other free public server, immediately upon publication, provided a link is included between the web page containing the Article and the Journal's website at http://jeb.biologists.org/.

Copyright and reproduction

Articles in JEB are published under an exclusive, worldwide licence granted to the publisher by the authors, who retain copyright. For full details of Open Access article use, see Open Access rights above.

Permission to use material from JEB in other publications

Authors are free to reproduce material from their own articles in other publications. Other individuals must first seek permission from The Company of Biologists to reproduce material by sending an email to permissions@biologists.com

Permission to use material from other publications in JEB

It is the responsibility of the author to obtain permission to use material (e.g. figures) from another publication in any article submitted to JEB and to ensure that any such use is credited to the source. Written permission from the author and/or publisher of the original material, if required, should be provided at the time of submission, otherwise publication may be delayed. If you have modified a figure from a previously published figure, please check with the copyright owners to see whether permission is required and include a complete citation/reference for the original article.

For all other matters relating to the reproduction of material, please email permissions@biologists.com

Appendix B: (continued)

B.2 Elsevier License (Figure 1.2)

ELSEVIER LICENSE
TERMS AND CONDITIONS

Jul 02, 2013

This is a License Agreement between Mayur Palankar ("You") and Elsevier ("Elsevier") provided by Copyright Clearance Center ("CCC"). The license consists of your order details, the terms and conditions provided by Elsevier, and the payment terms and conditions.

All payments must be made in full to CCC. For payment instructions, please see information listed at the bottom of this form.

Supplier	Elsevier Limited The Boulevard,Langford Lane Kidlington,Oxford,OX5 1GB,UK
Registered Company Number	1982084
Customer name	Mayur Palankar
Customer address	14162 Monterey Pines Dr. TAMPA, FL 33620
License number	3181080461933
License date	Jul 02, 2013
Licensed content publisher	Elsevier
Licensed content publication	Arthropod Structure & Development
Licensed content title	Mechanical aspects of legged locomotion control
Licensed content author	Daniel E. Koditschek,Robert J. Full,Martin Buehler
Licensed content date	1 July 2004
Licensed content volume number	33
Licensed content issue number	3
Number of pages	22
Start Page	251
End Page	272
Type of Use	reuse in a thesis/dissertation
Intended publisher of new work	other
Portion	figures/tables/illustrations
Number of figures/tables /illustrations	1
Format	both print and electronic
Are you the author of this Elsevier article?	No
Will you be translating?	No
Order reference number	None
Title of your thesis/dissertation	A Distributed local-leg feedback algorithm for robust walking on uneven terrian
Expected completion date	Aug 2013
Estimated size (number of pages)	150
Elsevier VAT number	GB 494 6272 12

134

Appendix B: (continued)

professional translator must perform all translations and reproduce the content word for word preserving the integrity of the article. If this license is to re-use 1 or 2 figures then permission is granted for non-exclusive world rights in all languages.

16. **Website**: The following terms and conditions apply to electronic reserve and author websites:

Electronic reserve: If licensed material is to be posted to website, the web site is to be password-protected and made available only to bona fide students registered on a relevant course if:

This license was made in connection with a course,

This permission is granted for 1 year only. You may obtain a license for future website posting,

All content posted to the web site must maintain the copyright information line on the bottom of each image,

A hyper-text must be included to the Homepage of the journal from which you are licensing at http://www.sciencedirect.com /science/journal/xxxxx or the Elsevier homepage for books at http://www.elsevier.com , and

Central Storage: This license does not include permission for a scanned version of the material to be stored in a central repository such as that provided by Heron/XanEdu.

17. **Author website** for journals with the following additional clauses:

All content posted to the web site must maintain the copyright information line on the bottom of each image, and the permission granted is limited to the personal version of your paper. You are not allowed to download and post the published electronic version of your article (whether PDF or HTML, proof or final version), nor may you scan the printed edition to create an electronic version. A hyper-text must be included to the Homepage of the journal from which you are licensing at http://www.sciencedirect.com/science/journal/xxxxx . As part of our normal production process, you will receive an e-mail notice when your article appears on Elsevier's online service ScienceDirect (www.sciencedirect.com). That e-mail will include the article's Digital Object Identifier (DOI). This number provides the electronic link to the published article and should be included in the posting of your personal version. We ask that you wait until you receive this e-mail and have the DOI to do any posting.

Central Storage: This license does not include permission for a scanned version of the material to be stored in a central repository such as that provided by Heron/XanEdu.

18. **Author website** for books with the following additional clauses:

Authors are permitted to place a brief summary of their work online only.

A hyper-text must be included to the Elsevier homepage at http://www.elsevier.com . All content posted to the web site must maintain the copyright information line on the bottom of each image. You are not allowed to download and post the published electronic version of your chapter, nor may you scan the printed edition to create an electronic version.

Central Storage: This license does not include permission for a scanned version of the material to be stored in a central repository such as that provided by Heron/XanEdu.

19. **Website** (regular and for author): A hyper-text must be included to the Homepage of the journal from which you are licensing at http://www.sciencedirect.com/science/journal/xxxxx. or for books to the Elsevier homepage at http://www.elsevier.com

20. **Thesis/Dissertation**: If your license is for use in a thesis/dissertation your thesis may be submitted to your institution in either print or electronic form. Should your thesis be published commercially, please reapply for permission. These requirements include permission for the Library and Archives of Canada to supply single copies, on demand, of the complete thesis and include permission for UMI to supply single copies, on demand, of the complete thesis. Should your thesis be published commercially, please reapply for permission.

21. **Other Conditions**:

v1.6

Appendix B: (continued)

B.3   Springer License (Figure 2.4 and 2.5)

SPRINGER LICENSE
TERMS AND CONDITIONS

Jul 02, 2013

This is a License Agreement between Mayur Palankar ("You") and Springer ("Springer") provided by Copyright Clearance Center ("CCC"). The license consists of your order details, the terms and conditions provided by Springer, and the payment terms and conditions.

All payments must be made in full to CCC. For payment instructions, please see information listed at the bottom of this form.

License Number	3180840970800
License date	Jul 02, 2013
Licensed content publisher	Springer
Licensed content publication	Biological Cybernetics
Licensed content title	The control of body position in the stick insect (Carausius morosus), when walking over uneven surfaces
Licensed content author	H. Cruse
Licensed content date	Jan 1, 1976
Volume number	24
Issue number	1
Type of Use	Thesis/Dissertation
Portion	Figures
Author of this Springer article	No
Order reference number	None
Title of your thesis / dissertation	A Distributed local-leg feedback algorithm for robust walking on uneven terrian
Expected completion date	Aug 2013
Estimated size(pages)	150
Total	**0.00 USD**

Terms and Conditions

Introduction
The publisher for this copyrighted material is Springer Science + Business Media. By clicking "accept" in connection with completing this licensing transaction, you agree that the following terms and conditions apply to this transaction (along with the Billing and Payment terms and conditions established by Copyright Clearance Center, Inc. ("CCC"), at the time that you opened your Rightslink account and that are available at any time at http://myaccount.copyright.com).
Limited License
With reference to your request to reprint in your thesis material on which Springer Science and Business Media control the copyright, permission is granted, free of charge, for the use indicated in your enquiry.
Licenses are for one-time use only with a maximum distribution equal to the number that you identified in the licensing process.
This License includes use in an electronic form, provided its password protected or on the university's intranet or repository, including UMI (according to the definition at the Sherpa website: http://www.sherpa.ac.uk/romeo/). For any other electronic use, please contact Springer at (permissions.dordrecht@springer.com or permissions.heidelberg@springer.com).
The material can only be used for the purpose of defending your thesis, and with a maximum of 100 extra copies in paper.
Although Springer holds copyright to the material and is entitled to negotiate on rights, this license is only valid, subject to a courtesy information to the author (address is given with the article/chapter) and provided it concerns original material which does not carry references to other sources (if material in question appears with credit to another source, authorization from that source is required as well).
Permission free of charge on this occasion does not prejudice any rights we might have to charge for reproduction of our copyrighted material in the future.
Altering/Modifying Material: Not Permitted

Appendix B: (continued)

You may not alter or modify the material in any manner. Abbreviations, additions, deletions and/or any other alterations shall be made only with prior written authorization of the author(s) and/or Springer Science + Business Media. (Please contact Springer at (permissions.dordrecht@springer.com or permissions.heidelberg@springer.com)

Reservation of Rights

Springer Science + Business Media reserves all rights not specifically granted in the combination of (i) the license details provided by you and accepted in the course of this licensing transaction, (ii) these terms and conditions and (iii) CCC's Billing and Payment terms and conditions.

Copyright Notice:Disclaimer

You must include the following copyright and permission notice in connection with any reproduction of the licensed material: "Springer and the original publisher /journal title, volume, year of publication, page, chapter/article title, name(s) of author(s), figure number(s), original copyright notice) is given to the publication in which the material was originally published, by adding; with kind permission from Springer Science and Business Media"

Warranties: None

Example 1: Springer Science + Business Media makes no representations or warranties with respect to the licensed material.

Example 2: Springer Science + Business Media makes no representations or warranties with respect to the licensed material and adopts on its own behalf the limitations and disclaimers established by CCC on its behalf in its Billing and Payment terms and conditions for this licensing transaction.

Indemnity

You hereby indemnify and agree to hold harmless Springer Science + Business Media and CCC, and their respective officers, directors, employees and agents, from and against any and all claims arising out of your use of the licensed material other than as specifically authorized pursuant to this license.

No Transfer of License

This license is personal to you and may not be sublicensed, assigned, or transferred by you to any other person without Springer Science + Business Media's written permission.

No Amendment Except in Writing

This license may not be amended except in a writing signed by both parties (or, in the case of Springer Science + Business Media, by CCC on Springer Science + Business Media's behalf).

Objection to Contrary Terms

Springer Science + Business Media hereby objects to any terms contained in any purchase order, acknowledgment, check endorsement or other writing prepared by you, which terms are inconsistent with these terms and conditions or CCC's Billing and Payment terms and conditions. These terms and conditions, together with CCC's Billing and Payment terms and conditions (which are incorporated herein), comprise the entire agreement between you and Springer Science + Business Media (and CCC) concerning this licensing transaction. In the event of any conflict between your obligations established by these terms and conditions and those established by CCC's Billing and Payment terms and conditions, these terms and conditions shall control.

Jurisdiction

All disputes that may arise in connection with this present License, or the breach thereof, shall be settled exclusively by arbitration, to be held in The Netherlands, in accordance with Dutch law, and to be conducted under the Rules of the 'Netherlands Arbitrage Instituut' (Netherlands Institute of Arbitration).*OR:*

All disputes that may arise in connection with this present License, or the breach thereof, shall be settled exclusively by arbitration, to be held in the Federal Republic of Germany, in accordance with German law.

Other terms and conditions:

v1.3

If you would like to pay for this license now, please remit this license along with your payment made payable to "COPYRIGHT CLEARANCE CENTER" otherwise you will be invoiced within 48 hours of the license date. Payment should be in the form of a check or money order referencing your account number and this invoice number RLNK501056635. Once you receive your invoice for this order, you may pay your invoice by credit card. Please follow instructions provided at that time.

Make Payment To:
Copyright Clearance Center
Dept 001
P.O. Box 843006
Boston, MA 02284-3006

For suggestions or comments regarding this order, contact RightsLink Customer Support: customercare@copyright.com or +1-877-622-5543 (toll free in the US) or +1-978-646-2777.

Gratis licenses (referencing $0 in the Total field) are free. Please retain this printable license for your reference. No payment is required.

ABOUT THE AUTHOR

Mayur Palankar was born in Mumbai (Bombay), India. He received his bachelor's degree in Computer Engineering at the University of Mumbai. He began his graduate studies in the field of Software Engineering at the New Mexico State University, Las Cruces, NM where he earned his M.S. degree in Computer Science. He then started his Ph.D. program in Computer Science and Engineering at the University of South Florida in Tampa, focusing on Robotics.